Design Methods for Reliable Interconnected Networks with Mutual Dependency: Drawing Inspiration from Human Brain Networks

Submitted to
Graduate School of Information Science and Technology
Osaka University

January 2020

Masaya MURAKAMI

List of publication

Journal papers

1. Masaya Murakami, Shu Ishikura, Daichi Kominami, Tetsuya Shimokawa, and Masayuki Murata, "Robustness and Efficiency in Interconnected Networks with Changes in Network Assortativity," *Applied Network Science*, vol. 2, no. 1, p. 6, March 2017.

2. Masaya Murakami, Daichi Kominami, Kenji Leibnitz, and Masayuki Murata, "Drawing Inspiration from Human Brain Networks: Construction of Interconnected Virtual Networks," *Sensors*, vol. 18, no. 4, p. 1133, April 2018.

3. Masaya Murakami, Daichi Kominami, Kenji Leibnitz, and Masayuki Murata, "Reliable Design for a Network-of-Networks with Inspiration from Brain Functional Networks," *Applied Sciences*, vol. 9, no. 18, p. 3809, September 2019.

Refereed Conference Papers

1. Masaya Murakami, Kenji Leibnitz, Daichi Kominami, Tetsuya Shimokawa, and Masayuki Murata, "Constructing Virtual IoT Network Topologies with a Brain-Inspired Connectivity Model," in *Proceedings of the 11th International Conference on Ubiquitous Information Management and Communication (ACM IMCOM 2017)*, pp. 1–8, January 2017.

2. Masaya Murakami, Kenji Leibnitz, Daichi Kominami, and Masayuki Murata, "Designing Interconnected Networks for Improving Robustness and Efficiency," in *Proceedings of the 23th*

IEEE International Symposium on Local and Metropolitan Area Networks (IEEE LANMAN 2017), pp. 1–6, June 2017.

Non-Refereed Technical Papers

1. Masaya Murakami, Daichi Kominami, Kenji Leibnitz, Tetsuya Shimokawa, and Masayuki Murata, "Constructing a Virtual IoT Network Using a Cerebral Cortical Connectivity Model," *Technical Report of IEICE (CCS2016-18)*, vol. 116, no. 180, pp. 9–14, August 2016 (in Japanese).

2. Masaya Murakami, Daichi Kominami, Kenji Leibnitz, and Masayuki Murata, "Analysis and Strategies for Improving Robustness and Efficiency in Interconnected Networks," *Technical Report of IEICE (IN2016-166)*, vol. 116, no. 485, pp. 413–418, March 2017.

3. Masaya Murakami, Kenji Leibnitz, Daichi Kominami, and Masayuki Murata, "Reliable Architecture for Network of Networks with Inspiration from Brain Networks," *Technical Report of IEICE (IN2017-111)*, vol. 117, no. 460, pp. 129–134, March 2018.

Preface

The Internet of Things (IoT) has seen an increasing number of practical implementations in recent years, regarding not only traditional Internet services but also other services of extreme societal importance, such as infrastructure (electricity grids, traffic, etc.) and life-critical services (security, medical treatment, etc.). That is, not only the scale but also the types of the networks have been increasing, which is resulting in the emergence of interconnected networks with mutual dependencies, known as a *network of networks* (NoN). For NoN, the potential of environmental fluctuations has been increasing where minor changes in one network are propagated onto other interconnected networks due to the dependency among the networks. In the upcoming IoT scenario, a partial malfunction in service networks will exert an increasing influence on society and human life. Consequently, it has become an urgent issue to establish methods for designing NoN with high reliability in order to sustain network services under environmental fluctuations.

In recent years, among the biological systems that have adapted their evolution to fluctuating environments, human brain networks have drawn a great deal of attention for their possible application in the engineering field. The human brain is composed of tens of billions of neurons and forms a modularly structured network with regions consisting of functional network components. Recent advancements in neuroimaging techniques, such as functional Magnetic Resonance Imaging (fMRI), have allowed the analysis of the human brain at a considerably detailed spatial resolution. Thus, it has been revealed that brain networks provide highly reliable services while dealing with topological fragility and metabolic cost for its huge modular structure and functional dependency between each pair of regions. We believe that brain networks contain fundamental properties that are also applicable to the aforementioned NoN in upcoming information network systems, but the

application of brain networks into information networks from an aspect of architectural design has not been investigated enough so far.

Therefore, in this thesis, we propose methods for designing reliable NoN drawing inspiration from human brain networks. We first investigate the NoN structural design from the topological aspect of node connectivity focusing on the application of network influencers (i.e., the most influential elements over the entire network), and on assortativity between the networks, which represents the distinctive node degree correlation. The high reliability of human brain networks is known to be obtained by the network assortativity, one of the essential topological properties of brain networks. Here, we deal with constructing not only a single network that possesses a specific degree of assortativity, but also an interconnected network where the assortativity between the component networks is specified, and therefore introduce a definition to measure assortativity between component networks based on the existing method of measuring assortativity between nodes. With respect to a single network, the results indicate that a decrease in assortativity provides high communication efficiency and distribution of communication load. Also we find, however, that excessive assortativity leads to poor network performance. On the other hand, for an interconnected network assortative connections between networks improve communication efficiency, whereas disassortative connections distribute the communication load.

Second, we investigate the reliable design of NoN from geographical aspect and consider connectivity between network components. When recapturing the structure of NoN from a wide-area viewpoint, it is necessary to take geometrical constraints into account and to consider how to efficiently connect network components with each other. Thus, we propose a method for assigning internetwork links based on a connectivity model observed in the cerebral cortex of the brain. Intermodular connectivity in the cerebral cortex achieves high reliability when dealing with the trade-off of geometrical constraints and communication performance on the large-scale networks composed of many modules (i.e., regions) and nodes (i.e., neurons). Furthermore, we consider how to assign endpoint nodes of the links between each component by controlling assortativity. Simulation experiments show that the proposed method based on the cerebral cortex model can construct an NoN topology with an optimal combination of communication efficiency, robustness, and wiring cost. For the selection of endpoint nodes for the internetwork links, the results show that high

assortativity enhances the robustness and communication efficiency due to the existence of many intramodular links attached to the high-degree endpoint nodes in either network component.

Only the structural reliability on an NoN is investigated in the studies described above, but it is also imperative to consider the dependency between network components, since there are many cases where the service availability of a network is closely tied with the other interdependent networks in the upcoming IoT scenario. To deal with a more concrete and fundamental interdependent network scenario that realizes an IoT environment, we focus on the network slicing technology. This enhances the utilization of physical networks while causing interdependence among sliced virtual networks due to traffic fluctuations from one network to the others. Among the NoN models that consider mutual dependence among networks, existing studies showed that the behavior of a NoN model based on brain functional networks reproduces the complementary internetwork dependence and elucidates the mechanisms that suppress the propagation of local fluctuations. Hence, we finally propose an NoN model assuming a virtualized network environment that describes the availability state of nodes to deal with traffic fluctuations and interdependence among the virtual and physical networks. We assume three fundamental types of interdependence among the networks for this model based on the existing NoN models, and confirm that the one applying complementary interdependence inspired by brain functional networks achieves high availability and communication performance while preventing interference among the sliced networks. Furthermore, we also investigate a method for designing a reliable network structure for the proposed model. To this end, the deployment of network influencers is configured from the perspective of intra-/internetwork assortativity. Simulation experiments confirm that availability or communication performance is improved when each sliced network is formed assortatively or disassortatively, respectively. Regarding internetwork assortativity, both the availability and communication performance are improved when the influencers are deployed disassortatively among the sliced networks.

Acknowledgments

This thesis could not have been accomplished without the assistance of many people, and I would like to acknowledge the contributions made by all of them.

Foremost, I would like to express my great thankfulness to my supervisor, Professor Masayuki Murata of the Graduate School of Information Science and Technology, Osaka University. His affectionate and invaluable guidance throughout my Ph.D. has made me grow not only as a researcher, but also as a human being.

I am heartily grateful to the members of my thesis committee, Professor Takashi Watanabe, Professor Teruo Higashino, and Professor Toru Hasegawa of the Graduate School of Information Science and Technology, Osaka University, and Professor Morito Matsuoka of the Cyber Media Center, Osaka University, for their multilateral reviews and perceptive comments.

I would like to owe my special thanks to Senior Researcher Kenji Leibnitz of the National Institute of Information and Communications Technology, and Assistant Professor Daichi Kominami of the Graduate School of Information Science and Technology, Osaka University. All the works would not have been possible without their firsthand advice, fruitful discussions, and attentive support.

Also, I would like to express my sincere appreciation for Specially Appointed Associate Professor Kazufumi Hosoda of the Institute for Academic Initiatives, Osaka University. His cordial support and thoughtful advice helped me a lot when I lost my direction.

I also acknowledge Senior Researcher Tetsuya Shimokawa of National Institute of Information and Communications Technology, Associate Professor Shin'ichi Arakawa, and Associate Professor Yuichi Ohsita of the Graduate School of Information Science and Technology, Osaka University,

for their valuable comments and suggestions on my study.

Furthermore, my appreciation goes to all of past and present staff members, colleagues and friends of the Advanced Network Architecture Research Laboratory, Graduate School of Information Science and Technology, Osaka University and the Humanware Innovation Program, Osaka University.

Finally, I cannot conclude my acknowledgement without expressing my thanks to my family. Thank you for your giving me invaluable support throughout my life.

Contents

List of Figures

List of Tables

Chapter 1

Introduction

1.1 Background

Information networks have been characterized by a rapid growth and increased complexity. Nowadays, the Internet of Things (IoT) has come to play an important role as a fundamental infrastructure in our society with billions of connected network devices and an increasing number of practical implementations [1–5]. In addition to the number of devices, the types of services provided over the Internet has been diversifying, including not only traditional Internet services for communication but also other indispensable services of extreme societal importance, such as public utility infrastructure (e.g., electricity grids, traffic) and life-critical services (security, medical treatment, etc.) [6, 7]. This situation is leading to the emergence of interconnected networks with mutual dependencies, which is known as a network of networks (NoN) [8].

When services are being provided over the NoNs, a local malfunction or fluctuation occurring in one of the networks can be propagated onto the other interconnected networks because of the mutual dependencies [8–11]. One of the most well-known cases is a real-world cascading failure on real-world interconnected networks consisting of power grid networks and supervisory control networks, which took place in Italy [12]. The functional availability of each infrastructure network depends on that of the other network: the power network must be operated by the control network, while the control network must be supplied with electricity by the power network. Hence, the

heavy mutual dependence between the two networks caused a small fraction of failures in one of the networks to increase to a large-scale cascading failure on the entire network, resulting in a massive blackout in a major part of the country.

Considering the upcoming IoT environment, such interdependent architectures regarded as NoNs can be assumed in the context of smart cities [13–15].To enhance the intelligence, efficiency, and operability of future cities, and to further the quality of human life, smart cities focus on the integration and coordination of different sectors of functional networks. Advanced metering, control, information, and communication technologies are the backbones of smart cities, and they are utilized by a combination of functional networks including electricity, healthcare, surveillance, transportation systems, and other public utilities. The availability of smart cities is guaranteed by the intelligent integration of decentralized information from an enormous number of IoT devices. Due to these synergistic interactions among different devices and networks, a processing halt in one service network also stops the functions on the others, and environmental changes in service networks will exert an increasing influence on society and human life. Consequently, an urgent issue is to establish methods for designing an NoN in the IoT context, in order to achieve high reliability, namely, the ability to sustain network services under unpredictable fluctuations.

On resolving complex issues in the field of engineering, biologically-inspired approaches have attracted significant research attention. In particular, the application of brain-like networks has progressed in recent years due to its superior characteristics as networks that have been optimized during the process of human growth and evolution [16, 17]. Remarkable advances in neuroimaging techniques, such as functional magnetic resonance imaging (fMRI), have allowed the analysis of the human brain at a considerably high spatial resolution [18–20]. Brain networks contain tens of billions of neurons to realize highly advanced functions, while providing a rapid information processing infrastructure and resilience against neuronal defects. This owes to the scalability and low metabolic cost realized by the modular network structure with its characteristic connectivity. In a human brain network, clusters of neurons are connected with each other and form subnetworks to provide a particular function (e.g., vision, emotion, or movement), and the underlying structural connectivity differs between and within the subnetworks. Further, the subnetworks are not just

interconnected from structural aspects but are also mutually dependent to complement their functionalities, and the brain networks are designed so that local fluctuations are not propagated onto the entire networks [21]. As for an NoN assuming the aforementioned environment of information networks today, it is indispensable to consider inter-network connectivity and dependency, and thus, brain networks are considered to possess fundamental characteristics that are necessary for the reliable design of an NoN. However, the insights from studying brain networks as mutually-dependent interconnected networks are yet to be applied to practical systems of information networks.

In this thesis, we investigate methods to design a reliable NoN considering the aforementioned problems of influence propagation against unpredictable fluctuations, particularly focusing on the inter-network connectivity and dependency, with inspiration from the mechanisms of brain functional networks.

1.2 Outline

Topology Design of Interconnected Networks to Improve Efficiency and Robustness [22]

In Chapter 2, the effect of assortativity on the robustness and efficiency of interconnected networks is investigated. This involves constructing a network that possessed the desired degree of assortativity, which is defined as the distinctive nodal degree correlation of human brain networks. Additionally, an interconnected network is constructed wherein the assortativity between component networks possesses a targeted value to configure a specific connectivity between the networks. With respect to individual networks, the results indicate that a decrease in assortativity provided low hop lengths, high information diffusion efficiency, and distribution of communication load on edges. The study also reveals that excessive assortativity lead to poor network performance. In addition, while in the usual case, assortativity is define as a metric over the entire network, we extend the definition to also define assortativity between networks. In this study, the assortativity between networks is defined and the following results were demonstrated: assortative connections between networks lowered the average hop lengths and enhanced information diffusion efficiency, whereas

disassortative connections between networks distributed the communication loads of internetwork links and enhanced robustness. Furthermore, it is necessary to carefully adjust assortativity based on the node degree distribution of networks. Finally, the application of the results to the design of robust and efficient information networks is discussed.

Configuring Interconnectivity of Interconnected Networks with a Trade-off of Geometric Constraints and Performance [23–25]

Virtualization of wireless sensor networks (WSN) is widely considered as a foundational block of edge/fog computing, which is a key technology that can help realize next-generation Internet of things (IoT) networks. In such scenarios, multiple IoT devices and service modules will be virtually deployed and interconnected over the Internet. Moreover, application services are expected to be more sophisticated and complex, thereby increasing the number of modifications required for the construction of network topologies. Therefore, it is imperative to establish a method for constructing a virtualized WSN (VWSN) topology that achieves low latency on information transmission and high resilience against network failures, while keeping the topological construction cost low. In Chapter 3, we draw inspiration from the intermodular connectivity in human brain networks, which achieves high performance in robustness and communication efficiency while suppressing metabolic cost, when dealing with large-scale networks composed of a large number of modules (i.e., regions) and nodes (i.e., neurons). We propose a method for assigning inter-modular links based on a connectivity model observed in the cerebral cortex of the brain, known as the exponential distance rule (EDR) model. We then choose endpoint nodes of these links by controlling intermodular assortativity, which characterizes the topological connectivity of brain networks. We test our proposed methods using simulation experiments. The results show that the proposed method based on the EDR model can construct a VWSN topology with an optimal combination of communication efficiency, robustness, and construction cost. Regarding the selection of endpoint nodes for the intermodular links, the results also show that high assortativity enhances the robustness and communication efficiency because of the existence of intermodular links connecting high-degree nodes in each module.

Design Method for Reliability of Interconnected Networks with Mutual Dependency [26–29]

In realizing the network environment assumed by the *Internet of Things*, network slicing has drawn considerable attention as a way to enhance the utilization of physical networks (PNs). Meanwhile, slicing has been shown to cause interdependence among the sliced virtual networks (VNs) by propagating traffic fluctuations from one network to the others. However, for interconnected networks with mutual dependencies, known as a *network of networks* (NoN), finding a reliable design method that can cope with environmental changes is an important issue that is yet to be addressed. Some NoN models exist that describe the behavior of interdependent networks in complex systems, and previous studies have shown that an NoN model based on the functional networks of the brain can achieve high robustness, but its application to dynamic and practical systems is yet to be considered. Consequently, in Chapter 4, we propose the *Physical–Virtual NoN* (PV-NoN) model assuming a network-slicing environment. This model defines an NoN availability state to deal with traffic fluctuations and interdependence among a PN and VNs. Further, we assume three basic types of interdependence among VNs for this model. Simulation experiments confirm that applying the complementary interdependence inspired by brain functional networks achieves high availability and communication performance while preventing interference among the VNs. Also investigated is a method for designing a reliable network structure for the PV-NoN model. To this end, the deployment of *network influencers* (i.e., the most influential elements over the entire network) is configured from the perspective of intra/internetwork *assortativity*. Simulation experiments confirm that availability or communication performance is improved when each VN is formed assortatively or disassortatively, respectively. Regarding internetwork assortativity, both the availability and communication performance are improved when the influencers are deployed disassortatively among the VNs.

Chapter 2

Topology Design of Interconnected Networks to Improve Efficiency and Robustness

2.1 Introduction

Information networks are characterized by rapid growth and increased complexity. Many sensor devices collect a varie, ty of environmental information and are placed at different locations and connected to the Internet [30, 31]. It is estimated that tens of billions of such devices will be connected to the Internet by 2020 [32]. Additionally, services operated over the network to improve human life will further diversify and the network will be considerably improved to meet changing requirements. Hence, control and management of huge networks, such as the Internet of Things (IoT), will be difficult and involve increasing communication and computational costs. As information networks constitute important infrastructure at present and in the future, high reliability, efficiency, and scalability are important for the control and management of these networks.

The interconnecting structure of multiple networks is important in ensuring the aforementioned properties in information networks. A set of networks with scales that are not too large to be controlled and managed is considered as a large network, which is termed as an interconnected

network. The Internet itself is an interconnected network wherein numerous mutually connected networks are operated by Internet service providers [33]. Future information networks, including the future Internet, will involve an enormous number of interconnected networks managed by different administrators [34]. It is not possible to guarantee the reliability and efficiency of the network since it is not feasible for a single administrator to manage the entire network. To limit this potential drawback, this study examines the design of interconnected networks to provide high robustness and efficiency.

Structures similar to those in the interconnected networks are observed in networks with modular structures, such as regulatory gene networks, protein-protein interaction networks, and human brain networks [35]. In a modular structure, a module is defined as a subset of network units wherein connections between subset members are denser when compared with connections in the rest of the network. Recent advancements in neuroimaging techniques have allowed the analysis of the human brain at a considerably finer spatial resolution. Thus, extant research has examined the structural network of the brain as represented by anatomical connections among the regions of interest. Previous studies indicated that brain networks possess high topological efficiency and robustness while minimizing wiring cost. Furthermore, the human brain can adaptively tackle a large variety of tasks. It was considered that these advantages were obtained during the process of human growth and evolution.

It is necessary to focus on human brain networks to examine the manner in which interconnected networks can be built. The human brain is a complicated network composed of neuronal cell bodies residing in cortical gray matter regions joined by myelin-insulated axons. Advances in methods to analyze human brains revealed that brain networks include topological features observed in complex networks including small-world properties, a hierarchical modular structure, and an assortative structure [16,36,37]. These topological features are considered to provide advantages to the brain such as robustness against node failure and efficiency at tackling tasks adaptively [38]. Extant studies discussed applying a human-brain structure to information networks [39].

It is essential to clarify the effects of the structural properties of the human brain to apply the structural properties of the human brain. It is considered that small-world properties of brain networks facilitate efficient communication. However, extant research does not focus on topological

advantages of hierarchical modularity. Current opinions on the same are divided. However, hierarchical modularity appears to be associated with communication efficiency, robustness, maintenance of dynamic activity, and adaptive evolution. An understanding of the manner in which the forementioned topological properties contribute to the function of brain networks would contribute significantly to understanding the human brain and the manner in which these properties can be applied.

This study accounted for the modular structure and investigated assortativity, which is defined as the distinctive nodal degree correlation of brain networks. Assortativity represents the degree of correlation between connected nodes. Nodes of similar degree tend to be connected to each other in networks that exhibit high assortativity (termed as assortative mixing). In contrast, in networks with low assortativity (disassortative mixing), nodes are more preferentially connect to each other if they have a larger gap on degree [40]. Generally, an assortative-mixing network is robust against selective node failure, and this accelerates the spread of information generated by high-degree nodes [41, 42]. Brain networks exhibit a modular structure in which nodes are densely connected to compose a module and modules are sparsely connected with each other. The modules exhibit assortative mixing in this structure. Previous research did not focus on the effect of degree correlation with respect to the formation of edges between modules.

In this study, the effect of assortativity in interconnected networks in terms of robustness and efficiency was investigated. To examine the interaction effects of assortativity within a network and assortativity between networks in detail, networks with different assortativities were constructed and analyzed with respect to the following metrics: (1) edge betweenness centrality [40], (2) average hop length, (3) robustness against node failure, and (4) information diffusion efficiency [43,44].

First, a single network was examined, and the basic properties of assortative networks were demonstrated. This involved constructing a network with a specified value of assortativity by using a rewiring-based method proposed in a previous study [45]. To analyze the assortativity between networks, assortativity was defined as the universal assortativity coefficient as proposed in an extant study [46]. This was followed by proposing a method with two networks connected such that the assortativity between the networks corresponded to the desired value.

First, we focus on a single network and show the basic properties of assortative networks. For

this, we construct a network that has a specified value of assortativity by the rewiring-based method proposed in [45]. For analyzing the assortativity between networks, we define assortativity as the universal assortativity coefficient proposed in [46]. Then, we propose a method of connected two networks in such a way that the assortativity between them is the desired value.

2.2 Method

2.2.1 Overview

This subsection provides an overview of the method that was used to reveal the effects of assortativity. Two types of assortativity were discussed, namely assortativity within a network and assortativity between networks. In order to examine the influence of these types of assortativity on robustness and efficiency, network construction methods were proposed to achieve the desired assortativity. First, a method to construct a single network with the specific assortativity was discussed. This was followed by proposing a method to construct an interconnected network that consisted of two networks constructed by the first method such that the set of edges connecting the networks yielded the specified assortativity. An example of an interconnected network is shown in Fig. 2.1.

First, single networks were examined, and the properties of assortativity within a network were demonstrated. This was followed by focusing on interconnected networks to examine the assortativity properties between networks. Additionally, the interaction between within-network assortativity and between-network assortativity was investigated. Networks with different assortativities were constructed to examine the influence of assortativity, and the constructed networks were analyzed relative to graph-theoretic metrics.

Subsection *Definition of Assortativity* provides an explanation of the definitions of assortativity within a network and of assortativity between networks. Its subsubsections discusses a method to construct a network with a specific assortativity. Assortativity could influence various metrics and four metrics were used for the evaluation in this study by considering requirements essential to information networks. Subsection *Metrics for Evaluation* describes these metrics in detail.

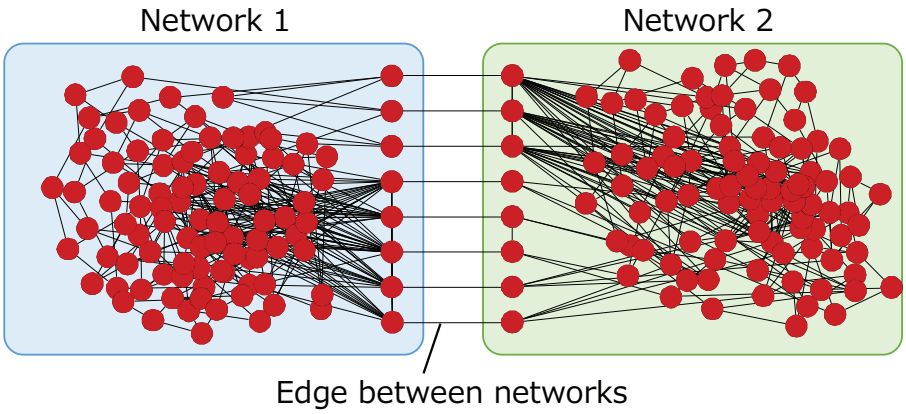

Figure 2.1: Interconnected modular network

2.2.2 Definition of Assortativity

This subsection focuses on an explanation of the definition of assortativity. Two types of assortativity were defined, namely assortativity within a network and between networks. Assortativity within a network is measured by the *assortativity coefficient* proposed by Newman [41]. The assortativity coefficient is shown in Subsection *Assortativity within a Network*. In contrast, a method to quantify assortativity between networks does not exist to the best of the authors' knowledge. Hence, the term *universal assortativity coefficient* [46] that corresponds to a dilatation of the assortativity coefficient was used to address this gap. The universal assortativity coefficient is described in Subsection *Assortativity between Networks*.

Assortativity Within a Network

Newman proposed measuring the assortativity of a network with the assortativity coefficient [40]. The assortativity coefficient is calculated from the remaining degree distribution $q(k)$ defined as follows:

$$q(k) = \frac{(k+1)p(k+1)}{\sum_j jp(j)}, \tag{2.1}$$

The remaining degree distribution is related to the degree distribution $p(k)$ that describes the probability that the degree of a randomly chosen node corresponds to k. The remaining degree of

a node in a path corresponds to the number of edges leaving a vertex separate from the vertex that was arrived along. In other words, the remaining degree of a node in a path is equal to the node's degree minus one. The joint probability distribution $e(j,k)$ can be introduced given $q(k)$ wherein the joint probability indicates the probability that two endpoints of a randomly chosen edge have the remaining degrees k and j. Hence, the assortativity coefficient r is defined as follows:

$$r = \frac{1}{\sigma_q^2}\left[\sum_{j,k} jke(j,k) - \left(\sum_j jq(j)\right)^2\right], \tag{2.2}$$

where σ_q denotes the standard deviation of the remaining degree distribution $q(k)$, given as follows: $\sigma_q^2 = \sum_k k^2 q(k) - \left(\sum_j jq(j)\right)^2$. The range of values that r can belong to corresponds to $[-1,\ 1]$. Positive and negative values of r indicate an assortative network and a disassortative network, respectively. When r corresponds to zero or is near zero, nodes are randomly connected with each other independent of their degrees. The range of feasible values of r is based on the degree distribution.

Assortativity Between Networks

Universal assortativity coefficient proposed in a previous study [46] was used to define the assortativity between networks. This coefficient reflects the contribution of an individual edge's to the global assortativity coefficient of the entire network. This was used to analyze the assortativity of any part of a network in a previous study [46]. The universal assortativity coefficient for a set of targeted edges E_{target} is represented as the sum of the contribution of each edge to the assortativity of the entire network as described in the previous subsubsection. The contribution of each edge to global assortativity is based on the global assortativity r in Eq. 2.2. Global assortativity r can be expressed as follows:

$$r = \frac{1}{\sigma_q^2}\Big(E[(J-U_q)(K-U_q)]\Big), \tag{2.3}$$

where $U_q = \sum_j jq(j)$ denotes the expected value of the remaining degree, and J and K denote variables of the remaining degree, which have the same expected value U_q. Then, the contribution

ρ_e of the edge e is then defined as follows:

$$\rho_e = \frac{(J - U_q)(K - U_q)}{M\sigma_q^2}, \tag{2.4}$$

where M denotes the number of edges in the whole network, and j and k denote the remaining degrees of the two endpoints of the edge e. Finally, the universal assortativity coefficient ρ is defined as follows:

$$\rho = \sum_{e \in E_{target}} \rho_e = \sum_{e \in E_{target}} \frac{(J - U_q)(K - U_q)}{M\sigma_q^2}. \tag{2.5}$$

The universal assortativity coefficient ρ is a part of global assortativity. Thus, if E_{target} is considered as the set of all edges, then ρ is equal to Newman's global assortativity. In this study, each edge between networks corresponds to an element of E_{target}. The assortativity between networks is calculated from Eq. (2.5) based on the E_{target}.

2.2.3 Network Construction Methods for Different Assortativities

This subsection presents two methods of constructing a network. The first subsubsection presented a method of constructing a single network that included the specified assortativity within the network as proposed in a previous study. The second subsubsection includes the proposal of a method to construct an interconnected network with the specified assortativity between two component networks.

Single Networks with Different Assortativities within a Network

A network with a target assortativity was constructed by repeatedly rewiring the edges of a given network. In this method, the assortativity was changed without changing the degree distribution because the individual rewirings did not change the degree distribution. Although this rewiring method did not necessarily achieve the overall maximum or minimum assortativity, this method has been widely used in previous researches relevant to assortativity due to its low computational cost [45, 47, 48], and it was also discussed that rewiring method can well approximate optimal solutions [49].

Repeated rewiring of the edges in the network proceeded in the following manner. First, two edges that did not share a common endpoint were randomly selected. This was followed by selecting four nodes as the new endpoints for the edges. Two pairs of nodes were rewired such that r approached the desired value, as shown in Figure 2.2. In the rewiring process, only the degree was considered to determine the nodes that should be connected with each other. Two nodes with degrees that exceeded the degrees of the other nodes were wired to increase assortativity. This contrasted with both the previously mentioned rewiring methods that decreased assortativity. Increasingly effective patterns to decrease assortativity were selected by calculating both assortativity coefficients. It should be noted that the two initially selected edges were not rewired when the connection pattern without rewiring was the most suitable and when the rewiring disconnect the network.

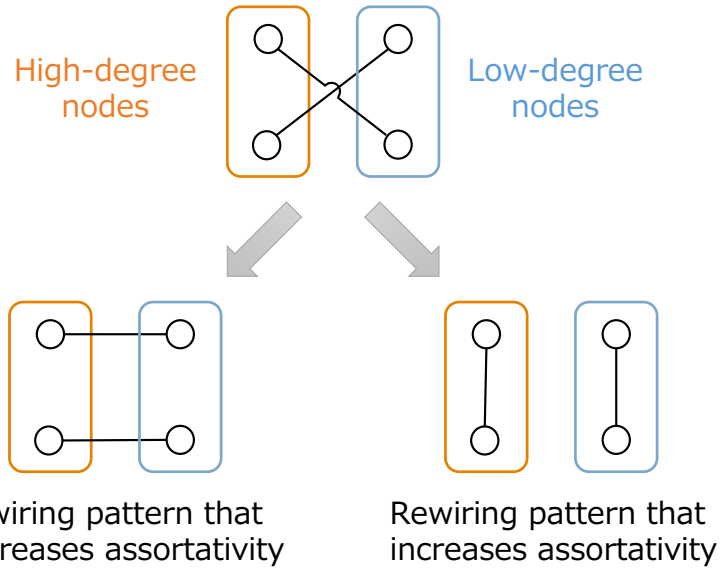

Figure 2.2: Rewiring patterns: decreasing assortativity (left) and increasing assortativity (right)

Inter-connected Network with Different Assortativities between networks

Interconnected Network with Different Assortativities Between Networks Two identical networks were connected to each other by M edges to construct an interconnected network with the specified

assortativity between networks. In order to obtain a suitable mixing pattern, edges between the networks were repeatedly deleted and added. This was performed stochastically with the mixing pattern determined by the following procedure:

1. Two networks were randomly connected via M edges. At this time, an endpoint node did not have multiple edges.

2. The assortativity between the networks was calculated. If the assortativity between the networks corresponded to the target value, then the set of connections at this point was adopted. Otherwise, the following steps were repeated until the assortativity between the networks reached the desired value.

3. An edge between the networks was randomly selected and deleted.

4. An edge was randomly added between the networks. If the assortativity did not approach the target value to a closer extant than the prior assortativity value, then the added edge was deleted, and the edge deleted in step 3) was re-added. The selection of an additional link was then repeated.

   In contrast with assortativity within a network, edges that influence assortativity could arbitrarily be chosen free from any degree constraints. Therefore, the maximum or minimum values of assortativity between networks for given networks were easily calculated.

2.2.4 Metrics for Evaluation

The metrics for the evaluation included the following: (1) the edge betweenness centrality, (2) the average hop length, (3) robustness relative to node failure, and (4) information diffusion efficiency. The details of these metrics are described in the following subsections.

Edge Betweenness Centrality The edge betweenness centrality of a network is defined as the number of shortest paths that passed through an edge in the network [40]. This could be considered as the communication load on the edges, and it indicated a possible concentration of the communication load. In the context of information networks, edges with high edge betweenness centrality

were associated with a higher probability of experiencing traffic congestion.

Average Hop Length The average path length corresponds to the average of the hop count of all shortest-hop paths. This is used widely in the field of graph theory and can be used to characterize data-transfer efficiency. Since we define the information diffusion efficiency in a network as a speed that information is diffused throughout the network in a probabilistic model for information diffusion, a network that has a small average hop length achieves a high information diffusion efficiency.

Robustness With respect to single networks, robustness was evaluated by using giant component size following the removal of a few nodes. The giant component size is the number of nodes in the largest connected component. Networks that maintained a high giant component size were considered to possess higher connectivity and consequently robustness.

With respect to the robustness of interconnected networks, it is inappropriate to use the giant component size because only a limited number of nodes include edges between networks, and the removal of other nodes corresponds to a considerably small influence on the performance of assortativity between networks. Removing nodes with the fore-mentioned interconnected edges could constitute a future research topic. However, all the nodes remain connected until all interconnecting edges are removed unless the endpoint nodes include extreme bottlenecks within the corresponding belonging network. Therefore, in order to evaluate the effect of interconnecting edges, average hop length between networks was used while removing endpoint nodes of the edges. With respect to the average hop length, paths between two nodes in the same network were ignored because they were barely influenced by the edges between networks. Thus, an interconnected network was considered robust if it retained its original value of average hop length following the removal of a few endpoint nodes.

Information diffusion efficiency The susceptible-infected-recovered (SIR) model in a previous study [50] was used to model the diffusion of information. In this model, each node could belong to three states, namely susceptible (S), infected (I), and recovered (R) state. An infected node

transmitted infection to neighbor nodes with probability β, and recovered with probability γ. A recovered node did not infect nor pass its infection to other nodes. When $\gamma = 0$ in the SIR model, it was termed as a susceptible-infected (SI) model [51] wherein when a node in a network was infected, all other susceptible nodes converged into an infected state. This SI model could purely measure the information diffusion speed of a network, i.e., the degree to which a network can diffuse information. Conversely, when $\gamma > 0$, all infected nodes eventually recovered and some nodes remained susceptible. In this case, areas that were more likely to be infected could be detected after a number of simulations selected an initial infected node randomly.

Several other models could be used to simulate the diffusion of information. However, the SIR model was used in the present study for two reasons. First, it was widely used in modeling the diffusion of information. Second, it offered immediate convergence.

2.3 Results

2.3.1 Single Networks

In this study, single networks with different assortativities were investigated. This involved using two types of networks that have different nodal degree distribution. The first type corresponded to a scale-free network (SF network) whose degree distribution follows power-law. Power-law distribution has been found in many complex networks, such as airline networks, social networks, the Internet, and so on. This type of networks is generated by two steps. First, we generate Barabási-Albert networks [52] which leads to the degree distribution $p(k) \sim k^{-3}$. Second, we keep its degree distribution and rewire all edges so that the characteristics of Barabási-Albert networks do not affect our evaluation. A single SF network consists of 100 nodes and 295 edges in which each node degree corresponded to a minimum of 3. Networks with different assortativities were generated by rewiring the edges of this network as described in the previous section. Assortativities within a range of $-0.69 \leq r \leq 0.58$ could be obtained by rewiring the edges of this network.

The second type corresponded to a Erdös-Eényi random network (RN network). The degree distribution of the RN network followed a Poisson distribution that is similar to the distribution

observed in wireless sensor networks. A single RN network consists of 100 nodes and 300 edges. The network was generated by repeatedly selecting pairs of nodes at random and connected these pairs. For this type of network, assortativities in the range of -0.79 and -0.97 were obtained. It was observed that the assortativity range of an SF network was narrower than that of a RN network, this reflected that the distribution of node degree was more strongly biased in SF networks. In particular, the number of nodes of high degree was lower, and thus, such nodes were rarely connected to other nodes of the same degree, thereby decreasing assortativity.

In the following results for single networks, we construct 25 topologies for each value of ρ; the results shown below are the averages across all 25 topologies.

Average Hop Length

The relation between average hop length and assortativity is shown in Figure 2.3. Both SF and RN networks exhibited the same tendency except with respect to the range of assortativity. As shown in Figure 2.3, the average hop length value increased when r increased. Specifically, the average hop length value rapidly increased when r approached its highest value for each network. With respect to information networks, an increase in the value of average hop length often degraded performance by increasing communication delays.

It was important to identify the reason for the sudden increase in average hop length when assortativity approached its highest value. This was performed by considering SF topology with assortativity $r = 0.58$ that corresponded to the peak. Figure 2.4 shows this network. Additionally, these clusters could be organized in order of degree. In this topology, almost all nodes were connected to other nodes of the same degree, and thus sets of same-degree nodes formed clusters. The results indicated that RN networks exhibited the same tendency. A chain-like topology possessed a high average hop length when compared with that of small-world topology, and thus a highly assortative topology implied a higher average hop length value. This tendency grew stronger as the assortativity of the network increased.

Hence, it was concluded that average hop length rapidly increased as assortativity approached its maximum value mainly because there were fewer shortcut edges and a few shortcut edges can

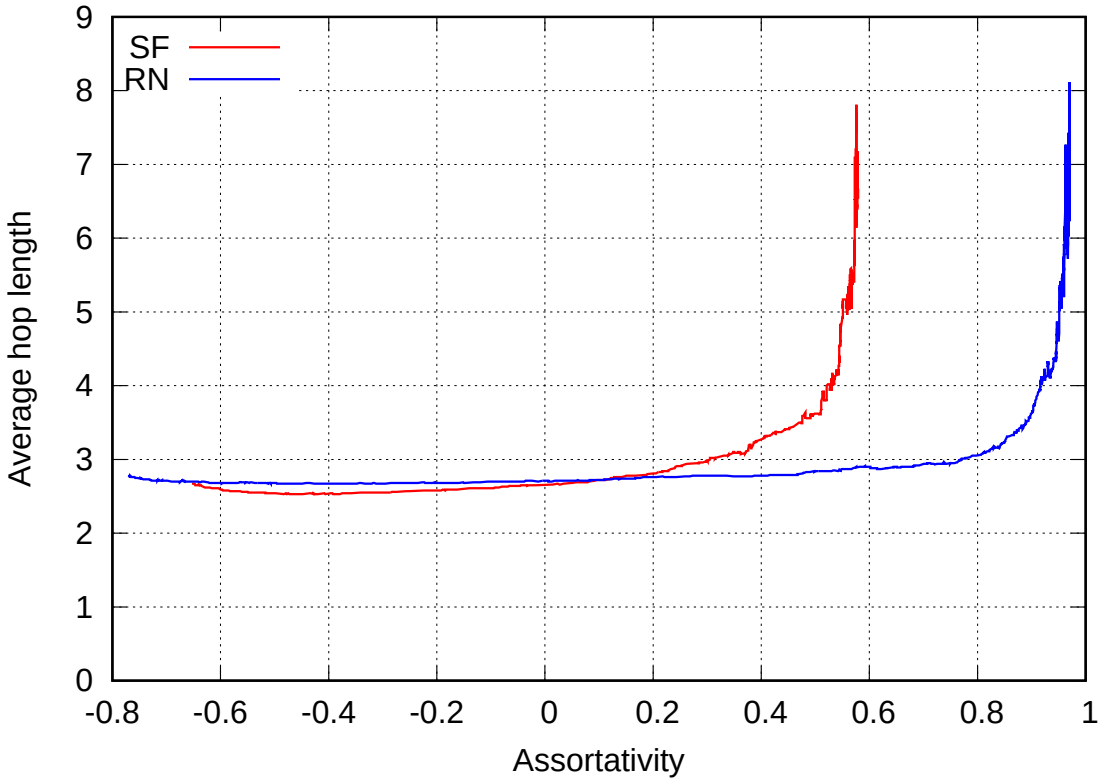

Figure 2.3: average hop length in single networks with different assortativities

markedly reduce average hop length, as demonstrated in a previous study [53]. However, these types of shortcut edges are likely to be lost when assortativity is very high because a clustered topology of the type shown in Figure 2.4 emerged. The observations indicated that the network lost these shortcut edges when the value of r was very high. Consequently, average hop length rapidly increased as assortativity approached a maximum value.

Edge Betweenness Centrality

Figure 2.5 shows edge betweenness centrality of each edge in a single SF and RN network. As shown in the figure, edges were arranged along the x-axis in increasing order of edge betweenness centrality. The figure indicated that with respect to the topology with maximum r (1), a few edges

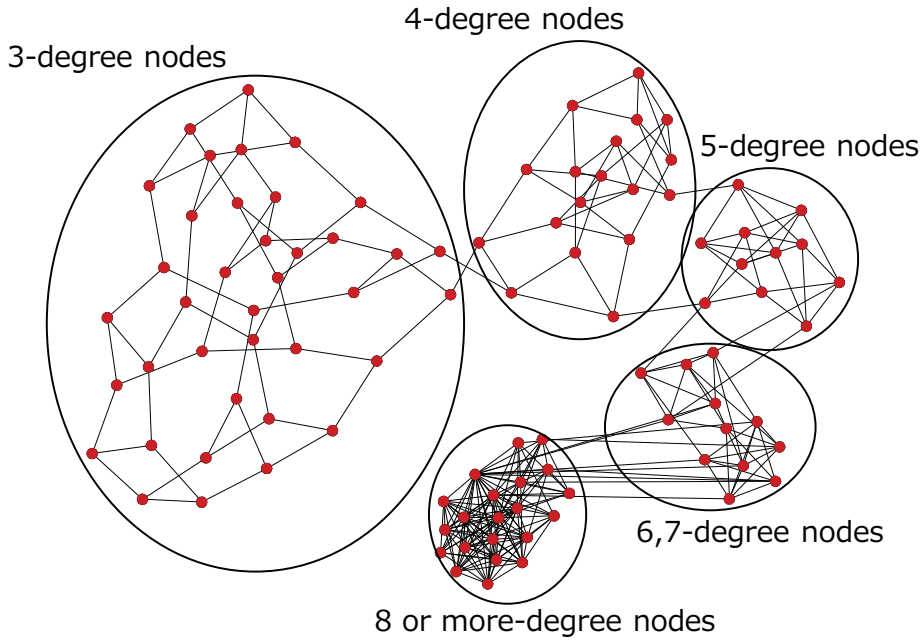

Figure 2.4: SF network topology with high assortativity ($r = 0.58$)

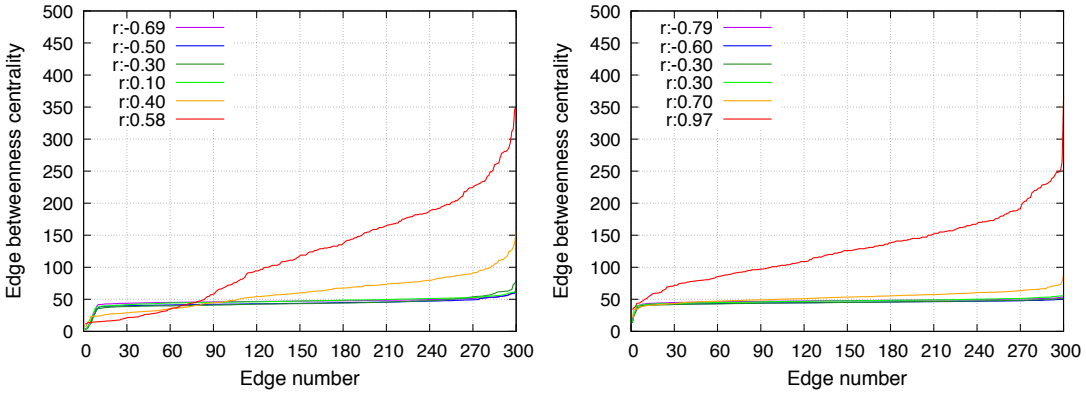

Figure 2.5: Edge betweenness centrality of all edges in a single SF network (left) and in a single RN network (right).

indicated extremely high edge betweenness centrality, and (2) the total edge betweenness centrality was also considerably high. This was attributed to the clustered structure shown in Figure 2.4. There were also very few shortcut edges in this topology, and the load on these edges increased. The lack of shortcut edges also caused an increase in the average hop length value as shown in the

Table 2.1: Relation between edge betweenness centrality and degrees of endpoints of edges in a SF network.

Most disassortative ($r = -0.69$)			Most assortative ($r = 0.58$)		
EBC	Endpoint 1	Endpoint 2	EBC	Endpoint 1	Endpoint 2
8.26	7	7	1.00	13	13
9.70	7	7	1.00	15	15
11.7	7	7	1.00	8	8
15.0	7	7	1.00	13	13
15.1	7	7	1.00	13	13
			⋮		
83.0	25	6	1070	6	5
88.8	19	6	1078	6	7
97.7	13	7	1136	4	4
100	15	7	1421	4	3
168	25	7	1455	5	4

previous section. Therefore, edges were included in the shortest paths several times. With respect to the other topologies, the total communication load over all edges drastically decreased due to the emergence of shortcut edges. Furthermore, it was observed that the distribution of edge betweenness centrality became more homogeneous as the assortativity decreased. This was because the connections between high-degree nodes changed into connections between a high-degree node and a low-degree node, and the communication load was distributed. Specifically, single RN networks with minimum assortativity r completely distributed the edge betweenness centrality since its node degree followed a Poisson distribution in contrast to SF networks that possess a Power law distribution.

Table 2.1 summarizes the relation between edge betweenness centrality and degrees of the endpoints of the edges in a single SF network. Only 5 out of 295 edges that correspond to the highest or lowest edge betweenness centrality are selected. High-degree nodes are important for a communication load in single disassortative networks, while low-degree nodes that connect different clusters are important in single assortative networks.

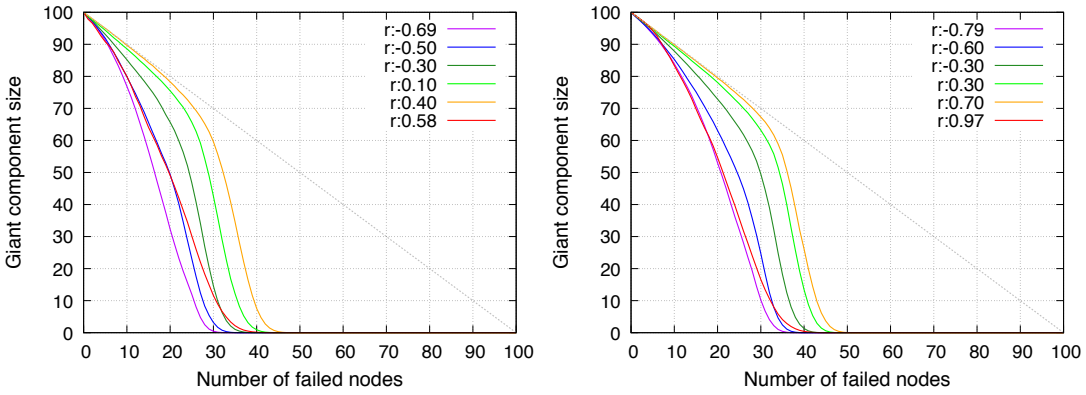

Figure 2.6: Change in giant component size with respect to deliberate node failure in a single SF network (left) and in a single RN network (right)

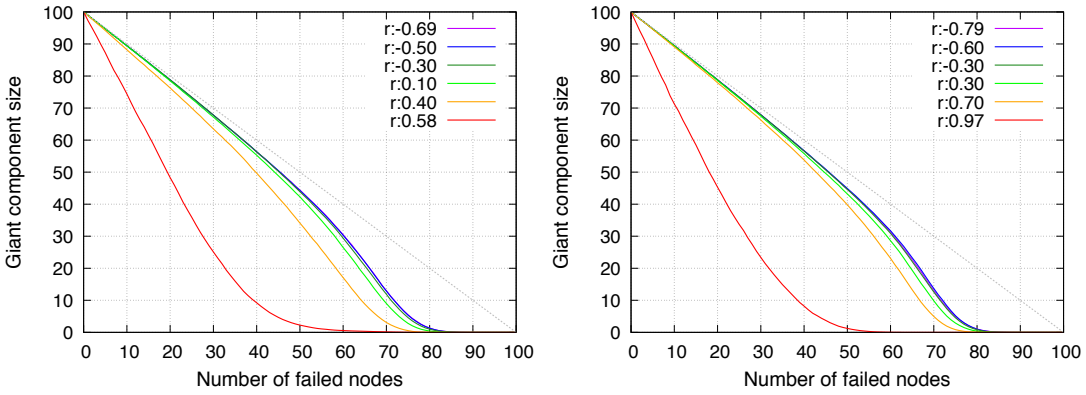

Figure 2.7: Change in giant component size with respect to random node failure in a single SF network (left) and in a single RN network (right)

Robustness

Figures 2.6 and 2.7 show the change in giant component size of networks when nodes are removed from the highest degree node either at each step or randomly. Simulations of removal were run 50 times with respect to each topology. With the exception of networks with maximum assortativity, assortative topologies were robust with respect to selective failure and weak with respect to random failure. As explained in the previous section, an assortative topology consisted of clusters connected in a chain. In the selective node-failure scenario, node failure commenced at the high-degree side

of this chain. Therefore, nodes with lower degrees remain connected to each other even when high-degree nodes failed. Conversely, the probability for the breaking of edges between clusters in the chain increased if the sequence of node failure did not follow any order. Thus, assortative topologies were fragile with respect to random node failure.

Robustness with respect to selective failure suddenly decreased when assortativity reached a maximum value. This corresponded to a topology with a minimum number of edges between clusters because the edges between clusters connected nodes of differing degrees. Thus, connectivity between clusters was fragile with respect to selective node failure.

An interesting point was that single RN networks exhibited considerably lower robustness when compared with that of SF networks given that both networks possessed maximum values of assortativity. This difference reflects the difference in the mode of degree. Many nodes in an SF network possess a minimal degree and they construct a cluster. Thus, selective node failure does not divide the giant component until additional nodes fail.

The aforementioned observations indicated that single assortative networks were robust with respect to selective failure albeit not with respect to random failure. However, when the forementioned networks were extremely assortative, then generated networks were weak with respect to both types of failures.

Information-diffusion Efficiency

As shown in Figure 2.8, speed of information diffusion is measured using a SI model with β set to 0.05. The x-axis represents time steps of diffusion, and the number of infected nodes is counted on the y-axis at each time step. Simulations of diffusion were executed 50 times with respect to each topology. A shown in Figure 2.8, information diffused poorly when the topology possessed high assortativity in both SF and RN networks. With respect to an assortative network, the low- and high-degree nodes involved few connections between them, and this resulted in a network with low efficiency of information diffusion.

Additionally, SIR models of $\beta = 0.05$ and $\gamma = 0.10$ were used to identify the areas that were more likely to be infected, and the number of infections on every node until a diffusion converged

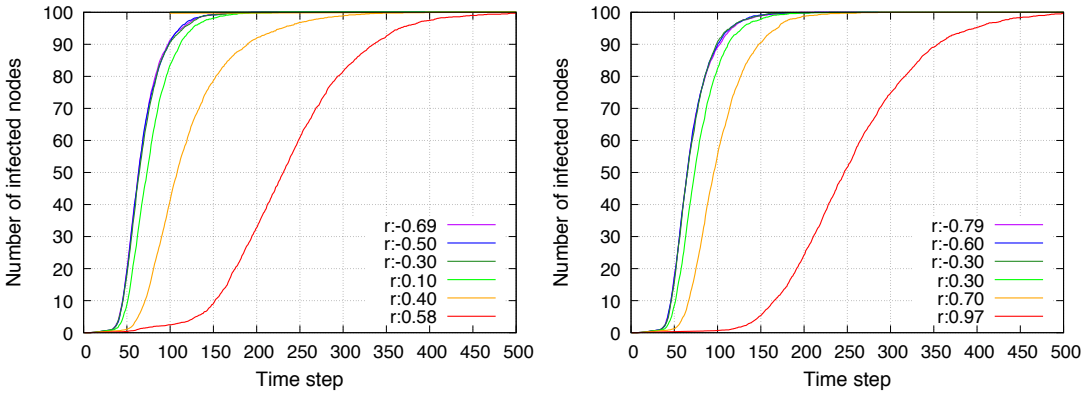

Figure 2.8: Information diffusion speed in a single SF network (left) and in a single RN network (right)

was counted. It should be noted that the SI model did not match this measurement because the infected nodes propagated infection permanently. Figure 2.9 shows the number of infections of each node in the SF topologies with $r = 0.55$ and -0.30. The total number of simulations run for each topology corresponded to 5,000 (50 simulations for every 100 node). All nodes were uniformly infected with respect to the topology with $r = -0.30$. In contrast, with respect to the assortative topology with $r = 0.55$, it was not likely that the information would diffuse in sparse areas and stack in high-degree dense areas.

2.3.2 Interconnected Networks

In this subsection, interconnected networks with differences between-network assortativities ρ were investigated. Each interconnected network consisted of two single networks of the same type that were connected to each other. Thus, a single SF network based on Barabási-Albert model included 1000 nodes and 2995 edges. Additionally, a RN network based on Erdös-Rényi model included 1000 nodes and 3000 edges. Two single networks of the same type were connected to each other via M edges, i.e., SF-SF networks and RN-RN networks.

Before starting the evaluation, it was important to clarify the appropriate value of M to measure the effect of changing assortativity ρ. Figure fig1:Inter-limit shows the relationship between the number of edges between networks and the maximum and minimum values of assortativity ρ. In

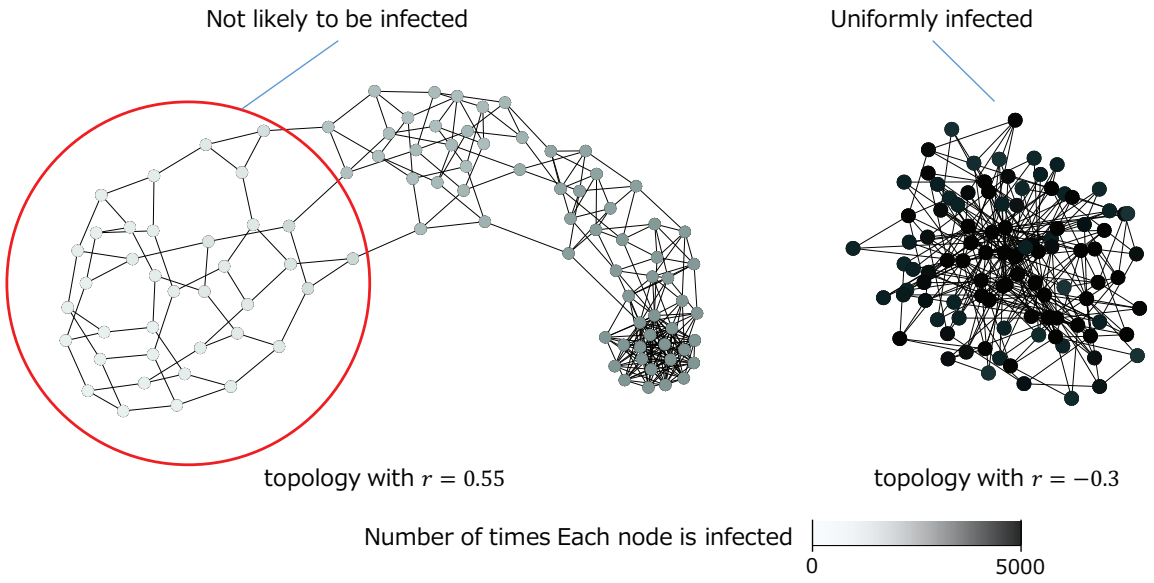

Figure 2.9: Number of infections of each node

this figure, edges were added in order of the influence on assortativity ρ. First, the range of ρ for RN-RN networks exceeded that of SF-SF networks since a SF network included a wider range of node degrees. However, it did not necessarily mean that larger limit of assortativity caused larger effect on the performance of RN-RN networks. We showed details about this point in the following evaluation of interconnected networks. Second, we also found that only a small fraction of edges could considerably increase or decrease assortativity ρ. Increment of all of the four curves was the largest at first, and as adding more edges the curves became gentler. To our surprise, the curve of SF-SF disassortative went so far as to cross the x-axis. This was because the average degree of a SF network is almost double of that of a RN network. Therefore, SF-SF networks has fewer combination of endpoints that contributes to increase disassortativity. Considering the above, M was set to 50 in the following evaluation.

The range of assortativity ρ between the networks was from -0.0054 to 0.0124 for SF-SF networks and from -0.037 to 0.0385 for RN networks. In the evaluation, the target assortativity ρ was changed, and edges were generated between networks. The construction method for interconnected networks included a probabilistic process. Thus, 25 topologies for each value of ρ were constructed and the results shown below correspond to the averages across all 25 topologies.

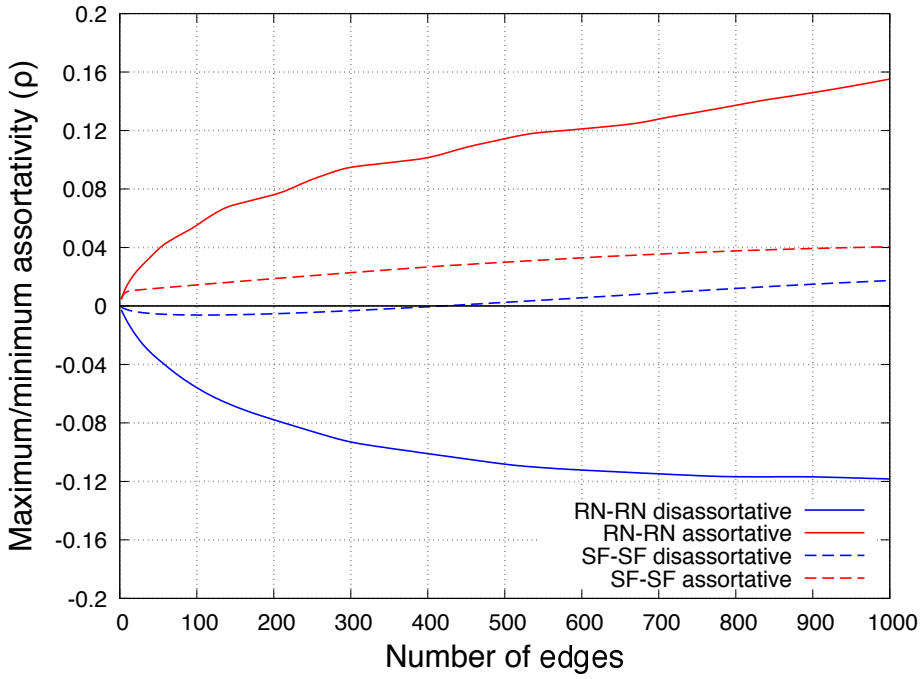

Figure 2.10: Relationship between the number of edges between networks and the maximum and minimum values of assortativity between networks.

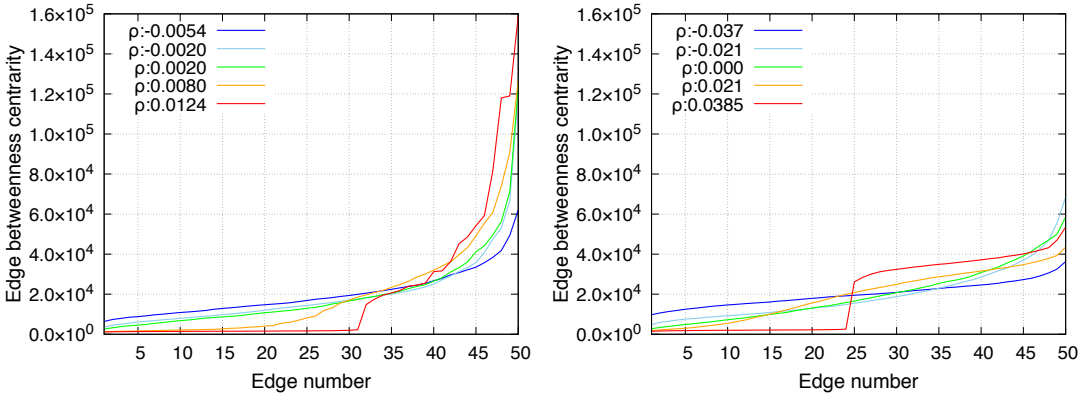

Figure 2.11: Edge betweenness centrality of every edges in SF-SF networks (left) and in RN-RN networks (right)

Edge Betweenness Centrality

Figure 2.11 shows the edge betweenness centrality of interconnecting edges. The edge betweenness centrality could be considered as the communication loads on edges. In a manner similar to

the single networks shown in Figure 2.5, disassortative edges between the networks could distribute communication loads in both SF-SF and RN-RN networks. All edges between networks connected high-degree nodes with low-degree nodes when networks were connected disassortatively. Therefore, communication loads were distributed to all edges between networks.

In contrast, topologies with larger ρ exhibited different and interesting properties when compared with those of single networks. First, edge betweenness centrality on the edges were more biased as ρ increased in single networks. However, a heavy communication load was assigned to edges with low-degree nodes in single assortative networks, as summarized in Table 2.1. In contrast, in interconnected networks, edges between the high-degree nodes carried a heavy communication load as shown in Tables 2.2-2.3 because those nodes were accessible to other nodes in each network. In Table 2.2, Only 5 out of 50 edges with the highest or lowest values of edge betweenness centrality are selected, whereas, In Table 2.3, only 5 out of 50 edges with the highest or lowest values of edge betweenness centrality are selected. Thus, features on node degrees of edges that possessed high edge betweenness centrality differed between single and interconnected networks. Another interesting property was that there was a sudden increase of edge betweenness centrality in the topologies with extremely high ρ. This was because the types of interconnecting edges were clearly separated into connection between high-degree nodes and connection between low-degree nodes. The ratio of increase in the edge betweenness centrality was more significant in SF-SF networks due to the power-law distribution of node degree. The relation between edge betweenness centrality and node degree is confirmed in Tables 2.2-2.3.

Robustness

With respect to the evaluation of robustness of interconnected networks, endpoint nodes of interconnecting edges were deliberately or randomly broken, and average hop length between networks was calculated. In this context, average hop length did not include paths between two nodes in the same network. Simulations of removal were executed 25 times with respect to each topology.

Figures 2.12–2.13 show the results, and it was observed that SF-SF and RN-RN networks exhibited almost identical tendencies. First, prior to checking the robustness, it was observed that the

Table 2.2: Relation between edge betweenness centrality and degrees of endpoints of the interconnecting edges in a SF-SF network.

Most disassortative ($\rho = -0.0054$)			Most assortative ($r = 0.012$)		
EBC	Network 1	Network 2	EBC	Network 1	Network 2
5.6×10^3	36	7	1.2×10^3	4	4
7.3×10^3	7	24	1.3×10^3	4	4
8.2×10^3	26	7	1.3×10^3	4	4
$9,2 \times 10^3$	22	7	1.4×10^3	4	4
1.0×10^4	7	22	1.4×10^3	4	4
			$\vdots$		
3.3×10^4	49	4	6.1×10^4	51	51
3.4×10^4	87	4	6.6×10^4	59	59
4.8×10^4	4	104	9.0×10^4	65	65
6.6×10^4	86	4	1.3×10^5	87	87
1.0×10^5	104	4	1.7×10^5	104	104

Table 2.3: Relation between edge betweenness centrality and degrees of endpoints of the interconnecting edges in a RN-RN network.

Most disassortative ($\rho = -0.036$)			Most assortative ($r = 0.037$)		
EBC	Network 1	Network 2	EBC	Network 1	Network 2
8.0×10^3	2	13	1.7×10^3	2	2
1.1×10^4	14	2	1.8×10^3	2	2
1.1×10^4	14	2	1.8×10^3	2	3
1.1×10^4	2	13	2.1×10^3	2	2
1.2×10^4	13	2	2.1×10^3	3	2
			$\vdots$		
2.8×10^4	3	12	3.2×10^4	13	13
3.0×10^4	13	2	3.3×10^4	13	14
3.1×10^4	2	17	3.3×10^4	13	14
3.3×10^4	2	13	3.7×10^4	17	13
4.1×10^4	3	12	4.3×10^4	15	15

average hop length decreased with topologies with high ρ. The main reason for this corresponded to the connections between high-degree nodes. As observed in the previous section, assortatively interconnected networks involve several connections of high-degree nodes that include a high communication load. Therefore, they contribute to a decrease in the average hop length.

With respect to the selective failure shown in Figure 2.12, assortative networks possess lower

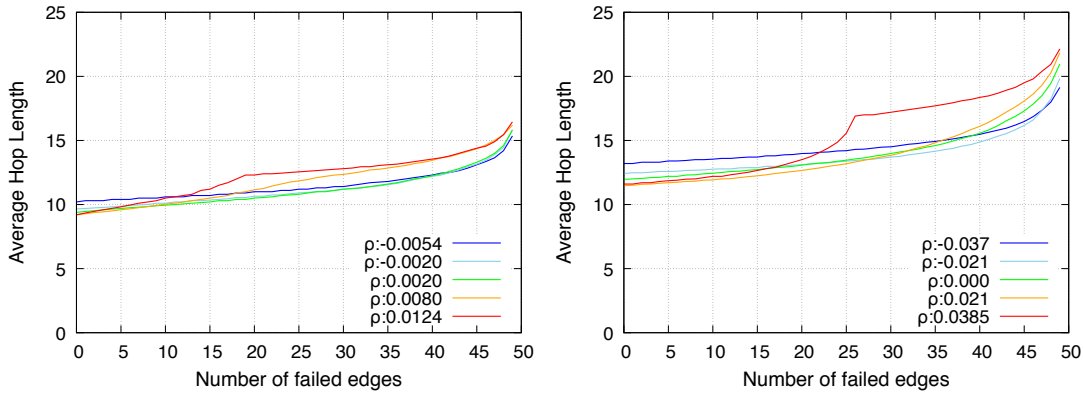

Figure 2.12: Change of average hop length against deliberate failure on endpoints of inter-connecting edges in SF-SF networks (left) and in RN-RN networks (right)

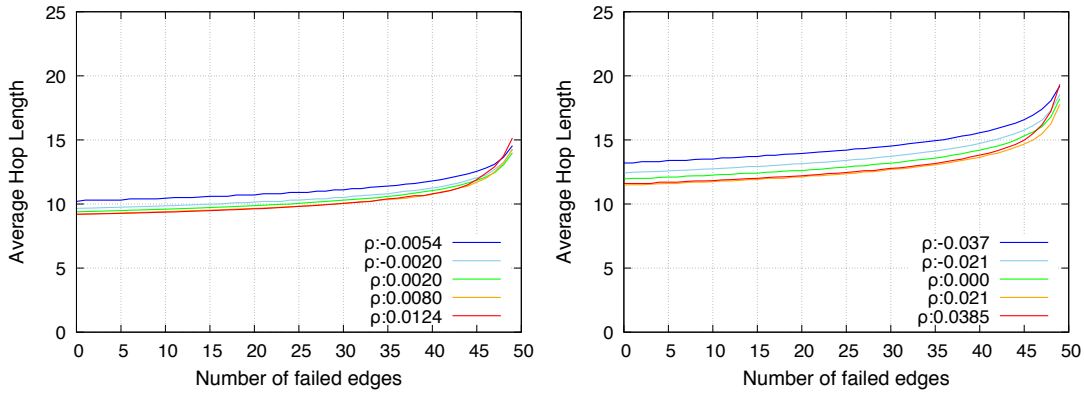

Figure 2.13: Change of average hop length against random failure on endpoints of inter-connecting edges in SF-SF networks (left) and in RN-RN networks (right)

average hop length, and are therefore initially efficient. However, subsequently as endpoint nodes were selectively removed, there was a performance reversal between assortative and disassortative networks. This could be attributed to the loss of connections between high-degree nodes. Conversely, as shown in Figure 2.13, the performance of average path length simply decreased while maintaining the order of assortativity.

In summary, as shown in Figure 2.14, topologies with low ρ were tolerant of both random and selective failure, while topologies with high ρ provided efficient average hop length and were tolerant of random failure albeit vulnerable to selective failure.

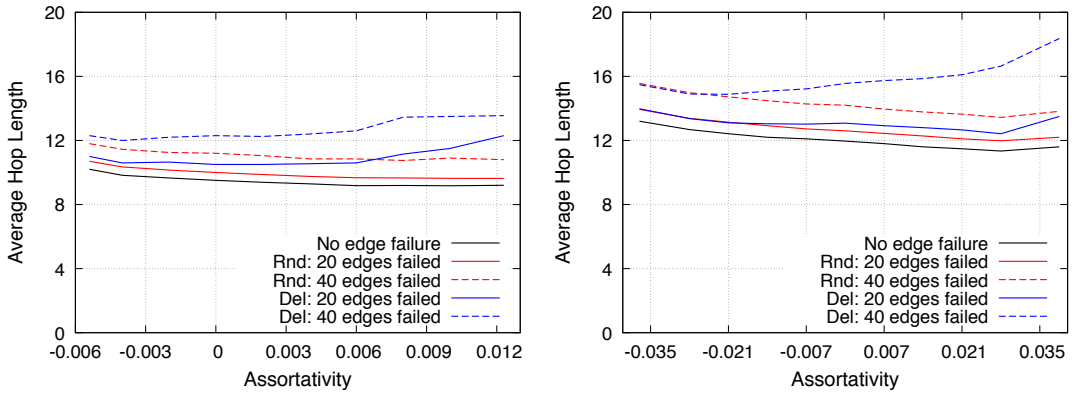

Figure 2.14: Relation between average hop length and assortativity between networks in SF-SF networks (left) and in RN-RN networks (right)

Information-diffusion Efficiency

Figure 2.15 shows the speed of information diffusion. Interestingly, SF-SF networks and RN-RN networks behaved differently. Assortative topologies spread information slightly faster in SF-SF networks. This was probably due to powerful highest-degree nodes termed as *hubs* in SF networks. However, a SF network itself constituted an efficient network with respect to information diffusion, and thus differences between topologies with different ρ were small. More interestingly, with respect to RN-RN networks, the efficiency of assortative and disassortative networks exceeded that of non-assortative networks. This could be because both assortative and disassortative interconnected networks involved edges with high-degree nodes, while non-assortative networks did not. Another interesting point was that although low assortativity led to a low performance in terms of average hop length, it also caused fast information diffusion. As summarized in Table 2.3, endpoints of edges in disassortative RN-RN network homogeneously contained high-degree nodes, and this property could help in the diffusion of information over all the nodes. These results indicated that information-diffusion efficiency could not be uniquely defined by assortativity between networks and instead depended on types of each network.

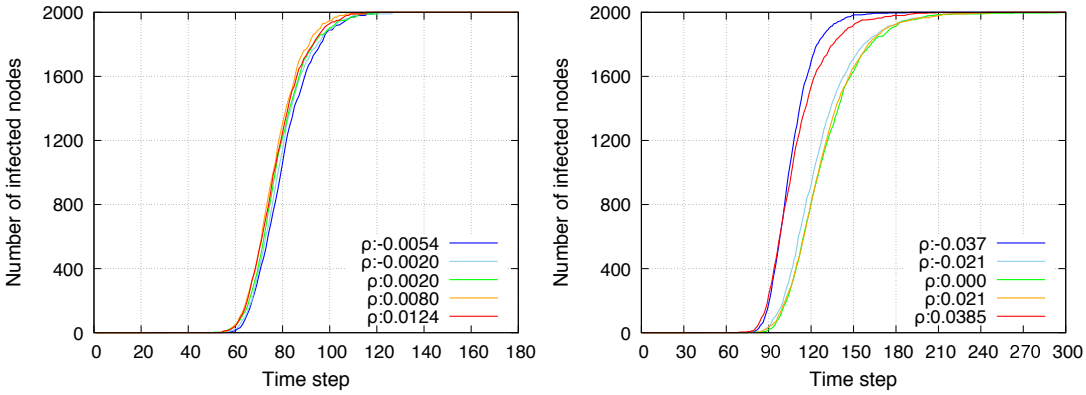

Figure 2.15: Information diffusion speed in SF–SF networks (left) and in RN–RN networks (right)

2.4 Discussion

2.4.1 Effect of Assortativity on Robustness and Efficiency

With respect to single networks, the results of the present study indicated that an increase in assortativity caused the following

1. High average hop count
2. High robustness relative to the failure of high-degree nodes
3. Low robustness relative to random node failure
4. Low efficiency of information diffusion
5. Concentration of communication loads on the edges connecting clusters

It should be noted that disassortative networks exhibited opposite features, i.e., a decrease in assortativity caused a low hop count, high information diffusion efficiency, and distribution of communication load. An intuitive explanation of the effects as detailed in the aforementioned points 1-5 was that high assortativity resulted in fewer shortcut links between high-degree nodes and low-degree nodes and formed a chain-shape network. It should be noted that extremely high assortativity led to fragile connectivity. The results indicated that the assortativity of a network should be within an appropriate range of values.

With respect to interconnected networks, the results revealed that an increase in assortativity led to the following:

1. Low average hop count
2. Low robustness against the failure of high-degree nodes
3. Normal robustness against random node failure
4. High efficiency of information diffusion
5. Concentration of communication loads on edges connecting hub nodes

In this case, disassortative networks exhibited opposite features with the exception of the efficiency in information diffusion (it also exhibited high efficiency). The results also indicated that the performance of assortativity between networks was based on the degree distribution of each network. For example, communication loads of interconnecting edges were considerably biased when networks possessed power-law of degree distribution. The range of assortativity was also influenced by the degree distribution. Thus, the fore-mentioned results characterized the relations among robustness, efficiency, and assortativity within a network.

2.4.2 Assortativity in Brain Networks

In the study, assortativity in interconnected networks was evaluated, and the effect of assortativity on robustness and efficiency was demonstrated. In this section, the results of the present study were compared with those related to the assortativity of human brain networks as obtained in our previous study. Here, we briefly summarize the result of the study. We used datasets of human brain networks from [37]. These datasets contain the weighted connections between the regions of interests (ROI) in a brain. The number of ROIs is 998. We used a threshold on the weight of connections to define an undirected edge between ROIs. We measured the average assortativity within the ROIs and the average assortativity between ROIs using the Louvain method [54] to identify the modular structure. Figure 2.16 show the results for assortativity within and between ROIs. With respect to within-module assortativity, human brain networks exhibited an assortative mixing pattern when

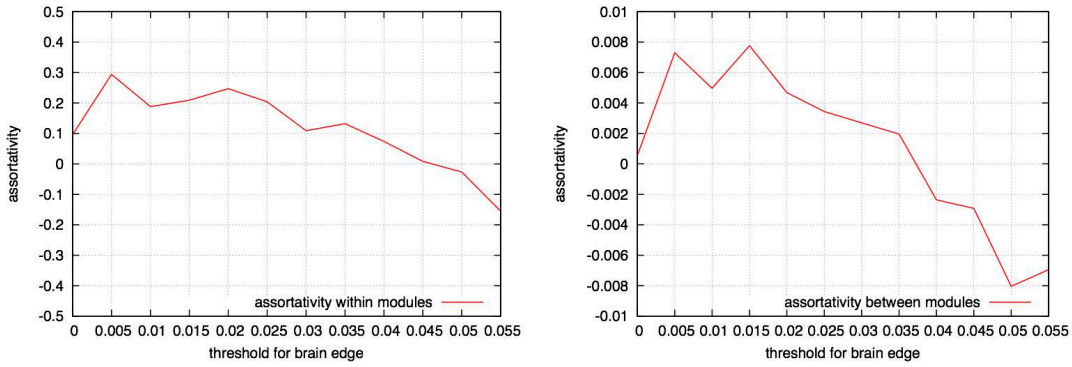

Figure 2.16: Average assortativity within ROIs (left) and between ROIs (right) in brain networks

weak edges were included, and this could indicate that weaker edges were important to robustness relative to node failure in the human brain, although they reduced the efficiency of communication. In contrast, strong edges exhibited a disassortative mixing pattern. This result indicated that the important edges in modules were connected such that the average hop length was reduced.

With respect to human brain networks, the network exhibited between-module assortativity when both strong and weak edges were included. This indicated that the human brain could communicate efficiently between modules. In contrast, modules were connected disassortatively when only strong edges were considered. This could facilitate concurrent processing between two modules. In order to design information networks, different values for assortativity were used based on the edge importance.

2.4.3 Information-Network Design with the Consideration of Assortativity

The effect of assortativity on the robustness and efficiency of interconnected networks was examined. The correlation of the assortativity with only the robustness and efficiency of a network were demonstrated previously, and thus assortativity could not be used to determine whether or not a given network was robust and efficient. However, it was important to discuss the construction of a new network such that it possessed good robustness and efficiency. Networks aimed at disseminating information should be constructed such that they possess low assortativity. In contrast, low assortativity was desirable to construct networks that could spread data quickly. Furthermore, when

multiple networks were integrated, the results indicated that the assortativity between networks could be adjusted to control the trade-off between efficiency and load balancing.

For an example, an ad-hoc network composed of IoT devices was considered as an application of the results of the present study. In this case, the entire network was composed of ad-hoc networks that were in turn composed of homogenous devices. The construction of an assortative network has various advantages in this case and include high robustness and good robustness with respect to computer-virus infections. This type of an assortative network also included disadvantages such as high average hop length and a concentration of communication loads. However, the average hop length of the network was not exceedingly high if the assortativity of the network was not too high. Thus, an appropriate setting for the assortativity is important.

A detailed method for constructing an assortative ad-hoc network is beyond the scope of this study. However, this could be achieved by selecting node deployment techniques and transmission-power control techniques. For example, nodes with similar degrees are likely to be connected when more nodes are arranged near the center of the field. Constructing shortcut links between nodes with similar degrees also contributed toward an assortative network and reflected cases in which nodes used directional beams or long-range omnidirectional transmission.

The following advantages were observed when networks were connected with each other assortatively. The connections between high-degree nodes reduced the average hop length. Connections between low-degree nodes improved the robustness relative to the failure of high-degree nodes. The type of network failures considered here reflected the depletion of electric power that resulted from the concentration of communication. Communication loads are distributed if networks are connected disassortatively.

2.5 Conclusion

In this study, the effect of assortativity on the robustness and efficiency of interconnected networks was examined. With respect to the assortativity of single networks, it was observed that an increase in assortativity caused (1) an increase in the hop count, (2) high robustness of connectivity with respect to the failure of high-degree nodes, (3) low robustness of connectivity with respect to random

node failure, (4) low efficiency for information diffusion, and (5) concentration of communication loads on a few edges. Simultaneously, these results implied that single disassortative networks involved opposite features. It was also observed that an increase in assortativity reduced the shortcut links in networks. Therefore, an excessive increase in assortativity harmed the network in terms of communication efficiency, robustness, and communication load on network links.

With respect to the assortativity between networks, the following results were observed: (1) a decrease in the hop count, (2) low robustness of connectivity with respect to the failure of high-degree nodes, (3) normal robustness of connectivity with respect to random node failure, (4) high efficiency with respect to information diffusion, and (5) concentration of communication loads on a few edges.

Additionally, it was observed that the performance of assortativity between networks depended on the degree distribution of each network. Although, the results of this study demonstrated the effect of assortativity on the robustness and efficiency of interconnected networks, the results were only applicable to networks involving the Barabási-Albert model and Erdös-Rényi random network model. The study also investigated assortativity in the case of networks with nodes of uniform degree. However, interconnected networks composed of networks with various degree distributions were not investigated, and this will be the subject of a future study.

The study also discussed methods to construct a network that was robust and efficient. In actual networks, various constraints affect the construction of assortative or disassortative networks. For example, with respect to ad-hoc networks of wireless sensor devices, it is necessary to consider the battery life of sensors and communication distances. This study did not propose a model to generate a network topology, and thus, a future study will include the proposal of a generation model for assortative or disassortative networks and the application in an actual network.

Chapter 3

Configuring Interconnectivity of Interconnected Networks with a Trade-off of Geometric Constraints and Performance

3.1 Introduction

Wireless sensor network (WSN) [55] refers to an ad hoc type of network that comprises spatially-distributed autonomous sensor devices. These sensor devices are connected to each other via a network, and they monitor the environment of a target area. Recent advancements in information and communication technology (ICT) has led to miniaturized and sophisticated sensor devices (e.g., low-power wide area (LPWA) networks [56, 57]), and WSNs are the foundational blocks for further advanced network systems, such as edge computing [58, 59] or fog computing [60, 61], which attract a great deal of attention for realizing the Internet of things (IoT) and cyber-physical systems (CPS) [5, 7, 62, 63]. In these scenarios, a number of ICT application services and other social infrastructure will be integrated and implemented on the Internet.

Virtualization techniques, such as network function virtualization (NFV) [64, 65], software defined networks (SDN) [66, 67], and network slicing [68, 69], have also been studied in combination with WSNs [70–74], and are considered key technologies to construct network systems for edge computing [75–78] and IoT [79–82]. A virtualized WSN (VWSN) is composed of two network layers: the infrastructure layer and the service layer (Figure 3.1). Multiple providers deploy physical network resources that can analyze the environment, collect and propagate data, and form IoT modules. Therefore, an infrastructure layer that comprises an interconnected structure of multiple IoT modules is realized. The service layer is virtually constructed by combining multiple IoT modules on this infrastructure layer, wirelessly connecting the edge servers, which process/transmit data and behave as gateways, based on millimeter-wave beam-forming techniques [83, 84]. In this scenario, the nodes in Figure 3.1 correspond to various types of IoT devices; some of them operate as endpoint nodes, which have the ability to serve as a representative nodes to communicate with the edge servers. The administrator of a virtualized service networks (VSN) operates edge servers and virtualized wireless connections among the IoT modules.

This virtualization architecture has several advantages for future IoT scenarios [70–72, 74]. For instance, even if the type of services to be implemented on the VWSN is not envisaged beforehand, administrators can construct the service layer for any purpose while flexibly reusing physical resources at relatively low costs. Second, virtualization in WSN can address the heterogeneity in the infrastructure layer, wherein diverse types of physical network modules are individually deployed by the infrastructure providers. In addition, separating infrastructure and service layers results in simplified operation and accelerated development.

VWSN architecture provides features that are conducive to the realization of IoT technology; however, no strategies have been proposed that efficiently generate virtualized topologies, wherein numerous networks are mutually interconnected. Virtualization techniques for the WSNs enable the administrators of the service providers to flexibly construct the VSN topologies [70, 71, 73, 74]. At the same time, the number of ICT services provided over the Internet has been skyrocketing, and their contents become more and more sophisticated [5, 7, 62, 63]. These situations demand frequent modification of the VWSN topologies: the administrators require addition/removal of network elements (i.e., nodes and links) on the existing VSNs, and the new VSNs will be constructed every time

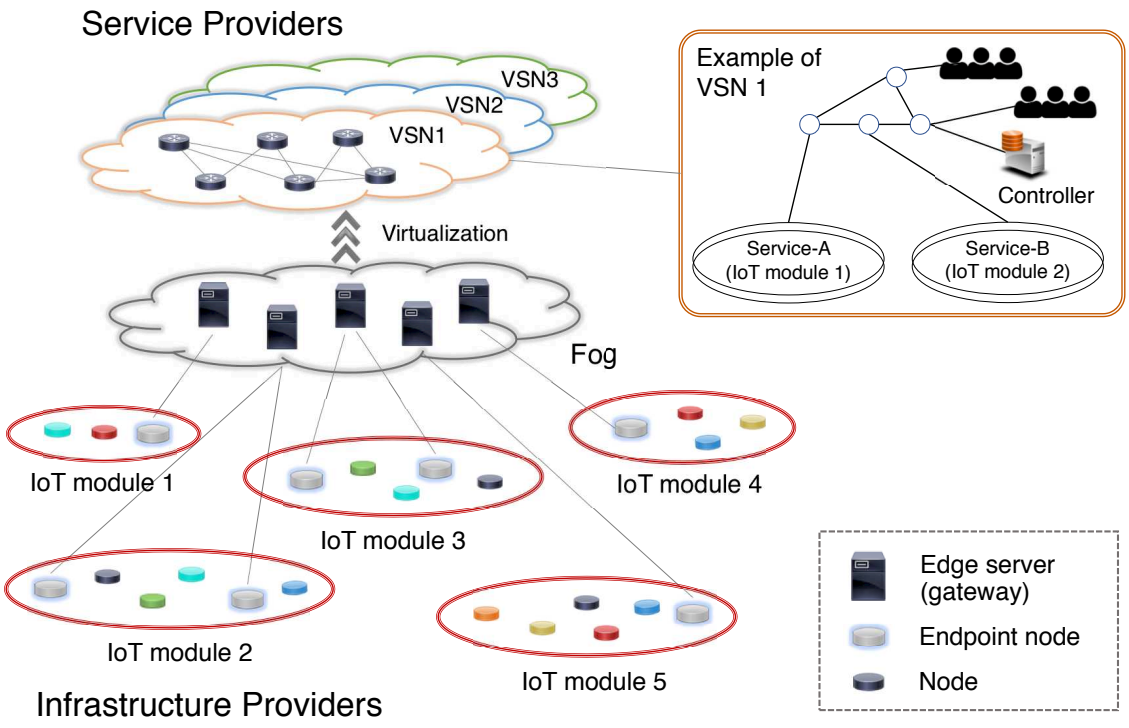

Figure 3.1: Architecture for virtualized wireless sensor networks (VWSNs).

a new service is launched. Furthermore, in the future, the Internet will be comprised of millions of interconnected IoT devices, and a substantial computational cost will be incurred when calculating the optimal topologies for the VSNs. Therefore, although optimizing topology shapes is virtually impossible due to the enormous number of devices and services, it is imperative to discover appropriate ways for constructing VWSN topologies that achieve a high level of performance, quick communication between any pair of nodes, high resilience against failures of network components, and low cost to sustain the wireless connectivity, prior to the determination of the optimal shape of topologies.

In recent years, the application of human brain networks in the engineering field has attracted significant research attention because brain networks possess excellent characteristics that have been optimized through the process of evolution [16, 17]. However, studies that have discussed the application of brain networks to information networking systems, particularly for the aforementioned modularly interconnected networks, are limited.

Remarkable advances of graph-theoretic analysis in neuroscience (e.g., functional Magnetic Resonance Imaging (fMRI)) have revealed that the modular structure of brain networks enables them to contain tens of billions of neurons, which can help a brain network adapt itself for a wide variety of tasks [16]. The inter-modular connectivity also enables the highly reliable information processing system of the brain, while optimizing the tradeoff between performance and metabolism [85]. Therefore, brain networks are considered to have fundamental characteristics that are necessary for designing an interconnected network of VWSNs. In this study, we investigate the relationship between the performance of information networks and the shape of the network topology based on recent findings in the field of neuroscience. In particular, we attempt to answer the following questions: *"which pair of modules should be connected by inter-modular links?"* and *"which nodes within modules should be selected as endpoints of these inter-modular links?"*.

First, we focus on the exponential distance rule (EDR) [85], which is a network model based on the modular connectivity in the cerebral cortex of a mammalian brain. The cerebral cortex is divided into multiple regions based on the local functional roles of those regions. The EDR model can reproduce the connectivity structure among those regions in the brain—the neural links among the areas are created based on a probability function that exponentially decays with inter-areal distance. In [85], Ercsey et al. showed that network topologies generated using the EDR model are similar to the topologies obtained from the fMRI experiments in terms of graph-topological features. The EDR model also explains how the human brain optimizes performance by considering the metabolic cost and inter-modular link length. In our previous work [24], we proposed a method to construct a VWSN topology and evaluated the performances regarding communication efficiency and wiring costs. In this study, we further reveal the performance of robustness against network failure, in relation to the communication efficiency and wiring costs.

However, the EDR model does not consider the endpoints of inter-modular links; therefore, this study accounts for the assortativity, which is defined as the correlation of node degrees in networks. Node degree is among the simplest and the most common centrality measures, and is used for measuring nodal importance on a network topology. In a network with high assortativity, a pair of nodes is likely to be interconnected if the two nodes have a similar node degree. By contrast, in networks with low assortativity, any two nodes are connected if they have a dissimilar

node degree [40]. As for the brain network, which is composed of multiple modules, assortativity can indicate different behaviors depending on whether the focus is on the connections between the modules or within the modules as well as depending on whether the connections between the modules are strong or weak. High reliability of brain networks can be attributed to the topological connectivity, which is based on the assortativity between and within network modules [22, 86].

The objective of this study is to design inter-modular network topologies for a VWSN that are robust against environmental changes and provide high communication efficiency at relatively low wiring costs. For the construction of the objective topology, we first assign links between modules based on our proposed method [24]. Second, by taking assortativity into account, we propose a method to assign inter-modular links on nodes within modules. The effects of the EDR model and assortativity can be controlled by a single parameter for each. Evaluation results reveal that the configuration of these two parameters is of critical importance to the performance: small communication delay between nodes, high robustness against network component failures, and low cost for constructing a VWSN topology. Therefore, the results of this study will guide future studies on the construction of inter-modular network topologies for VWSN that can realize high performance at relatively low wiring costs.

3.2 Related Work

3.2.1 Modular Human Brain Networks

The human brain can be regarded as a complex network comprising neuronal cell bodies that reside in the cortical gray matter regions joined by myelin-insulated axons. Recent advancements in neuroimaging techniques have enabled the analysis of the human brain at higher spatial resolutions. Previous studies have examined the structural network of the brain as represented by anatomical connections among the regions of interest [87–89].

To the best of the authors' knowledge, small-world and scale-free properties have been studied as main characteristics of brain networks [87–90]. Therefore, existing studies have not focused on

other topological properties of brain networks such as the hierarchical modular structure. Hierarchical modularity is considered to be associated with sparseness, robustness, transmission of signals, maintenance of dynamic activity, and adaptive evolution [17, 91, 92]. In other words, the modular structure is closely associated with the performance of the human brain, including robustness, communication efficiency, scalability, and metabolic cost. In this study, we focus on the similarity between the brain networks and information networks, and apply structural properties of brain networks to construct VWSN topologies with high performance.

Cerebral Cortical Inter-Modular Connectivity Model

Brain networks have recently been investigated from a topological viewpoint of complex networks. Moreover, previous studies have revealed the structure of brain networks in terms of small-world or scale-free properties. Although network models based on these two properties can generate topologies with characteristics found in brain networks (e.g., high modularity and low hop count), they do not consider the geometrical constraints [93]. Regarding the connectivity in brain networks, geometrical constraints should be considered because the metabolic cost of connecting two neurons increases with increasing length of the axons (i.e., physical distance between the neurons). Connecting distant neurons accelerates the information integration process in brain networks. However, long connections can add to the metabolic costs. In other words, we can conjecture that the connectivity structure of brain networks, i.e., the trade-off between metabolic cost and communication efficiency, has been optimized through the evolutionary process [94]. Regarding information networks, reducing the costs incurred owing to communication distances is necessary for both the wired and wireless networks. Long communication distances require higher wiring costs for the laying of physical cables for wired networks, and higher transmission power to overcome signal attenuation and interference in the case of wireless networks. At the same time, long connections are necessary for quick information transmission and robust connectivity.

Ercsey et al. proposed a novel network model [85] called the EDR model that is based on the neural connectivity in the cerebral cortex of the macaque monkey. When analyzing the neural

connectivity, the entire macaque cortex was divided into 91 regions of interest, i.e., areas of neurons with similar functions. The nodes in the resulting network topology represent each cortical area. In the process, 29 of the spatially distributed 91 cortical areas are selected such that the subgraph of the 29 areas can completely estimate the connectivity for the entire network. Retrograde tracer injections into those 29 areas revealed that 6,494,974 neural links and 1615 inter-areal links were present. The analysis revealed that the existence probability $p(d)$ of inter-areal connections exponentially decays with the inter-areal distance, which can be represented as follows:

$$p(d) = c \exp(-\lambda d), \tag{3.1}$$

where c denotes the normalization constant, d is the inter-areal distance, and λ is a parameter. For the approximation of the cerebral connectivity, $\lambda = 0.180\,\mathrm{mm}^{-1}$ is used in the EDR model [85]. It should be noted that links in the resulting topology are assigned weights corresponding to multiple neural connections between the areas. Given the trade-off between metabolic cost and performance, pairs of neurons that are in close proximity tend to have a higher number of connections; in addition, a few long-distance connections are present to accelerate information integration. Even though the EDR model is a relatively simple model that is controlled by only a single parameter λ, it can sufficiently reproduce various properties of topological connectivity in the cerebral network, such as communication efficiency, distribution of cliques, eigenvector spectra, and presence of a core structure [85].

Assortativity in Human Brain Networks

Assortativity, which indicates the correlation of node degrees, is a common characteristic that is used for the evaluation of complex networks. High assortativity implies that nodes are preferentially connected if their degrees are similar. By contrast, in the case of low assortativity, nodes of different degree are likely to be connected. Newman [40] proposed the concept of *global assortativity* to measure the assortativity of an entire network. In addition, *universal assortativity* was introduced to evaluate the assortativity of any part of a network [46]. This universal assortativity was also used to define the assortativity between networks in our previous work [22].

In [40], Newman proposed a method to measure the assortativity of a network topology by using the *global assortativity coefficient*. The global assortativity coefficient is calculated based on the remaining degree distribution $q(k)$, as follows:

$$q(k) = \frac{(k+1)p(k+1)}{\sum_j jp(j)}, \tag{3.2}$$

where $p(k)$ is called degree distribution, which denotes the probability that a randomly selected node has node degree k; $q(k)$ is referred to as the remaining degree distribution, which denotes the probability that either endpoint nodes of a randomly selected link have the remaining degree k. Here, the remaining degree of a node refers to the ordinary node degree minus the node itself. The global assortativity coefficient r is defined as follows:

$$r = \frac{1}{\sigma_q^2}\Big(E[(J-U_q)(K-U_q)]\Big), \tag{3.3}$$

where J and K denote variables of the remaining degree; both have the same expected value $U_q = \sum_j jq(j)$. The term $\sigma_q^2 = \sum_l j^2 q(j) - \Big(\sum_k kq(k)\Big)^2$ denotes the variance of the remaining degree distribution $q(k)$. The positive and negative values of r imply that a network is assortative and disassortative, respectively. When r tends to zero, the network becomes non-assortative; the shape of a network becomes similar to that of a random network. Theoretically, the range of feasible values of r is $[-1, 1]$; however, its range is rendered smaller due to the degree distribution.

Then, the *universal assortativity coefficient* ρ_l on a link l can be introduced, given $q(k)$. This coefficient corresponds to the contribution of an individual link to the global assortativity coefficient r. Therefore, ρ_l is defined as follows:

$$\rho_l = \frac{(j-U_q)(k-U_q)}{M\sigma_q^2}, \tag{3.4}$$

where j and k denote the remaining degrees of the two endpoints of link l. Here, M denotes the total number of links in the network. Then, the universal assortativity coefficient ρ can be defined

as follows:

$$\rho = \sum_{l \in S} \rho_l = \sum_{l \in S} \frac{(j - U_q)(k - U_q)}{M\sigma_q^2}, \tag{3.5}$$

where S denotes a set of links between modules. The assortativity between networks is determined using Equation (3.5). It can be said that the universal assortativity ρ is a part of global assortativity r. Hence, ρ is equal to r when S corresponds to all the nodes between modules. When $\rho_l > 0$, the link is called an assortative link; when $\rho_l < 0$, the link is called a disassortative link. A link with $\rho_l = 0$ has no correlation.

With respect to human brain networks, it has been shown that the connectivity between modules exhibits assortative mixing when both strong and weak connections are considered [22]. Therefore, it can be inferred that the assortative connections facilitate communication between modules in the human brain. In contrast, when only strong links were considered, inter-modular connectivity showed disassortative mixing, which can accelerate concurrent and robust processing between two modules.

3.3 Method to Construct a VWSN Network Topology

Virtualization in WSN is expected to play an important role on the IoT scenario [70–74], as explained in Section 3.2.1. It has enabled the construction of a VWSN topology over distributed wireless network resources with high flexibility and efficiency. In this study, we assume that a VWSN network is composed of two layers: *physical layer* and *virtual layer* (see Figure 3.2). On the physical layer, the physical network resources are deployed and connect to each other, and form heterogeneous network modules. Subsequently, the modules on the physical layer virtually connect to each other via wireless connections of inter-modular links between gateways (edge servers) and form the virtual layer. Regarding the assignment of endpoints of inter-modular links, all the nodes on the physical layer cannot behave as endpoints in a practical sense because the performance or role of the devices differ from each other. However, in this evaluation, we assume that all nodes have the ability to serve as an endpoint node. Therefore, our objective is to reveal the type of nodes that should be represented as an endpoint node from a topological viewpoint.

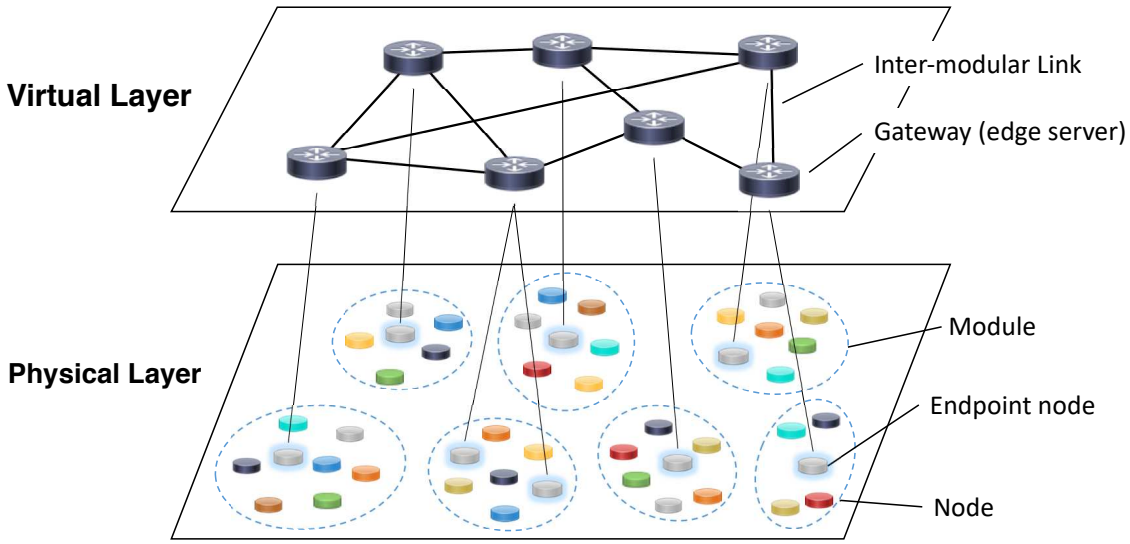

Figure 3.2: Architecture for virtualized wireless sensor network.

In the following subsections, the proposed method for constructing the topology of the virtual layer for the VWSN network architecture is described. First, the EDR model is modified and utilized to control the deployment of inter-modular links. Then, assortativity is applied to determine the assignment of endpoints of inter-modular links on nodes in the modules.

3.3.1 Physical Layer Assumption

Let us assume a simple network as the physical layer, which consists of multiple WSN modules. First, the given square area with a side length of E is divided into M smaller evenly sized squares. Each area has the same number of $N' = N/M$ nodes, and, in total, N nodes are deployed on the entire square region. Although there are many other possible ways to deploy modules, the aforementioned deployment sufficiently achieves our objective, which aims to reveal the relation between the performances and the geometrical distance.

The node degree distribution in each module is configured such that it follows a Gaussian or power-law distribution, which are commonly observed in topologies of complex networks [95]. L_{intra} links are deployed inside each module to form a connected topology. An intra-modular link does not have a direction or weight. Here, we assume that a gateway node is located at the

geometrical center of each module.

3.3.2 Virtual Layer Construction

In this model, the distance between any two modules is calculated based on Euclidean distance between the coordinates of the gateways. We assume that modules are wirelessly interconnected through these gateway nodes according to the probability function in the EDR model, thus forming inter-modular links. In this manner, the virtual layer is constructed. A certain number of L_{inter} inter-modular links are deployed on each network. Each inter-modular link does not have a direction or weight, but a pair of modules can have more than one inter-modular link.

For creating inter-modular links, we redefine Equation (3.1) as Equation (3.6) such that the variable and the parameter in the EDR model can be adapted to any scale of network topologies other than the cortical inter-areal connectivity:

$$p(d_n) = \exp\left(-d_n/\alpha\right), \tag{3.6}$$

where d_n denotes the relative distance between two modules. That is, $d_n = d/d_{max}$, where the actual Euclidian distance d is divided by the largest distance of all the pairs of modules d_{max}. Regarding the control parameter, λ is replaced in Equation (3.1) by a new parameter $\alpha = (\lambda d_{max})^{-1}$. The normalization constant c used in Equation (3.1) is eliminated because a predetermined number of inter-modular links are generated. Thus, $p(d_n)$ can be regarded as a probability function that generates inter-modular links between any two given modules.

When generating the virtual layer, the following process is repeated until the predefined number L_{inter} of inter-modular links are generated: (i) randomly choose a pair of modules; and (ii) probabilistically generate an inter-modular link according to $p(d_n)$. In our proposed method, more than one inter-modular link can be assigned to a pair of modules because of the presence of multiple nodes in each module. Thus, after the deployment of inter-modular links, the endpoints of inter-modular links are assigned to nodes in the modules.

Figure 3.3 shows the topologies generated using the procedure mentioned above. The circles represent modules, and the lines indicate the inter-modular links. The width of an inter-modular link

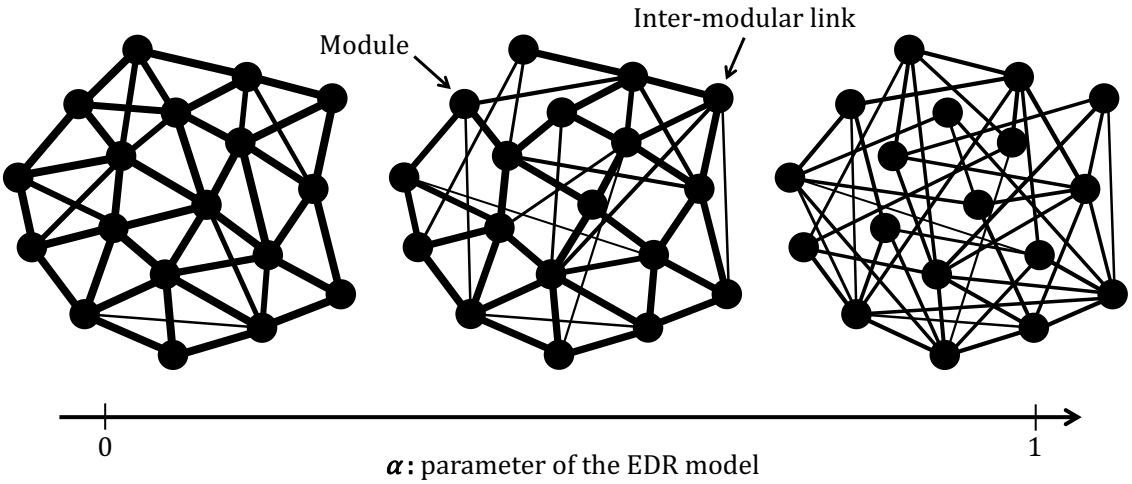

Figure 3.3: Relationship between parameter α and the topological shape.

corresponds to the number of links that exist between pairs of modules. As shown in Figure 3.3, when α is small, the inter-modular links are preferentially assigned to pairs of modules in close proximity. As α increases, the limitation on generating shorter inter-modular links is softened, and randomness on the connectivity increases.

3.3.3 Assigning Endpoints of Inter-Modular Links

As described in the previous subsection, inter-modular links are deployed among modules on the virtual layer. This subsection discusses the procedure to assign endpoints of inter-modular links to nodes from the viewpoint of node assortativity. That is, the endpoint nodes are chosen such that a specified value of assortativity ρ in Equation (3.5) is achieved on inter-modular connectivity for each pair of modules. By using this assignment scheme, the pairs of endpoints on which inter-modular links already exist are excluded. To obtain a suitable inter-modular connectivity that achieves a specified value of assortativity, the inter-modular links are repeatedly rewired. This process is performed stochastically by using the following procedure:

1. Two modules are randomly connected via a predetermined number of inter-modular links when constructing the virtual layer. Note that a pair of endpoint nodes does not have multiple edges.

2. The assortativity between the modules ρ is calculated. If ρ corresponds to the target value, then the set of connections at this point is retained. Otherwise, the following steps are executed.

3. An existing link between the modules, whose assortativity is farthest away from the target value, is deleted. If the current assortativity ρ is higher than the target value, the most assortative inter-modular link is selected, and vice versa.

4. A new link is created on two nodes in two different modules. The pair of nodes are randomly selected under the condition that the new link can move the assortativity ρ closer to the target value. Then, go back to Step 2.

The typical patterns of inter-modular connectivity corresponding to different values of the universal assortativity coefficient ρ are shown in Figure 3.4. When $\rho > 0$, the two nodes with similar node degrees are chosen as endpoints of links; thus, a pair of high-degree nodes or low-degree nodes is connected. It should be noted that, even if a pair of nodes has a similar node degree, the two nodes with the average node degree are not preferred because they do not wield significant influence, as indicated by Equation (3.5). On the other hand, when $\rho < 0$, a pair of two nodes with dissimilar degrees is assigned an inter-modular link. As ρ approaches to zero, the endpoint nodes for inter-modular links are more randomly chosen.

Figure 3.5 shows two example networks generated from the procedure above, where each link is unweighted and undirected.

3.4 Simulation Results

Extant research has studied the architecture for VWSN [70–74], but concrete strategies have not been investigated so far for constructing network topologies of the VWSN that satisfy various demands requested by the service providers. Since an enormous number of IoT devices and countless types of application services are deployed over the VWSN system, we consider that constructing the topologies focusing on basic topological nature is more essential than assuming a certain application service or traffic type. Therefore, our proposed method focuses on two points regarding topology

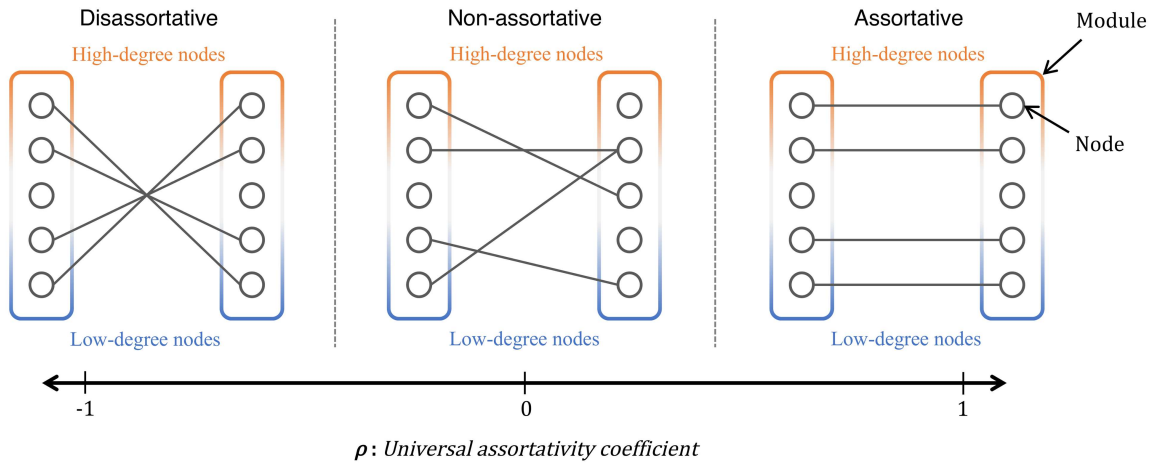

Figure 3.4: Relationship between universal assortativity coefficient and inter-modular connectivity.

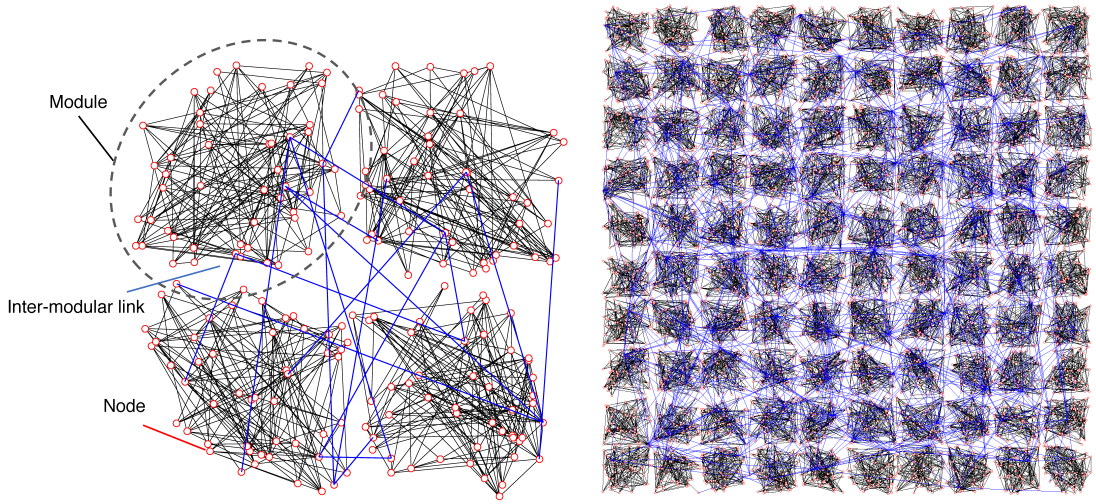

(a) Network of 4 modules

(b) Network of 100 modules

Figure 3.5: Examples of interconnected networks.

construction for VWSN: assigning inter-modular links among modules based on the EDR model, and assigning endpoints of those inter-modular links on nodes based on network assortativity.

In this section, we present the results from computer simulations and discuss the performance of the VWSN topologies constructed using the proposed method in comparison with other conceivable network models. First, multiple networks are generated and connected with each other, thereby generating a VWSN topology. Then, several types of simulations are performed on the VWSN

topologies, and their performance is measured in terms of communication efficiency, robustness, and network construction cost. The performance of the proposed method is evaluated relative to the performance of other comparative models.

3.4.1 Simulation Environment

First, we describe the computer simulation environment. This subsection describes the network models other than the EDR model that are used to assign links within and between modules. In addition, we also define the metrics to evaluate communication efficiency, robustness, and network construction cost. We also explain specific parameter settings for constructing the VWSN topologies for the computer simulations.

Metrics

In this work, we study the influence of connectivity among modules on the performance of the system in terms of communication efficiency, robustness, and wiring cost. The metrics used for the evaluation of the performance in computer simulations are described as follows.

Communication Efficiency To evaluate the communication efficiency of the VWSN topologies in terms of information transmission, we perform a packet routing simulation. We measure the time required for a data packet to pass from a source node to a destination node. In the realistic scenario for the IoT that is realized by the edge computing techniques, data collected and analyzed by the physical resources are passed to the edge servers. Then, the data are not uploaded to the cloud or the Internet side but the edge servers process by themselves in the edge computing scenario. When the data are proceeded and transmitted over the edge servers to the objective IoT module, they are delivered to the destination node. In the simulation, the packet routing is initiated at an arbitrary node, and the destination is also set on another arbitrary node. The packet is delivered according to the optimized path that minimizes the delay explained in the next paragraph. When a node receives a packet, the packet is forwarded to one of its neighbors that is included in the optimized path. The routing process is terminated when the data packet arrives at the destination node.

We conduct two types of packet routing simulation to measure the *service delay* and the *propagation delay*, respectively. At each instance that a packet arrives at a node, a service delay occurs according to an exponential distribution with service rate $\mu = 1/D\,\mathrm{s}^{-1}$. Furthermore, we assume that the propagation delay is D s per 100 m over the inter-modular links. These two types of delay are defined such that, on average, the service delay on a node is equal to the propagation delay over a 100 m link. We assume D to be an arbitrary value because the value does not affect the simulation results in this study. The packet routing simulation, which focuses on the service delay, indicates how the hop count between two arbitrary nodes changes when the inter-modular connectivity is configured. On the other hand, the propagation delay indicates the change in the average route length in a given network topology.

Robustness Robustness was evaluated by using algebraic connectivity [96]. Algebraic connectivity is a numeric value determined for a network topology from a graph-theoretical viewpoint. Fiedler et al. defined algebraic connectivity as the second smallest eigenvalue of the Laplacian matrix that is obtained from a network topology. It is well known that algebraic connectivity corresponds to the lower bound of both node connectivity and edge connectivity. The increase in algebraic connectivity leads to high robustness against node and link failures in the network topology because of the existence of multiple disjoint paths. In other words, a topology with high algebraic connectivity remains connected even if many nodes or links are removed [97–100].

Although there exist some other possible methods for evaluating the robustness of a network topology, in this study, we used algebraic connectivity because of the following advantages: (i) it does not depend on any parameter; (ii) it can uniquely specify robustness from just the shape of the network topology; and (iii) it can be calculated easily. Although the packet routing simulations for communication efficiency used in this study assume that bandwidth and network resources are sufficiently allocated and we do not consider network congestion, the metrics for robustness based on algebraic connectivity can indicate the degree of congestion in connection with the communication efficiency. When a generated VWSN topology shows high algebraic connectivity, the traffic can be distributed over many disjoint paths, and vice versa.

Wiring Cost We define the wiring cost to assume the required cost for deploying the wireless inter-modular links among the gateways on the virtual layer. Given that we focus on wireless networks and cost arises from geometrical constraints in this study, the wiring cost is calculated as the sum of squares of the lengths of all inter-modular links based on the Friis transmission equation [101]. This equation predicts that the energy consumption for a wireless signal transmission increases with the square of the distance between transmitter and receiver. We exclude links within modules in the simulations because we do not change the intra-modular connectivity when evaluating the performance of the VWSN topologies.

Network Models for Connectivity within Modules

Here, we describe the network models used to configure the connectivity within modules and between modules, respectively. First, we configure the connectivity patterns within modules. The effect of physical distance is considered to be negligible because the evaluation area for each module is considered to be sufficiently small. In this study, we focus on two types of common network models to determine the connectivity inside a module: the Barabási–Albert (BA) model [52] and the Erdös–Rényi (ER) model [102]. The BA model generates topologies whose degree distribution follows power-law, and, likewise, the ER model for Gaussian distribution. Both of the degree distributions are commonly observed in information networks.

Erdös–Rényi (ER) Model The ER model belongs to a class of random network models [102]. The degree distribution of the ER model follows a Gaussian distribution that is similar to the distribution observed in WSNs [103–105]. For the construction of networks based on the ER model, we randomly choose a pair of nodes and connect them until the total number of intra-modular links is L_{intra}.

Barabáshi–Albert (BA) Model The second type of networks corresponds to the BA model [52], which has been studied extensively as a class of complex networks. The BA model follows a power-law degree distribution and is characterized by the existence of extremely high-degree nodes (i.e., hub nodes) and a core cluster comprising hub nodes (i.e., rich-club). These characteristics

are often observed in the real-world networks, such as airline networks, social networks, and the Internet. Thus, the BA model is commonly used in the field of information networking to generate Internet-like topologies.

For the topology construction, we first select a small set of nodes to generate an initial full-mesh topology, which is referred to as a seed. Then, we repeatedly add nodes to the seed. After the addition of a new node, m nodes of the existing topology are probabilistically chosen and connected to the new node via a link. The probability that the node i is chosen from the existing topology is given by $p_i = k_i/\Sigma_j k_j$, where k_i denotes the degree of node i and $\Sigma_j k_j$ denotes the total degree of the existing topology; m is chosen such that almost the same number of intra-modular links (L_{intra}) are generated.

Network Models for Connectivity between Modules

After generating the connections in modules, the network models for generating links between modules are described. In addition to the proposed EDR model, the short-link model and the long-link model are described, which consider the physical distance between modules. We also prepare the ER model as a null model. In contrast with the connectivity within modules, wherein the physical distance is not considered, the short-link and long-link models are used to compare the performances from the viewpoint of physical distance. Another point of difference from the intra-modular connectivity is that any pair of modules can have more than one link, whereas a pair of nodes inside the modules can have at most one link. This is because, even when a pair of modules has multiple links, each link can be assigned to different nodes inside both of the modules.

It should be noted that the following models can determine the pair of modules having inter-modular links; however, they do not consider the nodes in modules that behave as the endpoints of these inter-modular links. Hence, we also use assortativity for determining the endpoints of the inter-modular links, as described in Section 3.3.3.

Exponential Distance Rule (EDR) Model Following the probability function $p(d_n)$ in Equation (3.6), a pair of modules is repeatedly chosen and an inter-modular link is generated between this pair. The procedure is terminated when the total number of inter-modular links reaches L_{inter}.

Erdös–Rényi (ER) Model We use the ER model to assign inter-modular links among modules to study the difference between our proposed model and a random model; the approach used is similar to the generation of links within modules. It should be noted that a pair of modules can have more than one link.

Short-Link (SL) Model A network topology based on the SL model is composed of only links shorter than a threshold R_{short} (in meters). We define this model for comparison with the EDR model and observe the difference in the performance if an inter-connected network does not contain long links. When constructing a topology, we randomly choose a pair of modules, generate a link if the distance is shorter than R_{short}, and repeat this process until L_{inter} links have been generated.

Long-Link (LL) model We define the LL model similar to the SL model by creating a topology with links longer than a threshold R_{long}.

Parameter Settings

Table 3.1 shows the list of parameters configured during the construction of VWSN topologies. Each row contains a variable, description, and values for each parameter.

In the computer simulations, we assume that VWSN topologies are constructed on an $E \times E\ \mathrm{m}^2$ square area and N nodes are deployed as physical nodes. The area is divided into M smaller regions in a grid pattern, and each area contains an equal number of $N' = N/M$ nodes. The physical nodes in an area are inter connected via L_{intra} links, and form a module on the physical layer. The value for L_{intra} is assumed such that a node corresponds to three intra-modular links. Then, the M modules are connected by L_{inter} inter-modular links to form the virtual layer. The details of the values of L_{inter} are provided in the following sections. Regarding the connectivity between modules, the parameter α controls the inter-modular connectivity of a topology based on the EDR model, and the parameter ρ controls the inter-modular assortativity of a pair of modules. R_{short} and R_{long} limit the length of links when constructing VWSN topologies based on the SL model and the LL model, respectively.

The values for parameter settings differ for each type of simulation, from Sections 3.4.2 to 3.4.4. Thus, the detailed values are described for each evaluation.

Table 3.1: Parameter description.

Variable	Description	Values for Section 3.4.2	Values for Section 3.4.3	Values for Section 3.4.4
E	Length of the side of evaluation area	100 m	500 m	500 m
N	Number of nodes	200	5000	5000
M	Number of modules	4	100	100
N'	Number of nodes in each module	50	50	50
L_{intra}	Number of intra-modular links	150	150	150
L_{inter}	Number of inter-modular links	30	300	300
ρ	Parameter of inter-modular assortativity (Eq. (3.5))	$variable$	$\rho_{min},\ \rho_{zero},\ \rho_{max}$	$\rho_{min},\ \rho_{zero},\ \rho_{max}$
α	Parameter of the EDR model (Eq. (3.6))	-	$[0.025,\ 0.8]$	$0.025,\ 0.1,\ 0.8$
R_{short}	Upper limit of link length for the SL model	-	-	10 m
R_{long}	Lower limit of link length for the LL model	-	-	20 m

3.4.2 Basic Property of Assortativity on 4-Module Networks

First, we conduct computer simulations using small-scale VWSN topologies. This subsection focuses on the assortativity of intra-modular connectivity and evaluates its influence on communication efficiency and robustness. In other words, before considering which pair of modules should have inter-modular links, we determine the nodes within the modules that should be assigned as endpoints of inter-modular links. Therefore, we do not consider the physical distance when evaluating the performance, and neither do we apply network models for connectivity between modules, as described in Section 3.4.1.

The parameter settings are shown in Table 3.1. A VWSN topology is composed of $M = 4$ modules, as shown in Figure 3.5. Each pair of modules is equally assigned five inter-modular links, and a VWSN topology has $L_{inter} = 5 \times 6 = 30$ inter-modular links given that there are ${}_4C_2 = 6$ possible combinations for connecting two out of four modules. The possible range of inter-modular assortativity for a VWSN topology is determined by the network models used for connectivity within the modules. Assortativity in the ER model varied from -0.05 to 0.05, whereas, in the BA model, it varied from -0.04 to 0.1. This difference is indicative of the fact that the distribution of node degree was more strongly biased in the BA model. In other words, the number of high-degree

nodes was lower in the BA model, and, thus, such nodes were rarely connected to other nodes of the same degree, thereby decreasing assortativity. In Fig. 3.6, (min, max) corresponds to $(-0.05, 0.05)$ and $(-0.04, 0.10)$ for the ER and BA models, respectively.

Robustness

Figure 3.6a shows the algebraic connectivity for the ER model and the BA model. The y-axis represents algebraic connectivity, and the x-axis represents intra-modular assortativity. Regarding the x-axis, we unite the different assortativity ranges of the ER and BA models to compare the performance more clearly. Each figure is the compilation of the results from 100 computer simulations, thus enabling the generation of a VWSN topology and measurement of the algebraic connectivity. As explained in the section above, high algebraic connectivity indicates that the network topology is robust against node and link failures.

Regarding the ER model, VWSN topologies with non-assortative or slightly assortative inter-modular connectivity exhibit higher robustness. It can also be said that assortative connectivity is a better indicator of high robustness than disassortative connectivity. These characteristics are closely associated with the degree of endpoint nodes of inter-modular links. When a topology is assortative, the nodes of similar degree are connected with each other. On the other hand, in a disassortative topology, the nodes tend to be connected if the degree is dissimilar. Therefore, all inter-modular links of a VWSN topology of disassortative connectivity have a high-degree node on one side, and a low-degree node on the other side. A low-degree node is located on the periphery of its module, and all the inter-modular links of a disassortative topology do not contribute to the creation of disjoint paths among nodes. This characteristic can explain why a disassortative topology exhibits the lowest robustness. Regarding an assortative topology, one half of the inter-modular links connect two high-degree nodes, and the other half connect two low-degree nodes. In contrast, in the non-assortative topology, endpoints for inter-modular links are randomly chosen. From the result in Figure 3.6a, we can conclude that inter-modular links of two low-degree nodes in an assortative topology offset the benefit of links between high-degree nodes, and random connectivity between

modules is preferred in terms of generating much more disjoint paths in a VWSN topology. Therefore, non-assortative topologies exhibit the highest robustness, followed by assortative topologies and disassortative topologies, in that order.

On the other hand, for the BA model, high assortative inter-modular connectivity of a VWSN topology is directly associated to a higher level of robustness. This interesting characteristic may be attributed to the small fraction of nodes contributing to high-degree nodes in the BA model owing to the power-law distribution. Assortativity is calculated based on the difference between the degree of each node to the average node degree. To achieve high assortativity, in the BA model, connection between two nodes with high degrees is preferred because node degree gap between high-degree nodes and the average-degree nodes is much greater than the gap between low-degree nodes and the average-degree nodes. Therefore, in an assortative VWSN topology of the BA model, almost all the inter-modular links contain high-degree nodes at both the endpoints and create many disjoint paths among nodes. On the other hand, for the ER model, only half of them are between two high-degree nodes. This results in the high robustness of an assortative VWSN topology based on the BA model.

When comparing results from the ER model and the BA model, the latter shows more robust features for any given value of assortativity. This can be attributed to the difference in node degree distribution. In a topology based on the BA model, the dense central core of hub nodes, i.e., rich club, tightly connects all the nodes and strengthens the connectivity. This decreases the diameter and shrinks the topological shape of the network. Thus, a few failures do not split the topology of the BA model. In contrast, a topology based on the ER model is more sparsely and uniformly connected, and can be broken easily into smaller clusters. These characteristics contribute to the difference in the algebraic connectivity between the ER and BA models.

Communication Efficiency

Figure 3.6b shows the results obtained from the packet routing simulations for the ER and BA models. The y-axis represents the average time required for the data packet to arrive at a destination node from another source node in the VWSN topology. Although in Section 3.4.1 we conducted two types of packet routing simulations that consider propagation delay on links and service delay

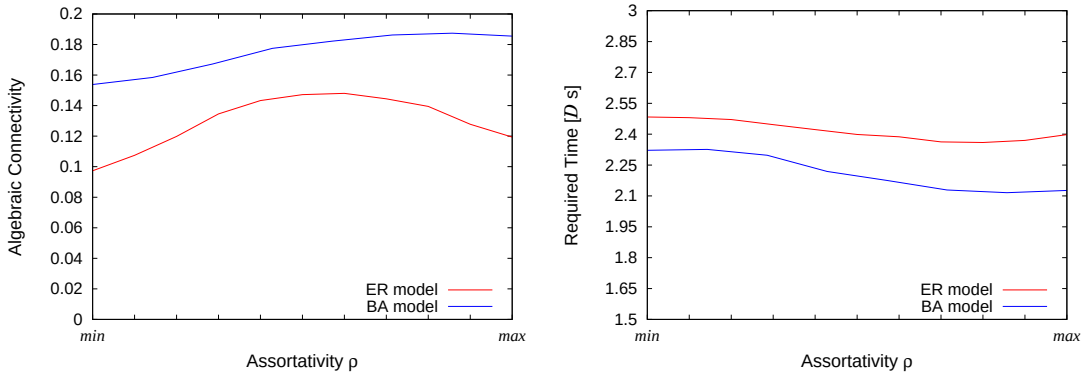

(a) Robustness (b) Communication efficiency

Figure 3.6: Simulation results for 4-module networks.

on nodes, this section provides only the results of simulations that consider service delay. This is because physical distance is assumed negligible for the 4-module VWSN networks. We generated 100 topologies for each model and 1000 packets on each topology to measure the communication delay.

The two results from the ER model and the BA model indicate a similar tendency in terms of information transmission speed. When inter-modular links of a VWSN topology are disassortatively connected, the transmission speed, i.e., communication efficiency, is the lowest. As the assortativity for inter-modular connectivity increases, the transmission speed also increases. This is because, for large values of assortativity, connections will be composed of two high-degree nodes as endpoints. Therefore, it is much easier for information to diffuse over the entire topology by passing through the connections of the two influential nodes. However, when the assortativity is maximized, the transmission speed decreases slightly. This reduction in transmission speed can be attributed to the fact that nodes with the highest or lowest degrees have to be connected to multiple inter-modular links at the same time so that assortativity is maximized; this results in inefficient spread of information over the network topology.

Moreover, it was observed that VWSN topologies based on the BA model diffuse information at a faster rate than those of the ER model. This can be explained by the fact that connecting the hub nodes in different modules based on the BA model enables faster transmission of information.

3.4.3 Evaluation of the Proposed Model

In the previous evaluation, VWSN topologies composed of four modules were used in order to focus on the assortativity between modules and its effect on the performance of communication efficiency and robustness. In this subsection, we also take geometric constraints and the lengths of inter-modular links into account. Therefore, we expand the scale of the topology into $M = 100$ modules and apply the network models explained in Section 3.4.1 for connectivity between modules.

As shown in Table 3.1, equal values are used for N' and L_{intra} because the VWSN topology has been shifted into a larger scale in the square region. The number of inter-modular links L_{inter} is determined to be $L_{inter} = 3 \times M = 300$ such that three inter-modular links are added per module. Because the detailed effect of assortativity ρ on the performance has been already investigated in the previous section, hereafter, we focus on just three values of ρ. ρ_{min} corresponds to the minimum ρ that leads to the most disassortative connectivity on a given VWSN topology, and, similarly, ρ_{max} corresponds to the maximum ρ. ρ_{zero} indicates that $\rho = 0$ and that the topology has non-assortative connectivity between modules. We vary the parameter α for the EDR model in the range of $[0.025, 0.8]$ in order to configure the pattern of inter-modular connectivity. We affix the lower limit to 0.025 because of the difficulty in generation of a connected topology with smaller α; in addition, we affix the upper limit to 0.08 because we confirmed that the topology shape does not change significantly even if we use larger α; the topology becomes similar to that of the ER model. Each result is obtained from 100 repetitions of computer simulations for each pattern of a given VWSN topology.

Robustness

Figure 3.7 shows the relationship between algebraic connectivity, the parameter α from the EDR model, and the inter-modular assortativity. The y-axis represents algebraic connectivity, while the x-axis represents the parameter α. The two subfigures contain three curves, each corresponding to assortative, disassortative, and non-assortative connectivity between modules, respectively.

For every curve in both the subfigures for the ER and BA models, it can be said that a VWSN topology cannot achieve high robustness with a small parameter α. The smaller the parameter α is,

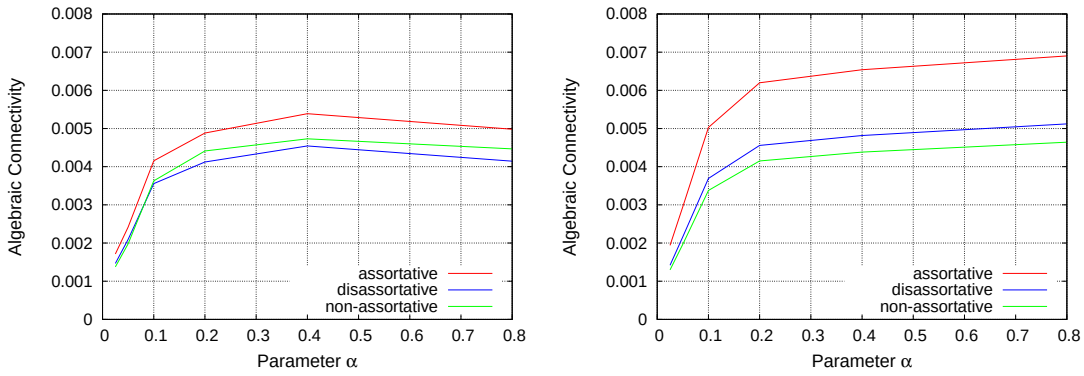

(a) ER model (b) BA model

Figure 3.7: Robustness of the proposed model.

the shorter the links that the VWSN topology has; that is, no long links exist that connect distant modules. Therefore, the modules are locally connected with each other and form several clusters. The topology is fragile and can be easily broken into clusters when node or link failure occurs. Increase in parameter α is characterized by the appearance of long links, and the connectivity between multiple modules is rendered more complicated, as in the case of a random graph (the ER model). Hence, the number of disjoint paths increases and the VWSN topology becomes redundant.

Regarding the assortativity, it should be noted that an assortative topology exhibits the highest algebraic connectivity, i.e., the most robust feature, in both the ER and BA models. In the ER model of the 4-module networks, however, we confirmed that non-assortative or slightly assortative connectivity achieves the highest robustness. This may be attributed to the difference in the number of modules; in a 4-module network, each module was connected to all the other modules by one hop. However, in this case, a VWSN topology is composed of 100 modules, and, therefore, most pairs of modules are indirectly connected. From this result, it can be conjectured that, when a path between two nodes passes through multiple modules, the inter-modular links composed of two high-degree nodes contribute to the increase in the number of disjoint paths. This results in the increase of algebraic connectivity, i.e., robustness. The effect of connections between high-degree nodes is larger in the BA model, and an assortative topology achieves significantly higher robustness.

Communication Efficiency

Although the physical distance and the propagation delay are not considered in the evaluation for 4-module networks, the packet routing simulations described in this section consider both the service delay and propagation delay. Figure 3.8 corresponds to the simulation that measures the propagation delay, and Figure 3.9 corresponds to the simulation that measures the service delay. The y-axis represents the average time required for the data packet to pass from a source node to a destination node in the VWSN topology, and the x-axis represents the parameter α from the EDR model.

Figure 3.8 shows that, as the parameter α decreases, the propagation delay is reduced. When α is small, the EDR model tends to generate shorter inter-modular links. As a result, the connectivity among modules approaches that of a grid topology. Therefore, any given pair of modules will be roughly connected in a straight line. This enables a VWSN topology with small α to decrease the propagation delay. On the other hand, when α is large, the number of long connections between modules increases. Hence, the shortest paths among modules follow a zigzag pattern, as opposed to a straight line. Such zigzag paths lead to an increase in the propagation delay. In contrast, the required time for information transmission increases for small α when considering service delay, as shown in Figure 3.9. Even if the shortest path for a pair of modules is along a straight line, the path is composed of many short inter-modular links. Since the service delay occurs on every hop, the time required for information transmission is large when α is small.

As for the inter-modular assortativity, in Section 3.4.2, we showed that assortative inter-modular connectivity can minimize the service delay for a 4-module network. In that sense, we can confirm a similar tendency in Figures 3.8 and 3.9, which indicates that assortative topology exhibits the best performance. However, the performance of a non-assortative topology is different for the ER model and the BA model. This may be attributed to the difference of node degree distribution. As mentioned earlier, half of the inter-modular links in an assortative topology are composed of low-degree nodes in the ER model. They offset the benefit of the rest of the inter-modular links composed of high-degree nodes. For the ER model, the results indicate that the performance of

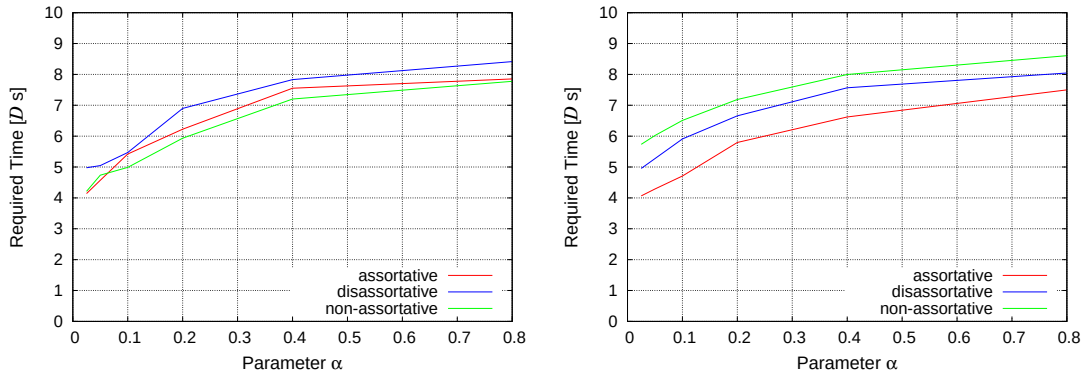

(a) ER model (b) BA model

Figure 3.8: Communication efficiency (propagation delay) of the proposed model

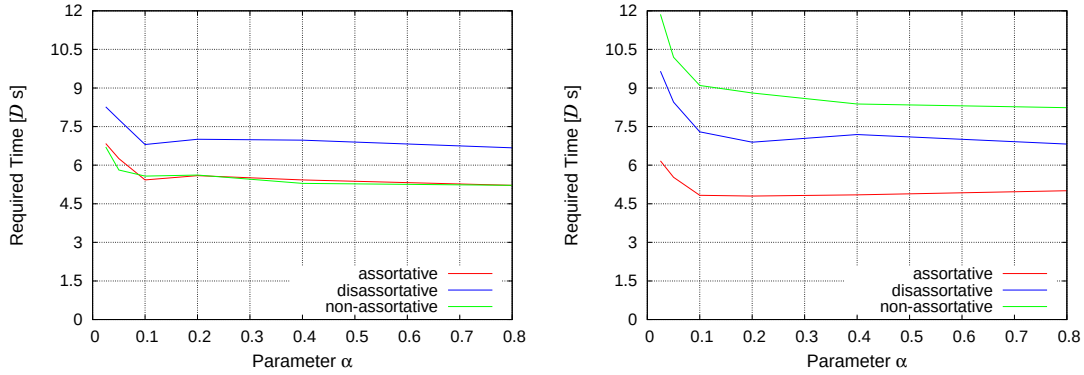

(a) ER model (b) BA model

Figure 3.9: Communication efficiency (service delay) of the proposed model.

random connectivity in a non-assortative topology is almost similar to that of a mixture of high-degree connections and low-degree connections in an assortative topology. Meanwhile, the non-assortative topology exhibits the slowest rate of information transmission for the BA model, even though a non-assortative topology is slightly better than the disassortative topology for 4-module networks, as shown in Figure 3.6b. This is because, when information passes through multiple modules, hub nodes, i.e., extremely high-degree nodes, have greater influence for the BA model, and inter-modular links of a non-assortative topology do not contain hub nodes.

Wiring Cost

In Figure 3.10, the y-axis represents the sum of squares of the lengths of all inter-modular links, as wiring cost is based on the *Friis transmission equation* [101]. As explained in Section 3.4.1, we do not consider the cost of links within modules. The x-axis corresponds to the parameter α of the EDR model. In Figure 3.10, assortativity or network models for intra-modular connectivity are assumed to have no effect on the evaluation, and hence are omitted.

The result shows a monotonous change in the wiring cost when the parameter α is varied. For small values of α, the EDR model probabilistically tends to generate shorter links according to Equation (3.6). As the parameter α increases, the restriction on generating long links is softened.

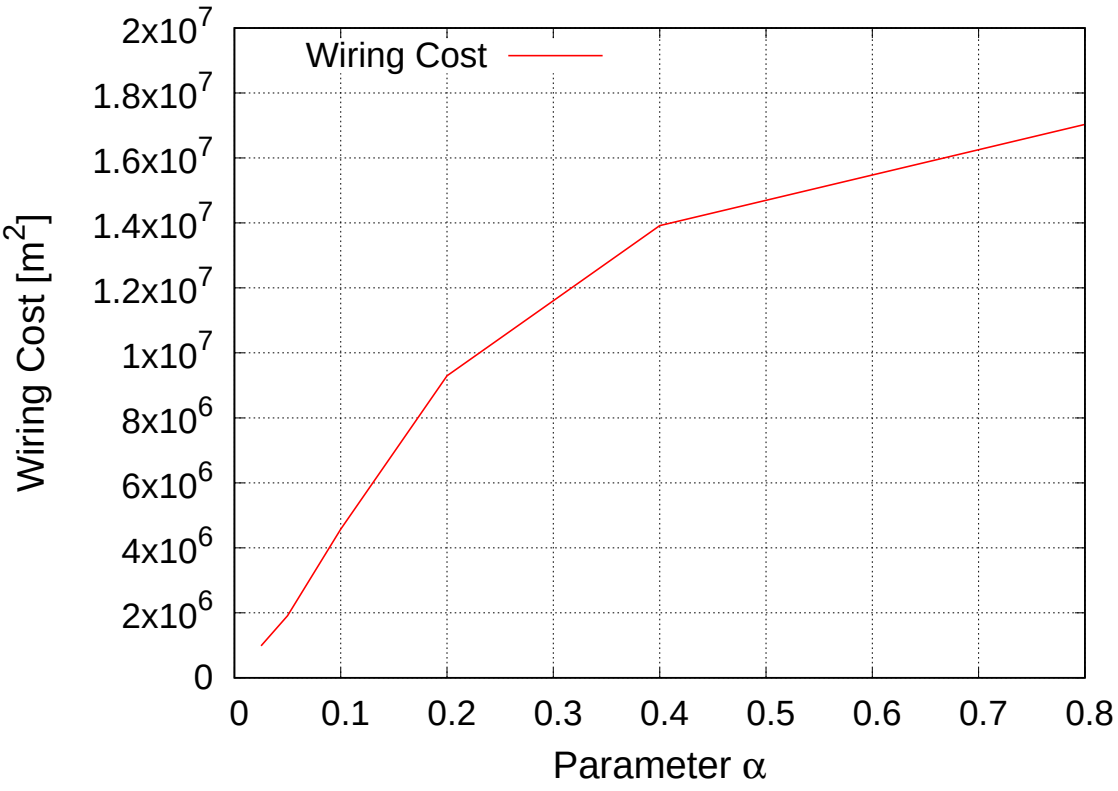

Figure 3.10: Wiring cost of the proposed model.

3.4.4 Comparison with Other Network Models

We investigate the effect on the performances of the difference in network models for inter-modular connectivity. We choose 0.025, 0.1, and 0.4 as representative values for the parameter α of the EDR model to construct a VWSN topology. In addition, we prepare the ER model, SL model, and LL model, which are explained in Section 3.4.1, and compare the performance of these models. As shown in Table 3.1, only the parameters of α, R_{short}, and R_{long} are changed from those in Section 3.4.3. Each result is obtained from 100 repetitions of computer simulations for each pattern of a given VWSN topology.

Robustness

Figure 3.11 shows the algebraic connectivity for each network model. The order of the algebraic connectivity of the network models on the x-axis is similar for the ER and BA models. The $\mathrm{EDR}_{0.025}$ and the SL model equally mark the lowest values for the algebraic connectivity. The SL model generates no long links, and the $\mathrm{EDR}_{0.025}$ also does not generate long links due to the limitation imposed by Equation (3.6). The resultant grid-like topologies are easily broken into small clusters in the event of failures, as mentioned in Section 3.4.3. On the other hand, the $\mathrm{EDR}_{0.4}$, ER, and LL models equally exhibit the highest algebraic connectivity. This result is interesting because the LL model generates only long links and no short links, unlike the other two models. From this viewpoint, it can be said that long inter-modular links are more important for the creation of disjoint paths and to improve redundancy of a VWSN topology. The assortative topology has the highest robustness, as explained in Section 3.4.3.

Communication Efficiency

Figures 3.12 and 3.13 show the time required for packet routing, and focus on the propagation delay and service delay, respectively. Regarding propagation delay, the $\mathrm{EDR}_{0.025}$ model exhibits the smallest delay, followed by the $\mathrm{EDR}_{0.1}$ and SL models. For shorter inter-modular links, the VWSN topology approaches a grid-like topology; the route between two nodes is along a straight line. On the other hand, the LL model shows a considerably slow diffusion speed. In a topology

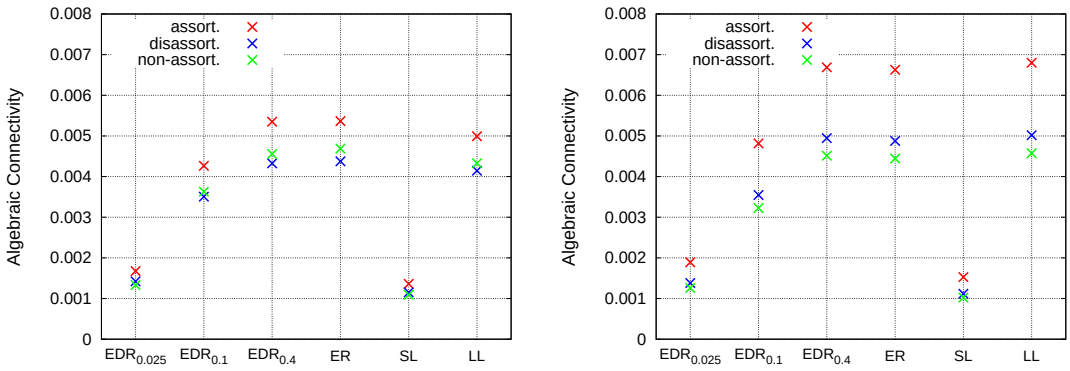

(a) ER model (b) BA model

Figure 3.11: Robustness comparing multiple network models

based on the LL model, there are no short links, and the data is required to undertake a detour when it passes around the topology. Regarding service delay, the SL model exhibits the poorest performance, followed by the $\mathrm{EDR}_{0.0.025}$ model. All the other models equally show the smallest delay.

Notable characteristics are observed on the $\mathrm{EDR}_{0.1}$, which achieves the best performance in terms of propagation delay and service delay. The procedure for generating links in the EDR model is probabilistic. Hence, the topologies of $\mathrm{EDR}_{0.1}$ can contain a small number of long inter-modular links, though almost all the links are short. From Figures 3.12 and 3.13, it can be confirmed that many short links in the $\mathrm{EDR}_{0.1}$ can help achieve a propagation similar to that of the SL model, and only a small number of long links are required to achieve a small service delay as that of the LL model.

Wiring Cost

The performance for wiring cost shown in Figure 3.14 is similar to that of communication efficiency of the propagation delay in Figure 3.12. It can be said that the ratio of short inter-modular links is closely linked to both results. The $\mathrm{EDR}_{0.025}$ and the SL model display the lowest cost, whereas the LL model exhibits an extremely high cost. The results simply reflect the procedure of generating inter-modular links: $\mathrm{EDR}_{0.025}$ and the SL models generate short links, and the LL model generates

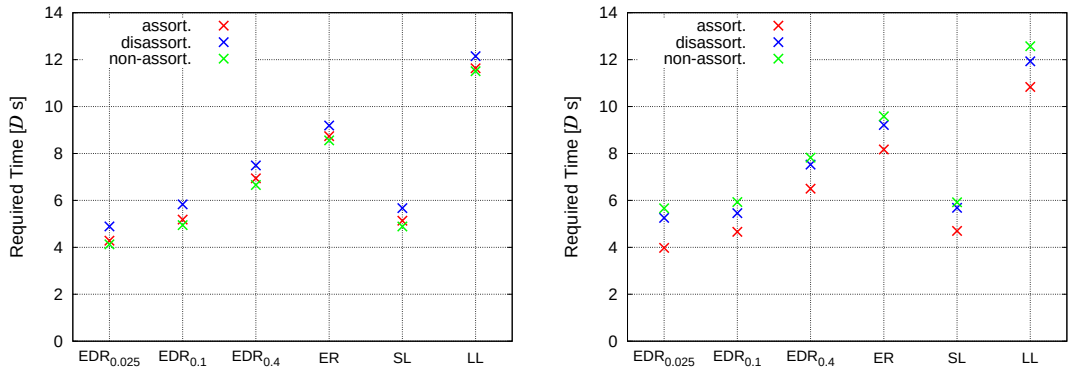

(a) ER model (b) BA model

Figure 3.12: Communication efficiency (propagation delay) comparing multiple network models.

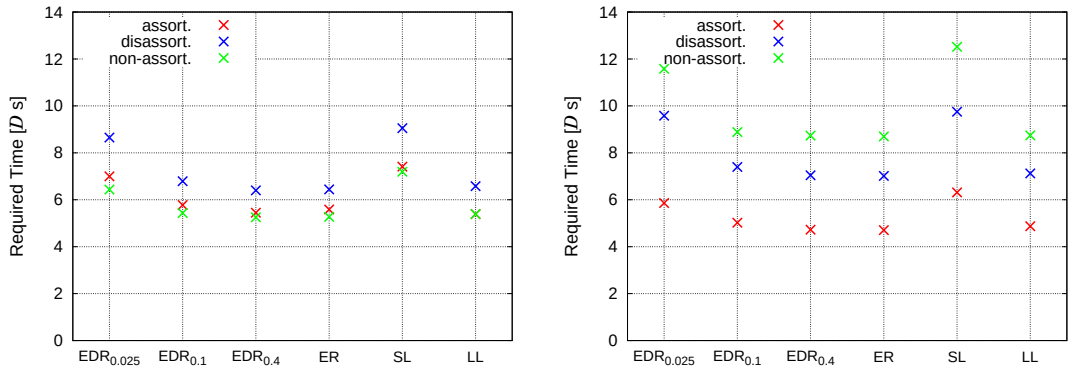

(a) ER model (b) BA model

Figure 3.13: Communication efficiency (service delay) comparing multiple network models.

long links. We can confirm that the cost of $\mathrm{EDR}_{0.1}$ is also much smaller than the other models except for $\mathrm{EDR}_{0.025}$ and SL models. This implies that, although the performance of the $\mathrm{EDR}_{0.1}$ and ER models shown in Figures 3.11 and 3.13 is similar, $\mathrm{EDR}_{0.1}$ is still biased towards generating shorter links when compared with the ER model, which generates links of the average length. If α is further increased, the inter-modular connectivity approaches that of the ER model.

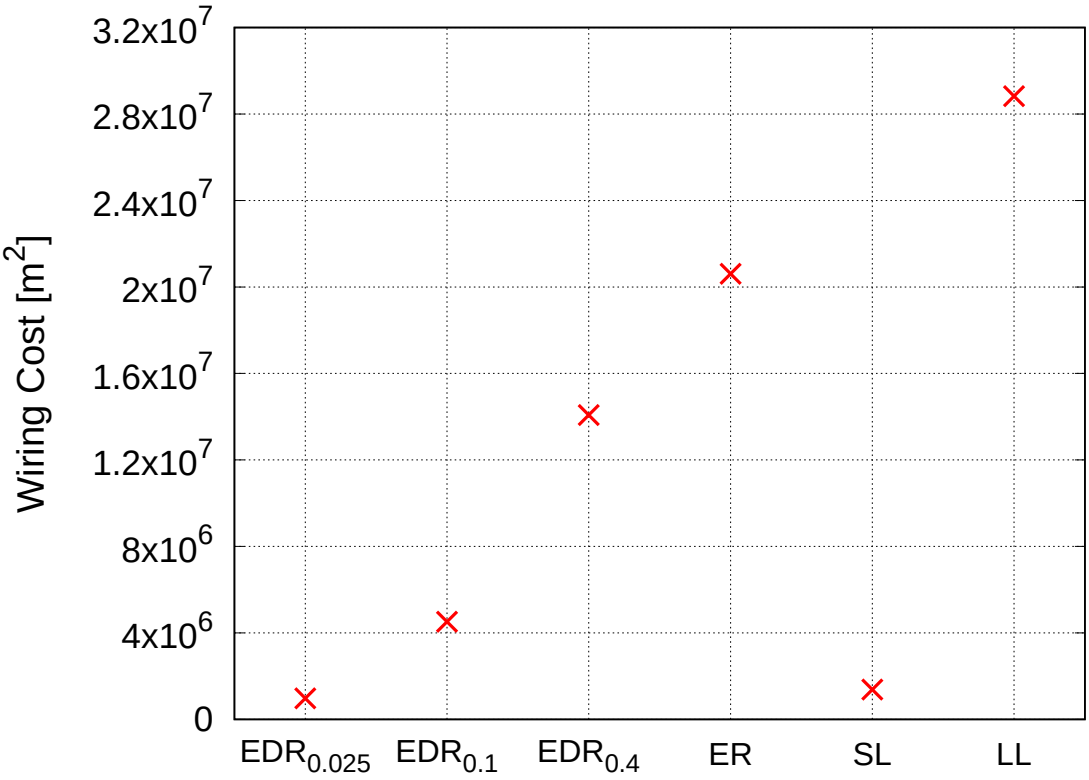

Figure 3.14: Wiring cost comparing multiple network models.

3.5 Conclusion

In this study, we proposed and evaluated a method to construct a VWSN topology. Since there are an enormous number of IoT devices and countless types of application services on the future VWSN, in order to satisfy the required performances such as communication efficiency, robustness, and construction cost, we focused on two basic topological properties: *which pair of modules should be assigned inter-modular links*, and *which nodes in the modules should be assigned endpoints of the inter-modular links*. For the former, we focused on an inter-modular connectivity model based on the cerebral cortex of a mammalian brain, which is referred to as the EDR model. For the latter, we focused on assortativity, which is an important property that characterizes the modular connectivity structure of human brain networks.

The proposed brain-inspired method constructs the virtual layer based on the EDR model, i.e., inter-modular links are assigned among a set of modules. The proposed method exhibited a trade-off between the metrics used in the computer simulations. When the parameter α shifted towards zero, service delay increased and robustness decreased, while propagation delay and wiring cost decreased. By contrast, if α is increased, the performance is good in terms of service delay and robustness, whereas propagation delay and wiring costs tend to deteriorate.

In comparison with other network models, we also confirmed that the proposed model can simultaneously achieve high performance in terms of robustness, communication efficiency, and construction cost when the parameter α is set around 0.1 in the above-mentioned trade-off. We revealed that robustness could be enhanced while suppressing service delay, when a small number of long inter-modular links are generated in a VWSN topology. This leads to a reduction in the construction cost, and propagation delay is also reduced by the existence of dozens of short inter-modular links in the topology. When α is approximately 0.1, most inter-modular links generated in the construction process are short, but a few long links are also probabilistically generated at the same time. These long links enable our proposed model to achieve high robustness and low service delay. Correspondingly, when an inter-modular topology of the cerebral cortex is reproduced, Markov et al. used a similar parameter setting of: $\alpha = (\lambda d_{max})^{-1} = (0.180 \times 58.2)^{-1} \simeq 0.0954$ [106]. This implies that brain networks also deal with this trade-off and realize high performance. In that sense, we also showed that the characteristics of brain networks are applicable to the VWSN topology.

With respect to inter-modular assortativity, topologies with high asssortativity revealed high performance with regard to both robustness and communication efficiency. We can also confirm that there exists a difference when the ER and BA models are used for connectivity within modules. When using the BA model, most inter-modular links consist of hub nodes, which have greater topological importance. This characteristic of the BA model enables the links to contribute the performance more than the ER model. We also confirmed that an assortative topology becomes superior when the number of modules is increased. This is because inter-modular links of high-degree nodes exert a greater influence when a pair of nodes is connected through many more indirect routes. From these observations, we can establish that connecting two high-degree nodes to generate inter-modular links contributes to performance enhancement in terms of robustness and communication

efficiency. This is particularly applicable to the case when each module has scale-free-like connectivity and the number of modules is significantly large.

In real world IoT networks, various constraints in the environment or service demands from the providers may affect the construction of a VWSN topology over edge computing systems and WSNs. For instance, an enormous number of IoT devices are assumed to consist of a VWSN topology as a physical layer in this study. In such a situation, it is essential to take into consideration the battery life of the devices and communication distances. Meanwhile, if the application service that runs over the VWSN topology is a life-critical system, high robustness against computer-virus infections or network failures are of critical importance. We consider that the application of the proposed method of topology construction based on the EDR model is not limited onto the virtualized networks, but other types of massive heterogeneous interconnected networks. Regarding the assignment of inter-modular links among modules, the infrastructure providers can construct a VWSN topology that is suited to specific situations by using our proposed model and setting the parameter α around 0.1. With respect to choosing endpoint nodes for the inter-modular links, it can be summarized that assortatively inter-connecting high-degree nodes enhances both robustness and communication efficiency. Through the discussion in this paper, we conclude that our proposed methods can help design VWSN architectures that can deal with various demands that may arise in actual IoT scenarios.

Chapter 4

Design Method for Reliability of Interconnected Networks with Mutual Dependency

4.1 Introduction

The *Internet of Things* (IoT) has seen an increasing number of practical implementations in recent years, regarding not only traditional Internet services but also other services of extreme societal importance, such as infrastructure (e.g., electricity grids, traffic) and life-critical services (security, medical treatment, etc.) [6, 7]. This situation is leading to the emergence of interconnected networks with mutual dependencies, known as a *network of networks* (NoN) [8]. Network slicing based on network virtualization technology can be regarded as an NoN case and has been attracting much attention as a way to realize the assumed IoT network environment [68, 69]. In this architecture, sliced networks [i.e., virtual networks (VNs)] are created by service providers to offer specific services on physical networks (PNs) provided by the infrastructure providers. To enhance the flexibility and efficiency of resource utilization, recent studies have investigated new methods for reallocating resources dynamically between VNs according to traffic fluctuations instead of dividing the PN resources statically [107–110]. However, although the above methods have several

advantages, traffic fluctuations in one VN can be propagated to other VNs because of the mutual dependences between the VNs sharing the same PN resources [9, 10]. In the upcoming IoT network scenario, environmental changes in service networks will exert an increasing influence on society and human life. Consequently, an urgent issue is to establish a method for designing an NoN with high reliability, namely, the ability to sustain network services under traffic fluctuation, assuming the network-slicing environment.

The *Catastrophic NoN* (C-NoN) was presented as a model expressing NoN availability based on actual interconnected networks comprising infrastructure networks in Italy, namely, a power network and a control network [12]. The functional availability of each infrastructure network depends on that of the other network: the power network must be operated by the control network, while the control network must be supplied with electricity by the power network. The C-NoN model reproduces the dependence between both networks, revealing how partial fluctuations spread their influence over the entire NoN.

On the other hand, Morone *et al.* argued that not all complex networks existing in nature are vulnerable to fluctuations [21]. Brain functional networks comprise a number of mutually connected network modules (i.e., regions) of neural cells. The regions are interdependent to complement their functionalities. Advances in neuroimaging technology, such as *functional magnetic resonance imaging* (fMRI), now make it possible to identify the interregional dependence of brain functional networks, for which Morone *et al.* proposed the *Brain NoN* (B-NoN) model [21]. The B-NoN model reproduces the complementary interregional dependence and elucidates the mechanisms that suppress the propagation of local fluctuations. However, insights from studying NoN models are yet to be applied to practical systems of information networks including the aforementioned network-slicing environment.

As an NoN system, we consider herein layered VNs with slicing, and we propose the *Physical–Virtual NoN* (PV-NoN) model based on existing NoN models. To deal with traffic conditions and interdependence among a PN and VNs, this model describes NoN availability, focusing on the states of the node interfaces. For the PV-NoN model, we assume three different types of interdependence according to how the resources (e.g., packet buffer, network I/O) are assigned on the physical interfaces. To investigate NoN reliability, we measured availability and communication performance

through simulation experiments. We confirm that among the three types of PV-NoN model, the one based on the B-NoN model, which reproduces the complementary interdependence of brain functional networks, achieves high availability and communication performance while preventing interference among the VNs.

We also investigate a method for designing reliable network structures in the PV-NoN model. To this end, we configure the deployment of *network influencers*, which are the network components whose fluctuations have the largest influence on the entire network [111–113], from the perspective of inter/intranetwork *assortativity*. Assortativity is a network metric for evaluating the correlation of node centrality, that is, node influence [41]. Evaluation results show that configuring the assortativity within each VN and among the VNs can improve NoN availability and communication performance. Obtaining guidelines on influencer design with the PV-NoN model contributes directly to controlling the performance of network slicing under unpredictable environmental change, thereby leading to the design of highly reliable interdependent network architectures in future IoT scenarios. Our results also suggest the potential of the NoN model to be applied to other interconnected network systems wherein there is mutual internetwork dependence.

4.2 Related Work

In this section, we introduce related studies of NoN models and describe the definitions of the B-NoN and C-NoN models. We also explain the details of the *Collective Influence* algorithm for detecting NoN network influencers.

4.2.1 Network of networks

Variables in NoN models

The existing NoN model is characterized by modeling the node states to express the NoN availability. The state of an arbitrary node in the NoN is determined by those of its neighbors. A node can be in one of four states, each of which is characterized by three variables (Table 4.1), and state

transitions occur in three steps (Fig 4.1), where the node symbols correspond to those defined in Table 4.1. The black lines indicate intranetwork links and the blue dashed lines indicate internetwork links. The variable n_i indicates the existence of node i, and its value is predetermined as shown by Fig 4.1(a). The value of σ_i, which expresses the *local effectiveness* of node i, is then determined based on the values n_j of all nodes j that are connected via internetwork links, and shifts to the states shown in Fig 4.1(b). ρ_i is the *global effectiveness* of node i and is determined by whether the node is included in the *giant component* (GC) composed of locally effective nodes, which is shown in Fig 4.1(c).

Table 4.1: Definition of network-of-networks (NoN) node states.

Symbol	Node state	n_i	σ_i	ρ_i
○	removed	0	0	0
●	exists	1	0	0
◉	locally available	1	1	0
●	globally available	1	1	1

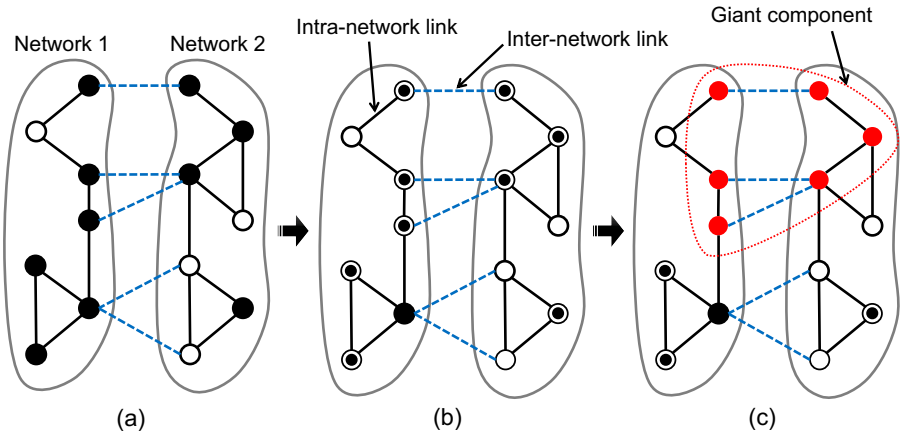

Figure 4.1: Example of state transition in Brain NoN (B-NoN) model.

The B-NoN and C-NoN models define the local effectiveness σ_i in the same way but the GC in different ways. This results in different definitions of the global effectiveness ρ_i, leading to a large difference in reliability between the two NoN models. In the following sections, we describe the definitions of σ_i and ρ_i in detail, along with the state-transition mechanisms shown in Fig 4.1.

Definition of local effectiveness

In a realistic NoN assumed by the B-NoN and C-NoN models, arbitrary nodes cannot be locally effective unless there is a node that is also locally effective in the interconnected network. For example, in brain functional networks, the function of "recognizing an image" can be achieved only by the cooperation of neural cells in two regions, namely the *posterior occipital cortex* (vision) and the *anterior cingulate cortex* (recognition) [21]. In the same manner, an electric power supply system is realized by the cooperation of nodes in a power network and a control communication network [12]. As such, the NoN models express the local effectiveness of node i by defining the variable σ_i as follows:

$$\sigma_i = n_i \Bigg[1 - \prod_{j \in \mathcal{F}(i)} (1 - n_i) \Bigg], \tag{4.1}$$

where $\mathcal{F}(i)$ is the set of nodes connected to node i via internetwork links. For node i to be locally effective, Eq (4.1) requires (i) node i to exist and (ii) there to be at least one node connected to node i via internetwork links. If node i has no internetwork links, then the condition reduces to (i) node i exists. For example, the node colored black in Fig 4.1(b) cannot become locally effective because both nodes connected via internetwork links are removed.

Definition of global effectiveness

The global effectiveness of a node is based on its connectivity to the GC consisting of locally effective nodes. The size of the GC is calculated using a method known as *message passing*, where a node (i) sends the probability of it being connected to the GC to all its adjacent nodes and (ii) updates this probability whenever the node receives the corresponding information from its neighboring nodes. A node can send information only when it is locally effective. At the beginning of message passing, the initial values of the probability are set by random binary configuration of $\{0, 1\}$, and the global effectiveness is determined by the converged value of this probability. The B-NoN and C-NoN models calculate the GC in different ways as explained in the following sections.

B-NoN model An image is recognized in the brain functional networks by the combination of the posterior occipital cortex, which is responsible for visual function, and the anterior cingulate

cortex, which deals with recognition. These two regions compensate complementarily for the lack of information in each; for instance, even if the posterior occipital cortex receives incomplete visual information from the eye, the anterior cingulate cortex can compensate for this lack and recognize the object. The B-NoN model reflects this as a *logical OR*-like dependence between the regions. A node is regarded as globally effective if *either* its adjacent nodes of the same network *or* those from other networks belong to the GC. For message passing in the B-NoN model, the variable $\rho_{i\to j}$ is defined as information sent from node i to node j within the same network and the variable $\varphi_{i\to j}$ is defined as information sent from node i to node j of a different network:

$$\begin{aligned}\rho_{i\to j} &= \sigma_i\Bigg[1-\prod_{k\in\mathcal{S}(i)\setminus j}(1-\rho_{k\to i})\prod_{l\in\mathcal{F}(i)}(1-\varphi_{l\to i})\Bigg],\\ \varphi_{i\to j} &= \sigma_i\Bigg[1-\prod_{k\in\mathcal{S}(i)}(1-\rho_{k\to i})\prod_{l\in\mathcal{F}(i)\setminus j}(1-\varphi_{l\to i})\Bigg],\end{aligned} \tag{4.2}$$

where $\mathcal{S}(i)$ is the set of adjacent nodes of node i within the same network and $\mathcal{F}(i)$ is the set of adjacent nodes of node i from other networks. By this formulation, $\rho_{i\to j}$ and $\varphi_{i\to j}$ become 1 if either $\rho_{k\to i}$ or $\varphi_{l\to i}$ is 1, reflecting the logical OR-like dependence. Starting with random configurations of $\rho_{i\to j}, \varphi_{i\to j} \in \{0,1\}$, the global effectiveness ρ_i as the converged probability of node i being connected to the GC through message passing is defined as

$$\rho_i = \sigma_i\Bigg[1-\prod_{k\in\mathcal{S}(i)}(1-\rho_{k\to i})\prod_{l\in\mathcal{F}(i)}(1-\varphi_{l\to i})\Bigg]. \tag{4.3}$$

C-NoN model In contrast to the B-NoN model, a node in the C-NoN model is globally effective if *both* its adjacent nodes of the same network *and* those from other networks belong to the GC. This model reflects the *logical AND*-like dependence that the power network and the control network are not mutually replaceable functions, whereas the functions in the inter-areal brain networks are

complementary. Based on this characteristic, the variables $\rho_{i\to j}$ and $\varphi_{i\to j}$ are defined as

$$\begin{aligned}\rho_{i\to j} &= \sigma_i\left[1-\prod_{k\in\mathcal{S}(i)\setminus j}(1-\rho_{k\to i})\right]\left[1-\prod_{l\in\mathcal{F}(i)}(1-\varphi_{l\to i})\right],\\ \varphi_{i\to j} &= \sigma_i\left[1-\prod_{k\in\mathcal{S}(i)}(1-\rho_{k\to i})\right]\left[1-\prod_{l\in\mathcal{F}(i)\setminus j}(1-\varphi_{l\to i})\right].\end{aligned} \tag{4.4}$$

In contrast to the formulation of the B-NoN model, $\rho_{i\to j}$ and $\varphi_{i\to j}$ become 1 if both $\rho_{k\to i}$ and $\varphi_{l\to i}$ are 1, reflecting the logical AND-like dependence. As the converged probability of node i being connected to the GC, the global effectiveness ρ_i is then defined as

$$\rho_i = \sigma_i\left[1-\prod_{k\in\mathcal{S}(i)}(1-\rho_{k\to i})\right]\left[1-\prod_{l\in\mathcal{F}(i)}(1-\varphi_{l\to i})\right]. \tag{4.5}$$

4.2.2 Influence identification in a network of networks

The identification of highly influential nodes, which play important roles in robustness and diffusion, has been studied in many research domains, such as social networks [111, 114], biology [115, 116], marketing [117, 118], and computer networks [113]. Because searching for the optimal influencers over a given network is an NP-hard problem [111], a number of heuristic methods have been proposed to date [119–121].

Herein, we also deal with influencer design to enhance NoN reliability, and therefore we focus on the recently proposed *Collective Influence* (CI) algorithm for influencer identification [122]. Not only does the CI algorithm outperform other existing methods in detecting influencers, it is also optimized for an NoN [21]. The influence on the network centered around node i is represented by CI_i, which is defined as

$$\mathrm{CI}_i = (k_i-1)\sum_{j\in\partial\mathrm{Ball}(i,l)}(k_j-1), \tag{4.6}$$

where k_i is the degree of node i and $\partial\mathrm{Ball}(i,l)$ is the set of nodes located exactly l hops away from node i (Fig 4.2). CI_i is depicted in Network 1. $\mathrm{Ball}(i,l)$ is the area of influence of node i, and $\partial\mathrm{Ball}(i,l)$ corresponds to the edge of $\mathrm{Ball}(i,l)$. Networks 1 and 2 are interdependent via an internetwork link. CI_i is calculated as the product of the degree of node i and the sum of the degree

of node j in $\partial\mathrm{Ball}(i,l)$. Furthermore, the definition of CI_i is expanded for an NoN as follows:

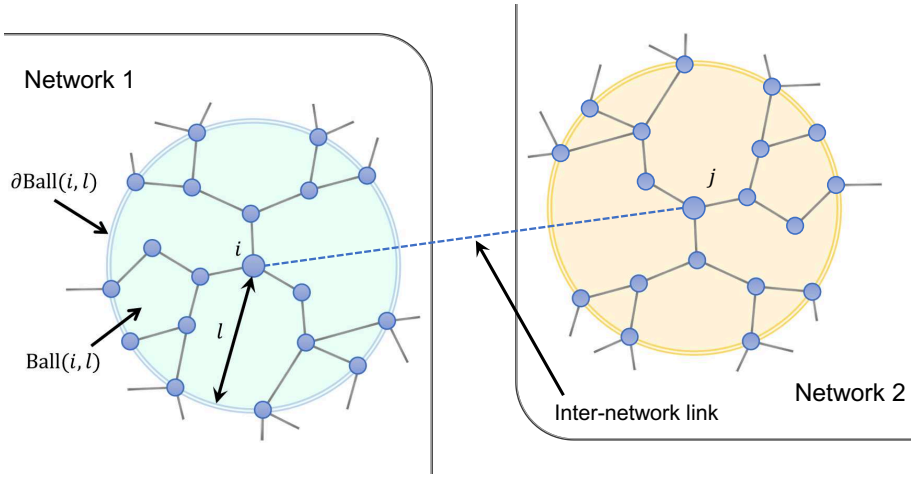

Figure 4.2: Expression of collective influence (CI).

$$\begin{aligned}\mathrm{CI}_i \;=\; & (k_i^{intra}+k_i^{inter}-1)\sum_{j\in\partial\mathrm{Ball}(i,l)}(k_j^{intra}+k_j^{inter}-1)\\ & +\sum_{j\in\mathcal{F}(i):k_j^{inter}=1}\Bigg[(k_j^{intra}+k_j^{inter}-1)\sum_{m\in\partial\mathrm{Ball}(j,l)}(k_m^{intra}+k_m^{inter}-1)\Bigg],\end{aligned}\tag{4.7}$$

where k_i^{intra} and k_i^{inter} are the degree of node i for intranetwork links and internetwork links, respectively. $\mathcal{F}(i)$ is the set of nodes connected to node i via internetwork links. The first term of Eq (4.7) corresponds to the CI of node i for Network 1 in Fig 4.2. The second term represents the sum of the CI of node j connected to node i via internetwork links, corresponding to Network 2 in Fig 4.2. The condition $k_j^{inter}=1$ indicates that node j is taken into account only if it has a single intermodular link. This is attributed to the NoN characteristic that the state of node j is not directly affected by node i if node j has more than one intermodular link according to Eq (4.1).

4.3 Network of Networks in virtualized networks

4.3.1 Interdependence of virtualized networks

In this study, we assume an interdependent layered network where a single PN is virtualized by network slicing, and multiple VNs are constructed on the PN as shown in Fig 4.3. A PN comprises *physical nodes* (P-nodes) and *physical links* (P-links). Similarly, *virtual nodes* (V-nodes) and *virtual links* (V-links) form a VN. Because of the virtualization of the PN, each V-node corresponds to exactly one P-node, while a V-link comprises multiple P-nodes and P-links that realize the shortest path connecting the two endpoint V-nodes. We assume that the connectivity structure of the PN is given by the infrastructure provider, whereas each VN realizes its own connectivity based on the requests of the service provider. In Fig 4.3, the P-node and V-node in VN k with common index i are represented as r_i^P and $r_i^{V_k}$, respectively. The P-interface j of P-node i and the V-interface j of V-node i in VN k are represented as $i_{i,j}^P$ and $i_{i,j}^{V_k}$, respectively. Refer to Table 4.2 for a description of all the main parameters defined in this paper.

Upon virtualization based on network slicing, the physical resources on the PN are shared among the VNs, thereby making the PN and VNs interdependent. Various services are being provided continuously over the VN, and environmental changes may occur at any instant because of traffic fluctuations. Consequently, our aim in this study is to model the VN availability under fluctuating traffic while considering the interdependence among the VNs caused by resource sharing. Although various physical resources on the P-nodes can be considered for virtualization (e.g., CPU, memory, storage, network I/O), we focus on the packet buffer memory (hereinafter referred to as the buffer) and network I/O because they are influenced directly by the traffic conditions. Consequently, we segment the P-nodes into *physical interfaces* (P-interfaces) and model the state of each P-interface taking the buffer and network I/O into consideration. The P-interface and the *virtual interface* (V-interface) are distinguished as shown in Fig 4.3.

Various approaches have been studied for partitioning physical resources, the aim being to improve the flexibility and efficiency of the virtualized networks [123–125]. Here, we assume three basic types of interface partitioning (Table 4.3). The most fundamental is *type-SD* (Statically Divided), in which resources (i.e., the buffer and network I/O) for the P-interface are divided statically

Table 4.2: Parameter description.

Variable	**Value**	**Description**	**Equation**
n_i	{0,1}	Existing state of node i	–
σ_i	{0,1}	Local effectiveness of node i	Eq. (4.1)
ρ_i	{0,1}	Global effectiveness of node i	Eq. (4.3,4.5)
$\rho_{i\to j}$, $\varphi_{i\to j}$	{0,1}	Probability information for message passing sent from node i to j	Eq. (4.2,4.4)
CI_i	[0,∞]	Collective influence of node i	Eq. (4.6,4.7)
r_x^P, $r_x^{V_k}$	–	Index for P-node x and V-node x on VN k	–
$i_{x,y}^P$, $i_{x,y}^{V_k}$	–	Index for P-interface y of r_x^P and V-interface y of $r_x^{V_k}$	–
$B_{x,y}^P$	*given*	Buffer capacity for P-interface y of r_x^P	–
$n_{x,y}^P$	{0,1}	Availability state for P-interface y of r_x^P	–
$n_{x,y}^{V_k}(t)$	[0,∞]	Traffic state for V-interface y of $r_x^{V_k}$ at time t	–
$R_{x,y}^{V_k}(t)$	{0,1}	Vacancy state for V-interface y of $r_x^{V_k}$ at time t	Eq. (4.8,4.10)
$\rho_{x,y}^{V_k}(t)$	{0,1}	Traffic state for V-interface y of $r_x^{V_k}$ at time t	Eq. (4.9,4.11,4.12)
$\mathrm{CI}(r_x^P)$, $\mathrm{CI}(r_x^{V_k})$	[0,∞]	Collective influence of r_x^P and $r_x^{V_k}$	Eq. (4.13–4.15)
η	[-1,1]	Assortativity for intra-network connectivity	Eq. (4.17)
θ	[-1,1]	Assortativity for inter-network connectivity	Eq. (4.21)
N^P, N^{V_k}	*given*	Number of P-nodes and V-nodes on VN k	–
L^P, L^{V_k}	*given*	Number of P-links and V-links on VN k	–
W	*given*	Bandwidth for P-interfaces	–
λ	*given*	Arrival rate of packets	–
R	*given*	Number of packet re-transmission	–

for each VN; the upper limit of the number of packets stored and sent out from a V-interface is divided statically beforehand. With this type, constant performance is guaranteed for each VN and no traffic interference occurs, but the efficiency of resource utilization is not optimal. In contrast to type-SD, we also assume *type-UD* (UnDivided), in which the physical resource for each VN is not partitioned; the resource capacity for each VN is not guaranteed, and traffic in a VN can even occupy all the buffers and network I/O on the PN, but the physical resources can be utilized completely. As the third case, we assume *type-DD* (Dynamically Divided), in which the physical resources are allocated dynamically depending on the changing traffic conditions; the physical resources are not partitioned under normal conditions (as with type-UD), but they are partitioned when traffic congestion occurs. Therefore, type-DD allows physical resources to be used more efficiently while guaranteeing the resources for each VN. With all three types, resource virtualization

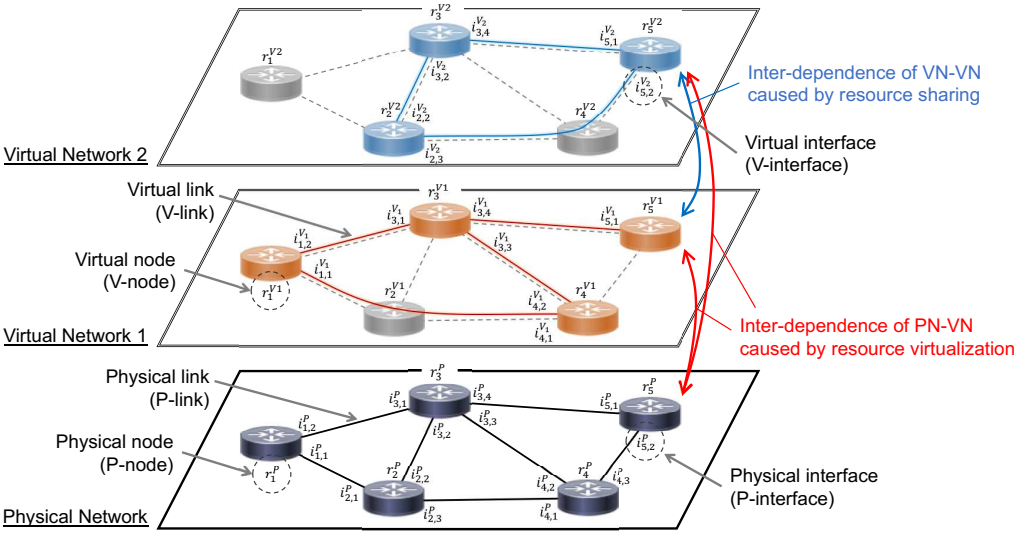

Figure 4.3: Example of virtualized network based on network slicing.

makes the PN and VNs interdependent. Furthermore, with type-UD and type-DD, the sharing of physical resources among multiple VNs makes the latter interdependent.

Table 4.3: Characteristics of three resource partitioning schemes for PV-NoN model.

	type-SD	type-UD	type-DD
Interdependence of PN-VN	yes	yes	yes
Interdependence of VN-VN	no	yes	yes
Utilization guarantee	yes	no	yes
Utilization efficiency	no	yes	yes

4.3.2 Model of network of networks with network slicing

The PV-NoN model defines the availability state of interfaces to deal with traffic fluctuations and interdependence among a PN and VNs. Here, the word *available* denotes the state in which packets are transmitted at interfaces with no packet overflow. In the following sections, we describe the definitions of the input states of V-interfaces and P-interfaces and the availability states of V-interfaces calculated based on those input states.

Input states of interfaces

In contrast to the existing NoN models, we introduce time in the form of the variable t because traffic conditions may change at any moment. The number of packets arriving at V-interface $i_{r,s}^{V_k}$ at time t is denoted as $n_{r,s}^{V_k}(t)$, which takes any positive value depending on the traffic conditions. The state of P-interface $i_{r,s}^{P}$ is expressed by the Boolean variable $n_{r,s}^{P}$, whose value is nominally 0 but becomes 1 if there is a malfunction and $i_{r,s}^{P}$ cannot send packets. The buffer capacity of $i_{r,s}^{P}$ is denoted as $B_{r,s}^{P}$.

Availability states of interfaces

We define $\sigma_{r,s}^{V_k}(t)$ to express the availability state of $i_{r,s}^{V_k}$ considering the dependence among the PN and VNs. If $i_{r,s}^{P}$ has no malfunction and $i_{r,s}^{V_k}$ has no packet overflow, then $i_{r,s}^{V_k}$ is regarded as available and $\sigma_{r,s}^{V_k}(t) = 1$ holds, otherwise $\sigma_{r,s}^{V_k}(t) = 0$. However, the threshold for judging the presence of packet overflow differs among the three types of PV-NoN model as explained above, and details of their definitions are described below.

Type-SD Because type-SD allocates the divided physical resources to each VN statically, there is no interdependence among the VNs. To derive the variable $\sigma_{r,s}^{V_k}(t)$ for $i_{r,s}^{V_k}$, we begin by defining a variable $R_{r,s}^{V_k}(t)$ that represents the presence of available capacity on $i_{r,s}^{V_k}$. $\sigma_{r,s}^{V_k}(t)$ for type-SD is then defined as follows using $R_{r,s}^{V_k}(t)$:

$$R_{r,s}^{V_k}(t) = \begin{cases} 1 & \text{if } \mathcal{B}_{r,s}^{P}/N_{r,s} > n_{r,s}^{V_k}(t), \\ 0 & \text{otherwise,} \end{cases} \tag{4.8}$$

$$\sigma_{r,s}^{V_k}(t) = R_{r,s}^{V_k}(t)\big(1 - n_{r,s}^{P}(t)\big), \tag{4.9}$$

where $N_{r,s}$ is the number of VNs that share $i_{r,s}^{P}$. $R_{r,s}^{V_k}(t)$ is defined so that it is 1 if the number of packets arriving at $i_{r,s}^{V_k}$ at time t does not exceed $\mathcal{B}_{r,s}^{P}/N_{r,s}$. Eq (4.9) defines the availability state of $i_{r,s}^{V_k}$ considering just VN k, which is in contrast to the other two types of PV-NoN model. By multiplying $R_{r,s}^{V_k}(t)$ and $\big(1 - n_{r,s}^{P}(t)\big)$, $\sigma_{r,s}^{V_k}(t)$ is configured to be 1 only if the interface is available

on both the virtual and physical levels.

Type-UD The resources of the P-interface are undivided in the case of type-UD, and thus there is the interdependence that a traffic increase on a VN can limit the performance of the other VNs. That is, type-UD has logical AND-like interdependence whereby the performance can be guaranteed only when *all* VNs that are interdependent with each other are not congested, similar to the characteristics of the C-NoN model explained in Sec. 4.2. Here, in contrast to $R^{V_k}_{r,s}(t)$, we define $R^{V}_{r,s}(t)$ to express the presence of available capacity considering all VNs. Using R^{V}, the availability $\sigma^{V_k}_{r,s}(t)$ for type-UD is expressed as

$$R^{V}_{r,s}(t) = \begin{cases} 1 & \text{if } \mathcal{B}^{P}_{r,s} > \sum_{l\in\mathcal{V}} n^{V_l}_{r,s}(t), \\ 0 & \text{otherwise,} \end{cases} \tag{4.10}$$

$$\sigma^{V_k}_{r,s}(t) = R^{V}_{r,s}(t)\big(1 - n^{P}_{r,s}(t)\big), \tag{4.11}$$

where $\mathcal{V}$ is the set of all VNs. $R^{V}_{r,s}(t)$ is 1 if the number of packets arriving at $i^{P}_{r,s}$ at time t does not exceed $\mathcal{B}^{P}_{r,s}(t)$. This reflects the characteristic of type-UD that each V-interface considers the states of all interdependent V-interfaces, in contrast to type-SD. Because traffic fluctuations in one VN can influence all the other VNs, Eq (4.11) defines $\sigma^{V_k}_{r,s}(t)$ so that $i^{V_k}_{r,s}$ can be regarded as being available only if *all* interdependent V-interfaces have room for packets.

Type-DD With type-DD, the resources of P-interfaces are reallocated among the VNs in a dynamic and complementary way depending on the traffic condition. This property allows type-DD to possess *logical OR*-like interdependence, which is seen in the B-NoN model described in Sec. 4.2: VN k can guarantee the performance if there is room in *either* VN k or the external VNs. Combining the characteristics of type-SD and type-UD, the availability of V-interfaces for type-DD is described as

$$\sigma^{V_k}_{r,s}(t) = \Big\{1 - \big(1 - R^{V_k}_{r,s}(t)\big)\big(1 - R^{V}_{r,s}(t)\big)\Big\}\big(1 - n^{P}_{r,s}(t)\big). \tag{4.12}$$

The first factor is 1 if the traffic condition satisfies either $R_{r,s}^{V_k}(t) = 1$ or $R_{r,s}^{V}(t) = 1$. This behavior expresses the *logical OR*-like interdependence that $i_{r,s}^{V_k}$ is available when either the allocated resources on VN k or the whole resources on the PN have room for packet processing.

4.3.3 Influencers in a network of networks with network slicing

In addition to modeling the availability state of an NoN with network virtualization, we aim to design NoN influencers to improve reliability. Consequently, we develop a method for detecting influencers in an NoN by applying the PV-NoN model based on the CI algorithm described in Sec. 4.2. As can be seen from the definition of the PV-NoN model described in the previous section, a failure of P-nodes occurring on the PN spreads to all interdependent VNs in any type of PV-NoN model. We therefore express the CI of P-node i as $\mathrm{CI}(r_i^P)$, and its definition is given based on Eq (4.7), corresponding to the sum of the influence on the PN centered around P-node i and the influence on each VN centered around V-node i. We define $\mathrm{CI}(r_i^P)$ as

$$\mathrm{CI}(r_i^P) = (k_i^P - 1) \sum_{j \in \partial \mathrm{Ball}(r_i^P, l)} (k_j^P - 1) + \sum_{k \in \mathcal{V}} \left[(k_i^{V_k} - 1) \sum_{h \in \partial \mathrm{Ball}(r_i^{V_k}, l)} (k_h^{V_k} - 1) \right], \tag{4.13}$$

where k_i^P and $k_i^{V_k}$ are the node degrees of r_i^P and $r_i^{V_k}$, respectively. The definition of $\partial \mathrm{Ball}$ is the same as that described in Fig 4.2. The first term accounts for the CI of P-node i within the PN, and the second term accounts for the sum of the CIs of all the V-nodes that are interdependent with P-node i because of resource virtualization.

Regarding the CIs of the V-nodes, in the case of type-SD and type-DD, a specific V-node influences neither the V-nodes on the external VN nor the P-node on the PN, and thus $\mathrm{CI}(r_i^{V_k})$ can be defined considering the influence on the VN to which the V-node belongs:

$$\mathrm{CI}(r_i^{V_k}) = (k_i^{V_k} - 1) \sum_{j \in \partial \mathrm{Ball}(r_i^{V_k}, l)} (k_j^{V_k} - 1). \tag{4.14}$$

On the other hand, in the case of type-UD, it is possible for a V-node to occupy all of the resources shared among the VNs, and eventually the interdependent P-node runs out of capacity.

Therefore, $\mathrm{CI}(r_i^{V_k})$ can be defined as the sum of the CIs of all the interdependent V-nodes including the CI of the interdependent P-node as given by Eq (4.13):

$$\mathrm{CI}(r_i^{V_k}) = \mathrm{CI}(r_i^P) = (k_i^P - 1) \sum_{j \in \partial \mathrm{Ball}(r_i^P, l)} (k_j^P - 1) + \sum_{k \in \mathcal{V}} \left[(k_i^{V_k} - 1) \sum_{h \in \partial \mathrm{Ball}(r_i^{V_k}, l)} (k_h^{V_k} - 1) \right]. \tag{4.15}$$

4.4 Evaluation

In this section, we conduct simulation experiments that generate traffic over the VNs to evaluate the availability of the PV-NoN model. We begin by describing the methods for the evaluation, and then we explain the evaluation results.

4.4.1 Network construction

This study assumes that an NoN comprises a PN and multiple VNs. The PN contains N^P P-nodes and E^P P-links, and similarly VN k contains N^{V_k} V-nodes and E^{V_k} V-links. If $N^P > N^{V_k}$, the VNs are mapped onto the PN so that the fewest P-nodes are shared among the VNs. The connectivity structure for the PN and VNs is determined based on a specific network model, for which we adopt the Erdös-Rényi (ER) model [102] and the Barabasi–Albert (BA) model [52] , which generate node degrees following a Poisson distribution and a power-law distribution, respectively. Because it is virtually impossible to predict connectivity patterns in an IoT scenario with numerous types of services, we use the aforementioned models because they have been observed widely in actual networks and used for network evaluation to date [103–105, 126]. Other types of network model are conceivable, such as the Watts–Strogatz (WS) model [127] , the Waxman model [128], and the random geometric graph (RGG) model [129] . However, the Waxman model belongs to the class of random networks; in other words, it is a special case of the ER model. The degree distributions of the WS and RGG models are close to a uniform distribution, making it difficult to evaluate how network influencers and configuration affect assortativity. Furthermore, the WS model is characterized by its small-worldness, which the BA model shows as well.

Regarding the VN topologies, demands from service providers for connectivity reconfiguration now arise more frequently because of the flexibility and cost-efficiency of virtualized networks [5, 9, 62, 63, 125]. Therefore, this paper deals with the configuration of VN connectivity from the perspective of *assortativity*. Assortativity is a network metric for evaluating the correlation of node centrality in a given topology [41]. For example, looking at assortativity based on degree centrality, an *assortative* node is one whose connected neighbors have similarly high (or low) degrees, while a *disassortative* node is one that has either a high degree compared to its low-degree neighbors or vice versa. In this study, we configure the assortativity of a VN (*intranetwork assortativity* and that among VNs (*internetwork assortativity*).

Intranetwork assortativity

When configuring topological connectivity within a network, the nodal degree is the only fixed metric that can evaluate the centrality of the nodes. Consequently, we focus on the degree assortativity η to configure the connectivity of a VN. We begin by introducing the *remaining degree distribution* $q(k)$, which is defined as

$$q(k) = \frac{(k+1)p(k+1)}{\sum_j jp(j)}. \tag{4.16}$$

The remaining degree distribution is related to the degree distribution $p(k)$ that describes the probability that the degree of a randomly chosen node corresponds to k. The remaining degree of a node in a path corresponds to the number of links of a node excluding the link it was arriving from. For a given $q(k)$, we can introduce the joint probability distribution $e(j,k)$, which indicates the probability that the two endpoints of a randomly chosen link have remaining degrees k and j. Consequently, the degree assortativity η is defined as

$$\eta = \frac{1}{\sigma_q^2}\left[\sum_{j,k} jke(j,k) - \Big(\sum_j jq(j)\Big)^2\right], \tag{4.17}$$

where σ_q is the standard deviation of the remaining degree distribution $q(k)$. η can take any value in the interval $[-1,1]$: $\eta > 0$ and $\eta < 0$ indicate an assortative network and a disassortative network, respectively, while $\eta = 0$ indicates that the nodes are connected with each other randomly

irrespective of their degrees. The degree distribution limits the range of feasible values of η.

Having constructed an initial VN topology with a specific degree distribution, we then set a target value of η' and rewire the links continuously [22, 130] until the assortativity η of the current topology approximates the given η_{target}. Note that we rewire a topology so that it is not split into submodules; if the generated VN topology is separated into more than one module, the former is reconstructed so that it is fully connected.

Internetwork assortativity

As well as configuring the connectivity within each VN, we must also consider how to map the dependence of V-nodes because traffic fluctuation along the VNs causes interference . For example, we must investigate whether a V-node with high influence in one VN should be interdependent with a V-node of high influence in another VN. We therefore introduce the variable θ to evaluate the assortativity among VNs, and we configure the NoN structure from the perspective of mapping V-nodes on the VNs. Although we use the degree assortativity for connectivity within a VN because of its conditional limitation, we use the CI as a centrality measurement for the assortativity between networks, which is described in Sec. 4.2.

In a previous study [22], we developed a method for measuring the assortativity between networks to evaluate the interdependence of information networks. The assortativity of a set of links is represented as the sum of each link's contribution to the assortativity of the entire network. Consequently, we begin by rewriting the definition of network assortativity described by Eq (4.17) as

$$\eta = \frac{1}{\sigma_q^2}\Big(E[(J-U_q)(K-U_q)]\Big), \tag{4.18}$$

where U_q is the expected value of the remaining degree, and J and K are variables of the remaining degree that have the same expected value U_q. To expand the definition of assortativity for centrality metrics other than degree centrality, we introduce $p'(c)$ as distribution of any kind of centrality metrics c on a VN. As for internetwork assortativity, the centrality of endpoint nodes of an internetwork link when the link is removed is equal to the centrality of those nodes on each VN topology. Hence,

generalized assortativity η' can be defined based on degree assortativity η in Eq. (4.18) as follows:

$$\eta' = \frac{1}{\sigma_{p'_j}\sigma_{p'_k}}\Big(E[(C_j - U_{p'_j})(C_k - U_{p'_k})]\Big), \tag{4.19}$$

where p'_j denotes centrality distribution on VN j. $U_{p'_j}$ and $\sigma_{p'_j}$ denote the expected value and the standard deviation of the centrality distribution p'_j, respectively. C_j denotes variables of the node centrality on VN j that have the same expected value $U_{p'_j}$. Based on Eq (4.19), the contribution θ_l of link l to the assortativity η' of the entire network is defined as follows:

$$\theta_l = \frac{(c_j - U_{p'_j})(c_k - U_{p'_k})}{\sigma_{p'_j}\sigma_{p'_k}}, \tag{4.20}$$

where c_j and c_k are the node centrality of the two endpoints of link l. Finally, the internetwork assortativity θ (i.e., the assortativity of the set of links L_{set} between two networks) is given by

$$\theta = \sum_{l \in L_{set}} \theta_l = \sum_{l \in L_{set}} \frac{(c_j - U_{p'_j})(c_k - U_{p'_k})}{\sigma_{p'_j}\sigma_{p'_k}}. \tag{4.21}$$

To map interdependent V-nodes among VNs, we begin by deploying the VNs randomly upon a PN. Then, similarly to the configuration of connectivity within a VN, we set a target value θ_{target} and repeatedly re-map until the θ calculated from the current VN interconnectivity approximates θ_{target} sufficiently.

4.4.2 Traffic model

Network virtualization is expected to be used in a wide variety of situations and scales in the IoT scenario, resulting in unforeseeable traffic patterns [5–7, 131, 132]. Consequently, this study deals with a basic traffic model for performance evaluation, and the packet processing is designed on the basis of the $M/D/1/K$ queuing model [133]. The traffic condition changes discretely every time unit. Here, the average arrival rate (i.e., the rate at which a new packet is generated on a V-node at time t) is expressed by λ. The destination V-node of the generated packet is selected randomly from the other V-nodes on the VN to which the V-node belongs.

The routing path for a packet is determined so as to minimize the total number of P-links from the source V-node to the destination V-node. If there are multiple candidates for the shortest path, then one of them is selected randomly. For a pair of V-nodes, each path is determined statically and then left unchanged during the simulation. The total packet delay consists of the propagation delay and the queuing delay. A packet sent from a V-node at time t arrives at the next V-node at time $t + 1$ because of the propagation delay (i.e., the propagation delay on each P-link is 1). Packets newly generated and packets arriving from neighbors at time t on a V-interface are stored on the buffer immediately. Because of the limitation of the bandwidth of P-links, the maximum number of packets that can be sent from one P-interface at time t is set uniformly to W, resulting in the queuing delay. Every P-interface holds a packet buffer that can store $\mathcal{B}^P_{r,s}$ packets, and packets waiting for their turn to be sent out are stored in the buffer. Packets are basically processed in a first in, first out (FIFO) manner, but the sending order is determined randomly when a V-interface receives multiple packets simultaneously. When a packet arrives at an intermediate full buffer (i.e., $\sigma^{V_k}_{r,s}(t) = 0$), it is re-transmitted from its source V-node at the next time step. Packets are removed from the VN after either being re-transmitted R times or arriving at the destination V-node.

4.4.3 Evaluation results

Comparing the availability of the three types of PV-NoN model

First, we compare the performance regarding the availability of the type-SD, type-UD, and type-DD versions of the PV-NoN model. We set $V = 2$ as the number of VNs, $N^P = 100$ and $N^{V_k} = 0.9N^P$ $(k \in \mathcal{V})$ for the number of nodes, and $L^P = 3N^P$ and $L^{V_k} = 3N^{V_k}$ $(k \in \mathcal{V})$ for the number of links. The ER model is used to construct the PN topology, while both the ER and BA models are used for the VNs. In this evaluation, the inter/intranetwork connectivity is determined randomly without considering the assortativity. The packet buffer size for the P-interfaces is set to $\forall\mathcal{B}^P_{r,s} = 20$, and the bandwidth for the P-interfaces is set to $W = 1$; that is, each P-interface can send W packets from the network I/O every time unit. We simulate two types of traffic conditions based on the arrival rate λ: (i) an equal amount of traffic flows on each VN and (ii) traffic is biased toward one of the two VNs. For (i), λ for both VNs is changed in the range $[0.1, 1.6]$, while for (ii)

λ is fixed at 0.2 on VN1 and varied in the range $[0.2, 3.2]$ on VN2.

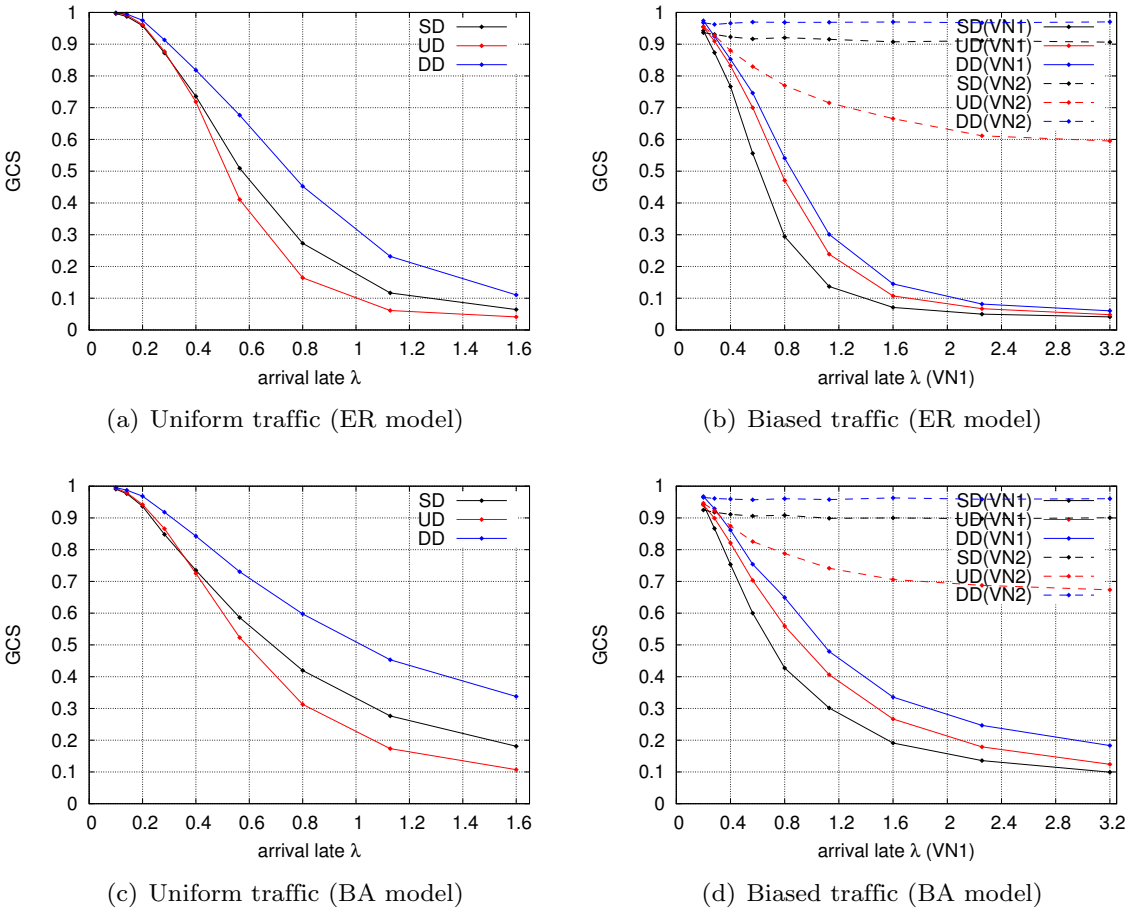

(a) Uniform traffic (ER model)

(b) Biased traffic (ER model)

(c) Uniform traffic (BA model)

(d) Biased traffic (BA model)

Figure 4.4: Variation of giant component size (GCS) with arrival rate λ.

We use the *giant component size* (GCS) and the *packet delay* as evaluation metrics to investigate NoN reliability from the perspectives of availability and communication performance. The GCS denotes the largest connected component on each VN consisting of available V-interfaces (i.e., $\sigma_{r,s}^{V_k}(t) = 1$), which we use to evaluate the availability of the entire network for each VN. The GCS is often used as a metric for complex networks [122, 126]. The packet delay denotes the average time required for a packet to be transmitted from its source to its destination, which is a more practical performance metric in communication networks. To see the impact of packet delay, we set the number of packet retransmissions to $R = 100$. In a realistic TCP/IP implementation, a much

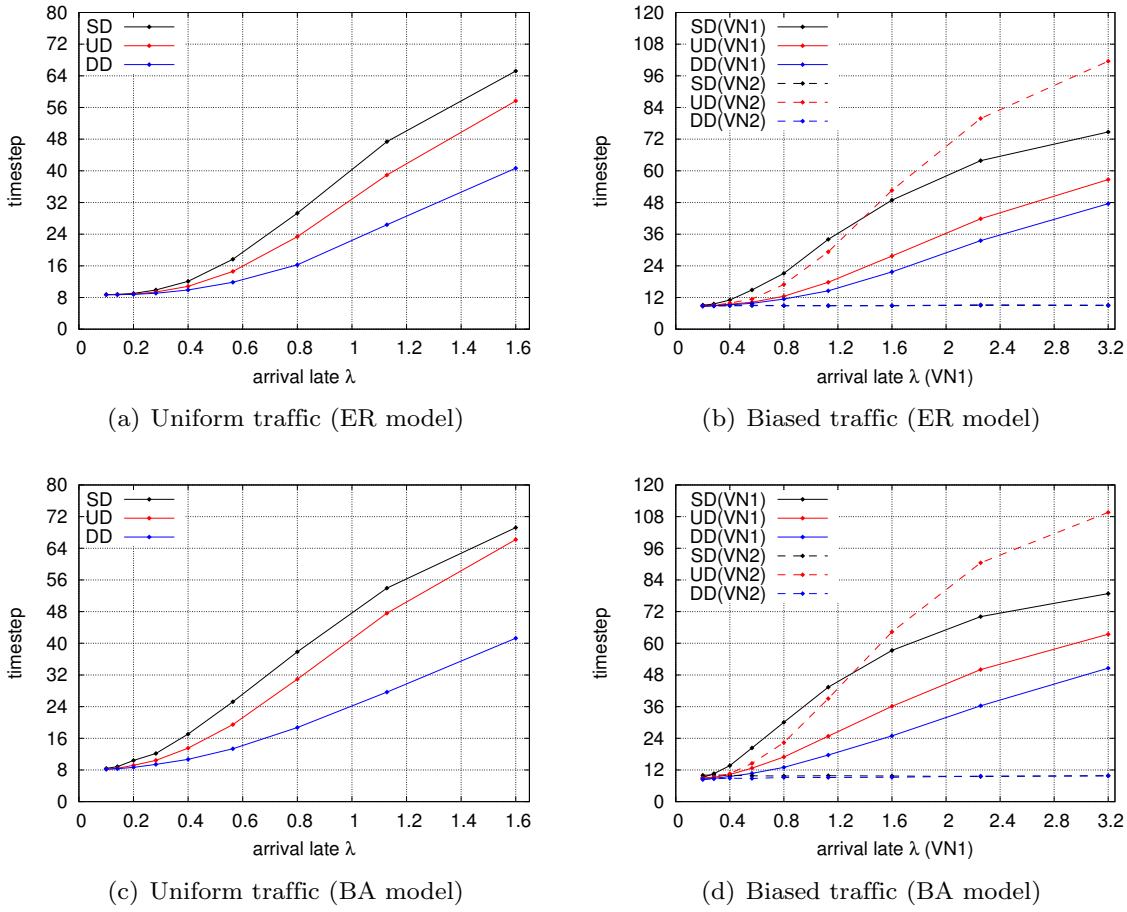

(a) Uniform traffic (ER model)

(b) Biased traffic (ER model)

(c) Uniform traffic (BA model)

(d) Biased traffic (BA model)

Figure 4.5: Variation of packet delay with arrival rate λ.

smaller number of around 10 would be used for the number of retransmissions. However, with such small values, only those packets whose source and destination are near each other can be transmitted successfully and longer routes do not work on the VN, thereby making it difficult to evaluate the impact of packet delay appropriately. Instead, we used $R = 100$ for the number of retransmissions. To evaluate the GCS, packets are created on the VN over 100 time steps and the GCS is measured at the 100th step, which is when the availability state of the V-interfaces is assumed to have converged and the simulation is finished. Regarding the packet delay, we create packets for the first 20 time steps and then continue the simulation until all the packets are either transmitted or removed from the VN. The packet delay is then counted for all the packets that were transmitted successfully

during the simulation. Each result shown is the mean value from 50 simulations.

The simulation results for the GCS are shown in Fig 4.4. The vertical axis represents the GCS: 1 indicates that all the nodes on a VN are connected, whereas 0 indicates that they are completely disconnected. The solid lines in (a) and (c) correspond to the average GCS of the two VNs, whereas the GCS for each VN is plotted separately in (b) and (d). The horizontal axis represents the arrival rate λ. In (b) and (d), note that λ is changed on VN1 but fixed on VN2. Each subfigure shows that type-DD gives the best availability of the three types of PV-NoN model. Although with type-SD traffic on one VN does not interfere with the other VN, neither VN can use its allocated physical resources fully because of the existence of the partition. Meanwhile, with type-UD the VNs can use their resources fully, but traffic between the VNs interferes with each other. Type-DD combines the characteristics of the other two types, thereby overcoming their shortcomings and improving the availability.

Another notable characteristic is observed in the simulation with biased traffic, as shown in Figs 4.4(b) and 4.4(d). Because there is no resource partition among the VNs in type-UD, traffic congestion in one VN influences the other interdependent VNs in a cascading manner. Therefore, of the three dotted lines, only the red one drops as the arrival rate λ increases. The extent to which cascades occur with type-UD is expected to increase further if the overlapping area of physical resources shared among the VNs increases. Meanwhile, even though type-DD also shares the physical resources of P-interfaces, the cascading of the performance degradation is prevented by the complementary dependence inspired by the B-NoN model.

Fig 4.5 shows the simulation results for the packet delay. The vertical axis represents the packet delay, required time steps for a packet to be transmitted. Similarly to Fig 4.4, the solid lines in (a) and (c) correspond to the average packet delay of the two VNs, whereas the packet delays for each VN are plotted separately in (b) and (d). The horizontal axis represents the arrival rate λ. In (b) and (d), note that λ is changed on VN1 but fixed on VN2. The performance of the packet delay can basically be explained in correspondence with the GCS results, and we confirm that the delay is lowest with type-DD. Type-DD can be said to be superior to the other two types regarding practical performance as a communication network. Another notable point is that the type-SD packet-delay performance degrades when compared with the GCS results in Fig 4.4. No matter how large the

buffer utilization (i.e., $\sum_{l \in \mathcal{V}} n_{r,s}^{V_l}(t)/\mathcal{B}_{r,s}^{P}$), the availability $\sigma_{r,s}^{V_k}(t)$, which is the basis of the GCS, is expressed as a binary state that does not take a negative value. On the other hand, the packet delay is expressed by taking any positive value reflecting the buffer utilization as it is. Based on these characteristics and results, we assume that interference among VNs with type-UD is likely to generate a number of moderately loaded V-interfaces to degrade the availability. Meanwhile, inefficient buffer allocation with type-SD is likely to generate rather few highly loaded V-interfaces to degrade the communication performance.

Designing influencers on the PV-NoN model

In this section, we investigate the importance of influencer deployment regarding inter/intranetwork assortativity. Because we confirmed above that type-DD prevails over the other two types, we focus on type-DD in this evaluation to investigate how to improve the performance further. The simulation settings are basically the same as those described in the previous evaluation, and we again use the GCS and packet delay to evaluate the availability and communication performance, respectively. However, to show the results concisely, we set the arrival rate for both VNs to $\lambda = 0.5$ because the evaluation above confirmed that changes in performance can be seen with that value. As for the inter/intranetwork assortativity of network influencers, we picked three cases for each assortativity: (i) *assort.* is the case in which the rewiring procedure described in Sec. 4.4.1 is repeated until the connectivity converges with the highest assortativity, (ii) *disassort.* corresponds to the analogous case with the lowest *assort.* value, and (iii) *non-assort.* is the case in which the original connectivity pattern is maintained.

Fig 4.6 shows to the GCS evaluation results, and Fig 4.7 shows those for the packet delay. The results are represented as heat maps in those figures. The GCS denotes the size of the largest connected component, and thus higher values indicate high performance (bright colors) in Fig. 4.6. Whereas, higher values indicate low performance (dark colors) in Fig. 4.7 in contrast to the GCS. First, we find that the GCS is increased when the intranetwork connectivity is assortative (i.e., $\eta > 0$) and the internetwork connectivity is disassortative (i.e., $\theta < 0$). We have shown previously that an assortative single network is fragile against random failures [22]. However, it is notable that

the results in Fig 4.7 tell us the opposite. We assume that when each VN topology is assortative, the overlapping of the shared physical resources among the VNs becomes concentrated on a local area of the entire NoN, thereby enhancing the availability when each VN is formed assortatively. By contrast, when $\theta < 0$, the high-influence nodes are likely to not be shared among the VNs but rather to be dedicated to each VN. Consequently, an efficient resource utilization is realized, resulting in improved availability.

The results also show that the assortativity configuration has greater influence on networks based on the BA model. Because of the biased degree distribution and the limitation in the procedure of topology construction, influencers have greater impact with the BA model. However, because the ER model (i) has a more uniform degree distribution compared to the BA model and (ii) its topological structure is generated randomly, the impact of the assortativity configuration is smaller.

By contrast, Fig 4.7 shows that the packet-delay performance is increased when the intranetwork connectivity is disassortative (i.e., $\eta < 0$). When a network topology is formed assortatively, the network diameter becomes large and the communication performance degrades. It is true that assortative connectivity within each VN has a positive impact on availability, as seen in Fig 4.6. However, from the practical viewpoint of communication performance, we find that the increase of network diameter has a larger negative impact, resulting in degraded communication performance. As for the internetwork assortativity, the packet delay is decreased when it is disassortative, similarly to the performance of GCS.

We ran simulations on type-UD and type-SD as well, but these merely confirmed that they show almost the same tendency in relation to the inter/intranetwork assortativity. A notable point is that the assortativity configuration had a larger influence on type-UD because the topological structure is closely related to the interference on the physical resources that is seen in type-UD.

4.4.4 Discussion and conclusion

With the growing use of network slicing to implement the IoT network environment, it has been pointed out that traffic fluctuation in a sliced network could propagate to other networks [9, 10].

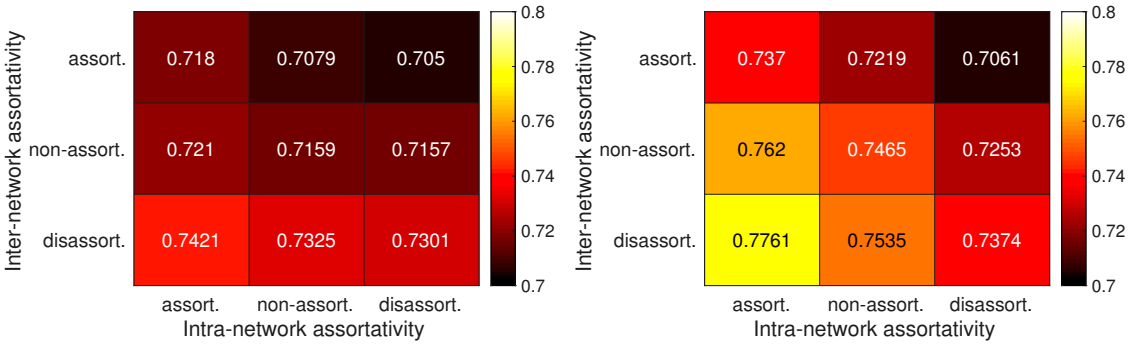

(a) ER model (b) BA model

Figure 4.6: GCS with changes in assortativity.

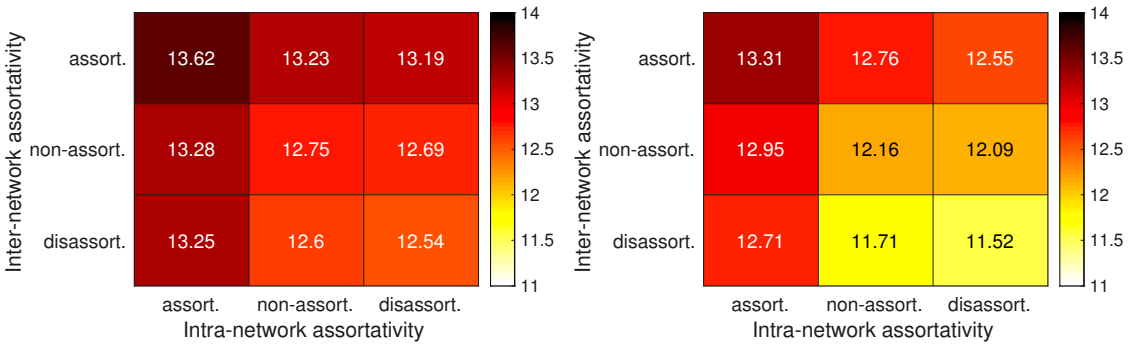

(a) ER model (b) BA model

Figure 4.7: Packet delay with changes in assortativity.

It has therefore become necessary to consider reliable design for not just single networks and interconnected networks but also interdependent networks, that is, an NoN. The existing NoN models [12, 21] describe the availability state of the NoN while considering the interdependence among the component networks, but are yet to be applied to practical systems of information networks. A contribution of the present work is that we considered layered VNs with network slicing as an NoN. We then proposed the PV-NoN model that expresses the availability state of an NoN that comprises a PN and VNs. The most notable aspect of our proposed model is that it considers traffic conditions and interdependence among the VNs. In this model, there are three types of interdependence according to the strategy used to divide the physical resources. With type-SD, the interface buffer

on the physical nodes is divided statically. With type-UD, the buffer is undivided and the traffic among the VNs interferes with itself in a logical AND-like way, as seen in the C-NoN model. With type-DD, the buffer is usually undivided but is divided when there is congestion, in which case interference occurs in a logical OR-like way similarly to the B-NoN model.

To investigate a reliable NoN design in the assumed network virtualization environment, in our simulation experiments we measured the GCS and packet delay on an NoN to evaluate the availability and communication performance. In the first experiment, we compared the performance of the three types of PV-NoN model, and we confirmed that in every case type-DD achieves the highest availability and communication performance. This superiority of type-DD arise from combining the guaranteed resource utilization of type-SD and the utilization efficiency of type-UD. Furthermore, we confirmed that type-DD prevents the cascading of performance degradation even though it shares physical resources on P-interfaces similarly to type-UD. In that aspect, even when dealing with interdependent network systems other than those based on network slicing, there appears to be potential for improving the availability of the system by adopting the complementary dependence inspired by the B-NoN model. Regarding the application of brain functional networks, it is also the case that type-DD appears to be highly resilient to network failures, which is one of the most notable characteristics of brain networks [16, 134].

We also conducted simulation experiments in which we configured the intra/internetwork assortativity of network influencers. The evaluation results confirmed that when the internetwork connectivity is disassortative (i.e., $\theta < 0$), both the availability and communication performance are improved because influential nodes are not shared among the VNs, thereby avoiding interference among those nodes. When the intranetwork connectivity is assortative (i.e., $\theta > 0$), the availability is improved while the communication performance is degraded. Although the internetwork connectivity affects only the interdependence among the VNs, the intranetwork connectivity also influences the structural performance of each VN in addition to the aforementioned interdependence. In detail, assortative connectivity within VNs localizes the area of physical resource sharing, thereby decreasing the interference among the VNs. At the same time, the assortative connectivity creates a long and narrow topology for each VN, thereby increasing the delay for packet communication. In a more practical scenario assuming the IoT environment, a larger-scale NoN must be

considered, wherein the number of VNs or network components increases greatly. In that sense, optimizing the NoN's structure would take an enormous amount of time and incur a huge computational cost. Consequently, structural configuration based on the assortativity of network influencers would help in designing reliable NoNs.

Because the main purpose of this paper was to deal with traffic fluctuations and interdependence on the assumed NoN environment, we configured the traffic pattern over the VNs in the simulation evaluation, which differentiates the performance among the three types of PV-NoN model. However, it would also be valuable to investigate the influence of network failures occurring on the PN as a future task. Because of the rapid development of the IoT network environment, where a skyrocketing of network scale, traffic amount, and service variety is expected, various types of NoN systems are expected to emerge in the IoT scenario. Consequently, it is our opinion that the findings in this paper will help to solve upcoming issues related to other NoN systems in the IoT environment besides VN environments based on network slicing.

Chapter 5

Conclusion

With the rapid development of information networks as social infrastructure, it has been imperative to establish methods for designing an NoN that is highly reliable under unpredictable fluctuations. To cope with this issue, we draw inspiration from brain functional networks: interdependent modular networks that have obtained robustness, scalability, and communication efficiency during the process of evolution. In this thesis, we investigated methods for designing reliable NoNs inspired by human brain networks, taking the connectivity and dependence between networks into consideration.

In Chap. 2, we first investigated the NoN structural design from the topological aspect of node connectivity focusing on the application of network influencers (i.e., the most influential elements over the entire network), and on assortativity between the networks, which represents the distinctive node degree correlation. The high reliability of human brain networks is known to be obtained by the network assortativity, one of the essential topological properties of brain networks. Here, we dealt with constructing not only a single network that possesses a specific degree of assortativity, but also an interconnected network where the assortativity between the component networks is specified, and therefore introduced a definition to measure assortativity between component networks based on the existing method of measuring assortativity between nodes. With respect to a single network, the results indicated that a decrease in assortativity provides high communication efficiency and distribution of communication load. Also we found, however, that excessive assortativity leads

to poor network performance. On the other hand, for an interconnected network assortative connections between networks improve communication efficiency, whereas disassortative connections distribute the communication load.

In Chap. 3, we then investigated the reliable design of NoN from geographical aspect and consider connectivity between network components. When recapturing the structure of NoN from a wide-area viewpoint, it is necessary to take geometrical constraints into account and to consider how to efficiently connect network components with each other. Thus, we proposed a method for assigning internetwork links based on a connectivity model observed in the cerebral cortex of the brain. Inter-modular connectivity in the cerebral cortex achieves high reliability when dealing with the trade-off of geometrical constraints and communication performance on the large-scale networks composed of many modules (i.e., regions) and nodes (i.e., neurons). Furthermore, we considered how to assign endpoint nodes of the links between each component by controlling assortativity. Simulation experiments showed that the proposed method based on the cerebral cortex model can construct an NoN topology with an optimal combination of communication efficiency, robustness, and wiring cost. For the selection of endpoint nodes for the internetwork links, the results showed that high assortativity enhances the robustness and communication efficiency due to the existence of many intramodular links attached to the high-degree endpoint nodes in either network component.

Only the structural reliability on an NoN was investigated in the studies described above, but it is also imperative to consider the dependency between network components, since there are many cases where the service availability of a network is closely tied with the other interdependent networks in the upcoming IoT scenario. In Chap. 4, to deal with a more concrete and fundamental interdependent network scenario that realizes an IoT environment, we focused on the network slicing technology. This enhances the utilization of physical networks while causing interdependence among sliced virtual networks due to traffic fluctuations from one network to the others. Among the NoN models that consider mutual dependence among networks, existing studies showed that the behavior of a NoN model based on brain functional networks reproduces the complementary internetwork dependence and elucidates the mechanisms that suppress the propagation of local fluctuations. Hence, we finally proposed an NoN model assuming a virtualized network environment

that describes the availability state of nodes to deal with traffic fluctuations and interdependence among the virtual and physical networks. We assumed three fundamental types of interdependence among the networks for this model based on the existing NoN models, and confirmed that the one applying complementary interdependence inspired by brain functional networks achieves high availability and communication performance while preventing interference among the sliced networks. Furthermore, we also investigated a method for designing a reliable network structure for the proposed model. To this end, the deployment of network influencers was configured from the perspective of intra-/internetwork assortativity. Simulation experiments confirmed that availability or communication performance is improved when each sliced network is formed assortatively or disassortatively, respectively. Regarding internetwork assortativity, both the availability and communication performance were improved when the influencers are deployed disassortatively among the sliced networks.

The emergence of interconnectivity and interdependence in the future Internet seem inevitable along with the anticipated increase of service diversity. Hence, the studies presented in this thesis capture the essential effects of the structure and interdependence of an NoN with respect to reliability, robustness, communication efficiency, construction cost, and scalability. We proposed methods for constructing interconnected network topologies and for configuring the interdependence of networks for a reliable design of NoNs. Future work entails further research in exploring a reliable design for NoN that is composed of more heterogeneous network components. In the era of smart cities, various types of communication services and infrastructure services are interconnected over the Internet. With the application of our proposed methods onto a specific scenario, it would also be required to consider the difference of network elements in each networks and their interdependencies. Another possible topic for future research is to simulate more realistic constraints that are assumed in the IoT environment. A variety of predictable and unpredictable application scenarios are expected in the IoT, and thus the simulations in our works targeted general metrics. On the basis of the proposed methods in our works, analysis based on actual constraints will help designing networks for a more specific environment, such as a hierarchical structure, which can appear when considering a more massive interconnected networks. Besides, there still exists technical limitation on analysing brain networks with the current neuroimaging techniques. The future development of

neuroscience will further reveal other characteristic mechanisms of brain networks, and it will help resolve complex issues occurring on the sophisticated information networks.

Bibliography

[1] F. Firouzi, A. M. Rahmani, K. Mankodiya, M. Badaroglu, G. Merrett, P. Wong, and B. Farahani, "Internet-of-things and big data for smarter healthcare: From device to architecture, applications and analytics," *Future Generation Computer Systems*, vol. 78, pp. 583 – 586, 2018. [Online]. Available: http://www.sciencedirect.com/science/article/pii/S0167739X17319726

[2] P. Ray, "A survey on internet of things architectures," *Journal of King Saud University - Computer and Information Sciences*, vol. 30, no. 3, pp. 291 – 319, 2018. [Online]. Available: http://www.sciencedirect.com/science/article/pii/S1319157816300799

[3] S. Li, L. D. Xu, and S. Zhao, "5g internet of things: A survey," *Journal of Industrial Information Integration*, vol. 10, pp. 1 – 9, 2018. [Online]. Available: http://www.sciencedirect.com/science/article/pii/S2452414X18300037

[4] I. Ud Din, M. Guizani, S. Hassan, B. Kim, M. Khurram Khan, M. Atiquzzaman, and S. H. Ahmed, "The internet of things: A review of enabled technologies and future challenges," *IEEE Access*, vol. 7, pp. 7606–7640, 2019.

[5] S. F. Ochoa, G. Fortino, and G. D. Fatta, "Cyber-physical systems, internet of things and big data," *Future Generation Computer Systems*, vol. 75, pp. 82 – 84, 2017.

[6] H. Arasteh, V. Hosseinnezhad, V. Loia, A. Tommasetti, O. Troisi, M. Shafie-khah, and P. Siano, "Iot-based smart cities: A survey," in *2016 IEEE 16th International Conference on Environment and Electrical Engineering (EEEIC)*, June 2016, pp. 1–6.

[7] A. Whitmore, A. Agarwal, and L. Da Xu, "The internet of things—a survey of topics and trends," *Information Systems Frontiers*, vol. 17, no. 2, pp. 261–274, Apr 2015. [Online]. Available: https://doi.org/10.1007/s10796-014-9489-2

[8] J. Gao, S. V. Buldyrev, H. E. Stanley, and S. Havlin, "Networks formed from interdependent networks," *Nature Physics*, vol. 8, p. 40, 12 2011.

[9] B. Han, V. Gopalakrishnan, L. Ji, and S. Lee, "Network function virtualization: Challenges and opportunities for innovations," *IEEE Communications Magazine*, vol. 53, no. 2, pp. 90–97, Feb 2015.

[10] J. Liu, Z. Jiang, N. Kato, O. Akashi, and A. Takahara, "Reliability evaluation for nfv deployment of future mobile broadband networks," *IEEE Wireless Communications*, vol. 23, no. 3, pp. 90–96, June 2016.

[11] Y.-Z. Chen, Z.-G. Huang, H.-F. Zhang, D. Eisenberg, T. P. Seager, and Y.-C. Lai, "Extreme events in multilayer, interdependent complex networks and control," *Scientific reports*, vol. 5, 2015.

[12] S. V. Buldyrev, R. Parshani, G. Paul, H. E. Stanley, and S. Havlin, "Catastrophic cascade of failures in interdependent networks," *Nature*, vol. 464, no. 7291, pp. 1025–1028, Apr. 2010.

[13] P. Neirotti, A. De Marco, A. C. Cagliano, G. Mangano, and F. Scorrano, "Current trends in smart city initiatives: Some stylised facts," *Cities*, vol. 38, pp. 25–36, Jun. 2014.

[14] A. I. Sarwat, A. Sundararajan, I. Parvez, M. Moghaddami, and A. Moghadasi, *Toward a Smart City of Interdependent Critical Infrastructure Networks*. Cham: Springer International Publishing, 2018, pp. 21–45. [Online]. Available: https://doi.org/10.1007/978-3-319-74412-4_3

[15] M. H. Amini, H. Arasteh, and P. Siano, *Sustainable Smart Cities Through the Lens of Complex Interdependent Infrastructures: Panorama and State-of-the-art*. Cham: Springer International Publishing, 2019, pp. 45–68. [Online]. Available: https://doi.org/10.1007/978-3-319-98923-5_3

[16] E. Bullmore and O. Sporns, "The economy of brain network organization," *Nature Reviews Neuroscience*, vol. 13, pp. 336–349, 04 2012.

[17] O. Sporns and R. F. Betzel, "Modular brain networks," *Annual review of psychology*, vol. 67, p. 613, 2016.

[18] A. Avena-Koenigsberger, B. Misic, and O. Sporns, "Communication dynamics in complex brain networks," *Nature Reviews Neuroscience*, vol. 19, no. 1, pp. 17–33, 2018. [Online]. Available: https://doi.org/10.1038/nrn.2017.149

[19] J. Z. Kim, J. M. Soffer, A. E. Kahn, J. M. Vettel, F. Pasqualetti, and D. S. Bassett, "Role of graph architecture in controlling dynamical networks with applications to neural systems," *Nature Physics*, vol. 14, no. 1, pp. 91–98, 2018. [Online]. Available: https://doi.org/10.1038/nphys4268

[20] O. Sporns, "Graph theory methods: applications in brain networks," *Dialogues in clinical neuroscience*, vol. 20, no. 2, pp. 111–121, 06 2018. [Online]. Available: https://www.ncbi.nlm.nih.gov/pubmed/30250388

[21] F. Morone, K. Roth, B. Min, H. E. Stanley, and H. A. Makse, "Model of brain activation predicts the neural collective influence map of the brain," *Proceedings of the National Academy of Sciences*, vol. 114, no. 15, pp. 3849–3854, 2017. [Online]. Available: http://www.pnas.org/content/114/15/3849

[22] M. Murakami, S. Ishikura, D. Kominami, T. Shimokawa, and M. Murata, "Robustness and efficiency in interconnected networks with changes in network assortativity," *Applied Network Science*, vol. 2, no. 1, p. 6, 2017. [Online]. Available: https://doi.org/10.1007/s41109-017-0025-4

[23] M. Murakami, K. Leibnitz, D. Kominami, T. Shimokawa, and M. Murata, "Constructing a virtual iot network using a cerebral cortical connectivity model," *Technical Report of IEICE (CCS2016-18)*, vol. 116, no. 180, August 2016.

[24] ——, "Constructing virtual iot network topologies with a brain-inspired connectivity model," in *Proceedings of the 11th International Conference on Ubiquitous Information Management and Communication*, ser. IMCOM '17. New York, NY, USA: ACM, 2017, pp. 78:1–78:8. [Online]. Available: http://doi.acm.org/10.1145/3022227.3022304

[25] M. Murakami, D. Kominami, K. Leibnitz, and M. Murata, "Drawing inspiration from human brain networks: Construction of interconnected virtual networks," *Sensors*, vol. 18, no. 4, 2018. [Online]. Available: https://www.mdpi.com/1424-8220/18/4/1133

[26] M. Murakami, K. Leibnitz, D. Kominami, and M. Murata, "Analysis and strategies for improving robustness and efficiency in interconnected networks," *Technical Report of IEICE (IN2016-166)*, vol. 116, no. 485, March 2017.

[27] ——, "Reliable architecture for network of networks with inspiration from brain networks," *Technical Report of IEICE (IN2017-111)*, vol. 117, no. 460, March 2017.

[28] ——, "Designing interconnected networks for improving robustness and efficiency," in *2017 IEEE International Symposium on Local and Metropolitan Area Networks (LANMAN)*, June 2017, pp. 1–6.

[29] M. Murakami, D. Kominami, K. Leibnitz, and M. Murata, "Reliable design for a network of networks with inspiration from brain functional networks," *Applied Sciences*, vol. 9, no. 18, 2019. [Online]. Available: https://www.mdpi.com/2076-3417/9/18/3809

[30] L. Atzori, A. Iera, and G. Morabito, "The Internet of Things: A survey," *Computer Networks*, vol. 54, no. 15, pp. 2787–2805, May 2010.

[31] A. Whitmore, A. Agarwal, and L. Da Xu, "The internet of things—a survey of topics and trends," *Information Systems Frontiers*, vol. 17, no. 2, pp. 261–274, 2015.

[32] D. Evans, "The internet of things," *How the Next Evolution of the Internet is Changing Everything, Whitepaper, Cisco Internet Business Solutions Group (IBSG)*, vol. 1, pp. 1–12, 2011.

[33] J. P. Bailey, "The economics of internet interconnection agreements," *Internet economics*, vol. 35, pp. 155–168, Mar. 1997.

[34] J. Gubbi, R. Buyya, S. Marusic, and M. Palaniswami, "Internet of Things (IoT): A vision, architectural elements, and future directions," *Future Generation Computer Systems*, vol. 29, no. 7, pp. 1645–1660, Sep. 2013.

[35] J.-D. J. Han, N. Bertin, T. Hao, D. S. Goldberg, G. F. Berriz, L. V. Zhang, D. Dupuy, A. J. Walhout, M. E. Cusick, F. P. Roth *et al.*, "Evidence for dynamically organized modularity in the yeast protein–protein interaction network," *Nature*, vol. 430, no. 6995, pp. 88–93, 2004.

[36] G. Zamora-López, C. Zhou, and J. Kurths, "Exploring brain function from anatomical connectivity," *Frontiers in neuroscience*, vol. 5, pp. 1–11, Jun. 2011.

[37] P. Hagmann, L. Cammoun, X. Gigandet, R. Meuli, C. J. Honey, V. J. Wedeen, and O. Sporns, "Mapping the structural core of human cerebral cortex," *PLoS biology*, vol. 6, no. 7, pp. 1479–1493, Jul. 2008.

[38] E. Bullmore and O. Sporns, "Complex brain networks: Graph theoretical analysis of structural and functional systems," *Nature Reviews Neuroscience*, vol. 10, no. 3, pp. 186–198, Apr. 2009.

[39] F. Klimm, D. S. Bassett, J. M. Carlson, and P. J. Mucha, "Resolving structural variability in network models and the brain," *arXiv preprint arXiv:1306.2893*, vol. 1, pp. 1–33, Jun. 2013.

[40] U. Brandes, "On variants of shortest-path betweenness centrality and their generic computation," *Social Networks*, vol. 30, no. 2, pp. 136–145, May 2008.

[41] M. E. J. Newman, "Assortative mixing in networks," *Phys. Rev. Lett.*, vol. 89, p. 208701, Oct 2002. [Online]. Available: https://link.aps.org/doi/10.1103/PhysRevLett.89.208701

[42] G. D'Agostino, A. Scala, V. Zlatić, and G. Caldarelli, "Robustness and assortativity for diffusion-like processes in scale-free networks," *Europhysics Letters (EPL)*, vol. 97, no. 6, pp. 1–5, May 2012.

[43] K. Klemm, M. Á. Serrano, V. M. Eguíluz, and M. San Miguel, "A measure of individual role in collective dynamics," *Scientific reports*, vol. 2, pp. 1–7, Feb. 2012.

[44] S. Bansal, B. T. Grenfell, and L. A. Meyers, "When individual behaviour matters: homogeneous and network models in epidemiology," *Journal of the Royal Society Interface*, vol. 4, no. 16, pp. 879–891, Oct. 2007.

[45] R. Xulvi-Brunet and I. Sokolov, "Reshuffling scale-free networks: From random to assortative," *Physical Review E*, vol. 70, no. 6, p. 066102, 2004.

[46] G.-Q. Zhang, S.-Q. Cheng, and G.-Q. Zhang, "A universal assortativity measure for network analysis," *arXiv preprint arXiv:1212.6456*, vol. 1, pp. 1–8, Dec. 2012.

[47] P. Van Mieghem, H. Wang, X. Ge, S. Tang, and F. Kuipers, "Influence of assortativity and degree-preserving rewiring on the spectra of networks," *The European Physical Journal B*, vol. 76, no. 4, pp. 643–652, 2010.

[48] R. Noldus and P. Van Mieghem, "Effect of degree-preserving, assortative rewiring on ospf router configuration," in *Proceedings of the 2013 25th International Teletraffic Congress (ITC)*. Shanghai, China: IEEE, 2013, pp. 1–4.

[49] W. Winterbach, D. de Ridder, H. Wang, M. Reinders, and P. Van Mieghem, "Do greedy assortativity optimization algorithms produce good results?" *The European Physical Journal B*, vol. 85, no. 5, pp. 1–9, 2012.

[50] W. O. Kermack and A. G. McKendrick, "A contribution to the mathematical theory of epidemics," *Proceedings of the Royal Society of London A: mathematical, physical and engineering sciences*, vol. 115, no. 772, pp. 700–721, May 1927.

[51] S. A. J. Marsden, L. S. S. Wiggins, L. Glass, R. Kohn, and S. Sastry, *Interdisciplinary Applied Mathematics*. New York City, Uniter States: Springer, 1993.

[52] A.-L. Barabási and R. Albert, "Emergence of scaling in random networks," *Science*, vol. 286, no. 5439, pp. 509–512, 1999.

[53] M. E. Newman, "Models of the small world," *Journal of Statistical Physics*, vol. 101, no. 3-4, pp. 819–841, Nov. 2000.

[54] V. D. Blondel, J.-L. Guillaume, R. Lambiotte, and E. Lefebvre, "Fast unfolding of communities in large networks," *Journal of statistical mechanics: theory and experiment*, vol. 2008, no. 10, p. P10008, Oct. 2008.

[55] I. Akyildiz, W. Su, Y. Sankarasubramaniam, and E. Cayirci, "Wireless sensor networks: a survey," *Computer Networks*, vol. 38, no. 4, pp. 393 – 422, 2002. [Online]. Available: http://www.sciencedirect.com/science/article/pii/S1389128601003024

[56] U. Raza, P. Kulkarni, and M. Sooriyabandara, "Low power wide area networks: An overview," *IEEE Communications Surveys Tutorials*, vol. 19, no. 2, pp. 855–873, Secondquarter 2017.

[57] K. E. Nolan, W. Guibene, and M. Y. Kelly, "An evaluation of low power wide area network technologies for the internet of things," in *2016 International Wireless Communications and Mobile Computing Conference (IWCMC)*, Sept 2016, pp. 439–444.

[58] W. Shi, J. Cao, Q. Zhang, Y. Li, and L. Xu, "Edge computing: Vision and challenges," *IEEE Internet of Things Journal*, vol. 3, no. 5, pp. 637–646, Oct 2016.

[59] M. Satyanarayanan, "The emergence of edge computing," *Computer*, vol. 50, no. 1, pp. 30–39, Jan 2017.

[60] S. Yi, Z. Hao, Z. Qin, and Q. Li, "Fog computing: Platform and applications," in *2015 Third IEEE Workshop on Hot Topics in Web Systems and Technologies (HotWeb)*, Nov 2015, pp. 73–78.

[61] A. V. Dastjerdi and R. Buyya, "Fog computing: Helping the internet of things realize its potential," *Computer*, vol. 49, no. 8, pp. 112–116, Aug 2016.

[62] J. A. Stankovic, "Research directions for the internet of things," *IEEE Internet of Things Journal*, vol. 1, no. 1, pp. 3–9, Feb 2014.

[63] L. D. Xu, W. He, and S. Li, "Internet of things in industries: A survey," *IEEE Transactions on Industrial Informatics*, vol. 10, no. 4, pp. 2233–2243, Nov 2014.

[64] B. Han, V. Gopalakrishnan, L. Ji, and S. Lee, "Network function virtualization: Challenges and opportunities for innovations," *IEEE Communications Magazine*, vol. 53, no. 2, pp. 90–97, Feb 2015.

[65] R. Mijumbi, J. Serrat, J. L. Gorricho, N. Bouten, F. D. Turck, and R. Boutaba, "Network function virtualization: State-of-the-art and research challenges," *IEEE Communications Surveys Tutorials*, vol. 18, no. 1, pp. 236–262, Firstquarter 2016.

[66] B. A. A. Nunes, M. Mendonca, X. N. Nguyen, K. Obraczka, and T. Turletti, "A survey of software-defined networking: Past, present, and future of programmable networks," *IEEE Communications Surveys Tutorials*, vol. 16, no. 3, pp. 1617–1634, Third 2014.

[67] D. Kreutz, F. M. V. Ramos, P. E. Veríssimo, C. E. Rothenberg, S. Azodolmolky, and S. Uhlig, "Software-defined networking: A comprehensive survey," *Proceedings of the IEEE*, vol. 103, no. 1, pp. 14–76, Jan 2015.

[68] X. Zhou, R. Li, T. Chen, and H. Zhang, "Network slicing as a service: enabling enterprises' own software-defined cellular networks," *IEEE Communications Magazine*, vol. 54, no. 7, pp. 146–153, July 2016.

[69] H. Zhang, N. Liu, X. Chu, K. Long, A. H. Aghvami, and V. C. M. Leung, "Network slicing based 5g and future mobile networks: Mobility, resource management, and challenges," *IEEE Communications Magazine*, vol. 55, no. 8, pp. 138–145, 2017.

[70] C. Liang and F. R. Yu, "Wireless network virtualization: A survey, some research issues and challenges," *IEEE Communications Surveys & Tutorials*, vol. 17, no. 1, pp. 358–380, 2015.

[71] I. Khan, F. Belqasmi, R. Glitho, N. Crespi, M. Morrow, and P. Polakos, "Wireless sensor network virtualization: A survey," *IEEE Communications Surveys Tutorials*, vol. 18, no. 1, pp. 553–576, Firstquarter 2016.

[72] M. Richart, J. Baliosian, J. Serrat, and J.-L. Gorricho, "Resource slicing in virtual wireless networks: A survey," *IEEE Transactions on Network and Service Management*, 2016.

[73] H. I. Kobo, A. M. Abu-Mahfouz, and G. P. Hancke, "A survey on software-defined wireless sensor networks: Challenges and design requirements," *IEEE Access*, vol. 5, pp. 1872–1899, 2017.

[74] K. M. Modieginyane, B. B. Letswamotse, R. Malekian, and A. M. Abu-Mahfouz, "Software defined wireless sensor networks application opportunities for efficient network management: A survey," *Computers & Electrical Engineering*, vol. 66, pp. 274 – 287, 2018. [Online]. Available: http://www.sciencedirect.com/science/article/pii/S0045790617304159

[75] R. Morabito, V. Cozzolino, A. Y. Ding, N. Beijar, and J. Ott, "Consolidate iot edge computing with lightweight virtualization," *IEEE Network*, vol. 32, no. 1, pp. 102–111, Jan 2018.

[76] A. C. Baktir, A. Ozgovde, and C. Ersoy, "How can edge computing benefit from software-defined networking: A survey, use cases, and future directions," *IEEE Communications Surveys Tutorials*, vol. 19, no. 4, pp. 2359–2391, Fourthquarter 2017.

[77] R. Morabito and N. Beijar, "Enabling data processing at the network edge through lightweight virtualization technologies," in *2016 IEEE International Conference on Sensing, Communication and Networking (SECON Workshops)*, June 2016, pp. 1–6.

[78] R. Morabito, R. Petrolo, V. Loscrí, and N. Mitton, "Enabling a lightweight edge gateway-as-a-service for the internet of things," in *2016 7th International Conference on the Network of the Future (NOF)*, Nov 2016, pp. 1–5.

[79] A. Mayoral, R. Vilalta, R. Casellas, R. Martinez, and R. Munoz, "Multi-tenant 5g network slicing architecture with dynamic deployment of virtualized tenant management and orchestration (mano) instances," in *ECOC 2016; 42nd European Conference on Optical Communication; Proceedings of*. VDE, Dec. 2016, pp. 1–3.

[80] O. Kaiwartya, A. H. Abdullah, Y. Cao, J. Lloret, S. Kumar, R. R. Shah, M. Prasad, and S. Prakash, "Virtualization in wireless sensor networks: Fault tolerant embedding for internet of things," *IEEE Internet of Things Journal*, vol. PP, no. 99, pp. 1–1, 2017.

[81] R. Morabito, "Virtualization on internet of things edge devices with container technologies: A performance evaluation," *IEEE Access*, vol. 5, pp. 8835–8850, 2017.

[82] J. Li, J. Jin, D. Yuan, and H. Zhang, "Virtual fog: A virtualization enabled fog computing framework for internet of things," *IEEE Internet of Things Journal*, vol. 5, no. 1, pp. 121–131, Feb 2018.

[83] W. Roh, J. Y. Seol, J. Park, B. Lee, J. Lee, Y. Kim, J. Cho, K. Cheun, and F. Aryanfar, "Millimeter-wave beamforming as an enabling technology for 5g cellular communications: theoretical feasibility and prototype results," *IEEE Communications Magazine*, vol. 52, no. 2, pp. 106–113, February 2014.

[84] S. Kutty and D. Sen, "Beamforming for millimeter wave communications: An inclusive survey," *IEEE Communications Surveys Tutorials*, vol. 18, no. 2, pp. 949–973, Secondquarter 2016.

[85] M. Ercsey-Ravasz, N. T. Markov, C. Lamy, D. C. Van Essen, K. Knoblauch, Z. Toroczkai, and H. Kennedy, "A predictive network model of cerebral cortical connectivity based on a distance rule," *Neuron*, vol. 80, no. 1, pp. 184–197, Oct. 2013.

[86] F. Klimm, D. S. Bassett, J. M. Carlson, and P. J. Mucha, "Resolving structural variability in network models and the brain," *PLOS Computational Biology*, vol. 10, no. 3, pp. 1–22, 03 2014. [Online]. Available: https://doi.org/10.1371/journal.pcbi.1003491

[87] D. S. Bassett and E. Bullmore, "Small-world brain networks," *The neuroscientist*, vol. 12, no. 6, pp. 512–523, 2006.

[88] V. M. Eguiluz, D. R. Chialvo, G. A. Cecchi, M. Baliki, and A. V. Apkarian, "Scale-free brain functional networks," *Physical review letters*, vol. 94, no. 1, p. 018102, 2005.

[89] M. P. van den Heuvel, C. J. Stam, M. Boersma, and H. H. Pol, "Small-world and scale-free organization of voxel-based resting-state functional connectivity in the human brain," *Neuroimage*, vol. 43, no. 3, pp. 528–539, 2008.

[90] O. Sporns, *Networks of the Brain*, 1st ed. The MIT Press, 2010.

[91] D. Meunier, R. Lambiotte, and E. T. Bullmore, "Modular and hierarchically modular organization of brain networks," *Frontiers in Neuroscience*, vol. 4, no. 200, pp. 1–11, Dec. 2010.

[92] D. Meunier, R. Lambiotte, A. Fornito, K. Ersche, and E. Bullmore, "Hierarchical modularity in human brain functional networks," *Frontiers in Neuroinformatics*, vol. 3, p. 37, 2009. [Online]. Available: https://www.frontiersin.org/article/10.3389/neuro.11.037.2009

[93] K. Knoblauch, M. Ercsey-Ravasz, H. Kennedy, and Z. Toroczkai, "The brain in space," in *Micro-, meso-and macro-connectomics of the brain*. Springer, 2016, pp. 45–74.

[94] M. Kaiser and C. C. Hilgetag, "Nonoptimal component placement, but short processing paths, due to long-distance projections in neural systems," *PLoS Comput Biol*, vol. 2, no. 7, p. e95, 2006.

[95] S. Boccaletti, V. Latora, Y. Moreno, M. Chavez, and D.-U. Hwang, "Complex networks: Structure and dynamics," *Physics Reports*, vol. 424, no. 4, pp. 175 – 308, 2006. [Online]. Available: http://www.sciencedirect.com/science/article/pii/S037015730500462X

[96] M. Fiedler, "Algebraic connectivity of graphs," *Czechoslovak Mathematical Journal*, vol. 23, no. 2, pp. 298–305, 1973. [Online]. Available: http://eudml.org/doc/12723

[97] A. Jamakovic and P. Van Mieghem, "On the robustness of complex networks by using the algebraic connectivity," in *NETWORKING 2008 Ad Hoc and Sensor Networks, Wireless Networks, Next Generation Internet: 7th International IFIP-TC6 Networking Conference Singapore, May 5-9, 2008 Proceedings*, A. Das, H. K. Pung, F. B. S. Lee, and L. W. C. Wong, Eds. Berlin, Heidelberg: Springer Berlin Heidelberg, May 2008, pp. 183–194. [Online]. Available: https://doi.org/10.1007/978-3-540-79549-0_16

[98] A. Jamakovic and S. Uhlig, "On the relationship between the algebraic connectivity and graph's robustness to node and link failures," in *2007 Next Generation Internet Networks*, May 2007, pp. 96–102.

[99] M. J. Alenazi, E. K. Çetinkaya, and J. P. Sterbenz, "Cost-efficient algebraic connectivity optimisation of backbone networks," *Optical Switching and Networking*, vol. 14, no. Part 2, pp. 107 – 116, 2014, special Issue on RNDM 2013. [Online]. Available: http://www.sciencedirect.com/science/article/pii/S157342771400037X

[100] A. Sydney, C. Scoglio, and D. Gruenbacher, "Optimizing algebraic connectivity by edge rewiring," *Applied Mathematics and Computation*, vol. 219, no. 10, pp. 5465 – 5479, 2013. [Online]. Available: http://www.sciencedirect.com/science/article/pii/S0096300312011551

[101] H. T. Friis, "A note on a simple transmission formula," *Proceedings of the Institute of Radio Engineers*, vol. 34, no. 5, pp. 254–256, May 1946.

[102] P. Erdös and A. Rényi, "On random graphs, i," *Publicationes Mathematicae (Debrecen)*, vol. 6, pp. 290–297, 1959.

[103] H. Kawahigashi, Y. Terashima, N. Miyauchi, and T. Nakakawaji, "Modeling ad hoc sensor networks using random graph theory," in *Second IEEE Consumer Communications and Networking Conference (CCNC 2005)*, Jan 2005, pp. 104–109.

[104] F. A. Onat and I. Stojmenovic, "Generating random graphs for wireless actuator networks," in *2007 IEEE International Symposium on a World of Wireless, Mobile and Multimedia Networks*, June 2007, pp. 1–12.

[105] L. Ding and Z.-H. Guan, "Modeling wireless sensor networks using random graph theory," *Physica A: Statistical Mechanics and its Applications*, vol. 387, no. 12, pp. 3008 – 3016, 2008.

[106] N. T. Markov, M. Ercsey-Ravasz, C. Lamy, A. R. Ribeiro Gomes, L. Magrou, P. Misery, P. Giroud, P. Barone, C. Dehay, Z. Toroczkai, K. Knoblauch, D. C. Van Essen, and

H. Kennedy, "The role of long-range connections on the specificity of the macaque interareal cortical network," *Proceedings of the National Academy of Sciences*, vol. 110, no. 13, pp. 5187–5192, 2013. [Online]. Available: http://www.pnas.org/content/110/13/5187.abstract

[107] D. S. Michalopoulos, M. Doll, V. Sciancalepore, D. Bega, P. Schneider, and P. Rost, "Network slicing via function decomposition and flexible network design," in *2017 IEEE 28th Annual International Symposium on Personal, Indoor, and Mobile Radio Communications (PIMRC)*, Oct 2017, pp. 1–6.

[108] F. Z. Yousaf, M. Gramaglia, V. Friderikos, B. Gajic, D. von Hugo, B. Sayadi, V. Sciancalepore, and M. R. Crippa, "Network slicing with flexible mobility and qos/qoe support for 5g networks," in *2017 IEEE International Conference on Communications Workshops (ICC Workshops)*, May 2017, pp. 1195–1201.

[109] P. Rost, C. Mannweiler, D. S. Michalopoulos, C. Sartori, V. Sciancalepore, N. Sastry, O. Holland, S. Tayade, B. Han, D. Bega, D. Aziz, and H. Bakker, "Network slicing to enable scalability and flexibility in 5g mobile networks," *IEEE Communications Magazine*, vol. 55, no. 5, pp. 72–79, May 2017.

[110] X. Li, R. Casellas, G. Landi, A. de la Oliva, X. Costa-Perez, A. Garcia-Saavedra, T. Deiss, L. Cominardi, and R. Vilalta, "5g-crosshaul network slicing: Enabling multi-tenancy in mobile transport networks," *IEEE Communications Magazine*, vol. 55, no. 8, pp. 128–137, 2017.

[111] D. Kempe, J. Kleinberg, and É. Tardos, "Maximizing the spread of influence through a social network," in *Proceedings of the ninth ACM SIGKDD international conference on Knowledge discovery and data mining*. ACM, Aug. 2003, pp. 137–146.

[112] R. Albert, H. Jeong, and A.-L. Barabási, "Error and attack tolerance of complex networks," *nature*, vol. 406, no. 6794, pp. 378–382, Jul. 2000.

[113] R. Cohen, K. Erez, D. ben Avraham, and S. Havlin, "Breakdown of the internet under intentional attack," *Phys. Rev. Lett.*, vol. 86, pp. 3682–3685, Apr 2001. [Online]. Available: https://link.aps.org/doi/10.1103/PhysRevLett.86.3682

[114] W. Chen, Y. Wang, and S. Yang, "Efficient influence maximization in social networks," in *Proceedings of the 15th ACM SIGKDD International Conference on Knowledge Discovery and Data Mining*, ser. KDD '09. New York, NY, USA: ACM, 2009, pp. 199–208.

[115] Y. Chen, G. Paul, S. Havlin, F. Liljeros, and H. E. Stanley, "Finding a better immunization strategy," *Phys. Rev. Lett.*, vol. 101, p. 058701, Jul 2008. [Online]. Available: https://link.aps.org/doi/10.1103/PhysRevLett.101.058701

[116] M. E. J. Newman, "Spread of epidemic disease on networks," *Phys. Rev. E*, vol. 66, p. 016128, Jul 2002.

[117] M. Richardson and P. Domingos, "Mining knowledge-sharing sites for viral marketing," in *Proceedings of the eighth ACM SIGKDD international conference on Knowledge discovery and data mining*. ACM, Jul. 2002, pp. 61–70.

[118] C. Kiss and M. Bichler, "Identification of influencers — measuring influence in customer networks," *Decision Support Systems*, vol. 46, no. 1, pp. 233 – 253, 2008. [Online]. Available: http://www.sciencedirect.com/science/article/pii/S0167923608001231

[119] M. Kitsak, L. K. Gallos, S. Havlin, F. Liljeros, L. Muchnik, H. E. Stanley, and H. A. Makse, "Identification of influential spreaders in complex networks," *Nature physics*, vol. 6, no. 11, pp. 888–893, Jul. 2010.

[120] Z.-K. Bao, C. Ma, B.-B. Xiang, and H.-F. Zhang, "Identification of influential nodes in complex networks: Method from spreading probability viewpoint," *Physica A: Statistical Mechanics and its Applications*, vol. 468, pp. 391–397, Feb. 2017.

[121] L. Lü, D. Chen, X.-L. Ren, Q.-M. Zhang, Y.-C. Zhang, and T. Zhou, "Vital nodes identification in complex networks," *Physics Reports*, vol. 650, pp. 1–63, Sep. 2016.

[122] F. Morone and H. A. Makse, "Influence maximization in complex networks through optimal percolation," *Nature*, vol. 524, p. 65, 07 2015.

[123] Z. Wang, X. Wang, F. Hou, Y. Luo, and Z. Wang, "Dynamic memory balancing for virtualization," *ACM Trans. Archit. Code Optim.*, vol. 13, no. 1, pp. 2:1–2:25, Mar. 2016. [Online]. Available: http://doi.acm.org/10.1145/2851501

[124] M. Beshley, V. Romanchuk, V. Chervenets, and A. Masiuk, "Ensuring the quality of service flows in multiservice infrastructure based on network node virtualization," in *2016 International Conference Radio Electronics Info Communications (UkrMiCo)*, Sept 2016, pp. 1–3.

[125] J. G. Herrera and J. F. Botero, "Resource allocation in nfv: A comprehensive survey," *IEEE Transactions on Network and Service Management*, vol. 13, no. 3, pp. 518–532, Sept 2016.

[126] D. S. Callaway, M. E. J. Newman, S. H. Strogatz, and D. J. Watts, "Network robustness and fragility: Percolation on random graphs," *Phys. Rev. Lett.*, vol. 85, pp. 5468–5471, Dec 2000. [Online]. Available: https://link.aps.org/doi/10.1103/PhysRevLett.85.5468

[127] D. J. Watts and S. H. Strogatz, "Collective dynamics of 'small-world'networks," *Nature*, vol. 393, p. 440, 06 1998.

[128] B. M. Waxman, "Routing of multipoint connections," *IEEE Journal on Selected Areas in Communications*, vol. 6, no. 9, pp. 1617–1622, Dec 1988.

[129] J. Dall and M. Christensen, "Random geometric graphs," *Phys. Rev. E*, vol. 66, p. 016121, Jul 2002.

[130] P. Van Mieghem, H. Wang, X. Ge, S. Tang, and F. A. Kuipers, "Influence of assortativity and degree-preserving rewiring on the spectra of networks," *The European Physical Journal B*, vol. 76, no. 4, pp. 643–652, Aug 2010. [Online]. Available: https://doi.org/10.1140/epjb/e2010-00219-x

[131] Z. Chang, Z. Zhou, S. Zhou, T. Chen, and T. Ristaniemi, "Towards service-oriented 5g: Virtualizing the networks for everything-as-a-service," *IEEE Access*, vol. 6, pp. 1480–1489, 2018.

[132] A. Gupta and R. K. Jha, "A survey of 5g network: Architecture and emerging technologies," *IEEE Access*, vol. 3, pp. 1206–1232, 2015.

[133] L. Kleinrock, *Queueing systems, volume 2: Computer applications*. wiley New York, 1976, vol. 66.

[134] S. Achard, R. Salvador, B. Whitcher, J. Suckling, and E. Bullmore, "A resilient, low-frequency, small-world human brain functional network with highly connected association cortical hubs," *Journal of Neuroscience*, vol. 26, no. 1, pp. 63–72, 2006. [Online]. Available: http://www.jneurosci.org/content/26/1/63